MISSIONE 4
ISTRUZIONE
RICERCA

Department of Earth and Environmental Sciences

PhD program in Chemical, Geological and Environmental Sciences

Curriculum in Chemical Sciences

Cycle XXXVIII

DESIGNING AND TESTING REAL-TIME SENSORS FOR AIR QUALITY ASSESSMENT IN INDOOR/OUTDOOR ENVIRONMENTS

Tutor:
Prof. Luca Ferrero

Candidate:
Andrea Doldi

Supervisor:
Prof. Ezio Giovanni Bolzacchini

Coordinator:
Prof. Marco Giovanni Malusà

Academic Year 2025/2026

Finanziato dall'Unione europea NextGenerationEU
Ministero dell'Università e della Ricerca
Italiadomani
PIANO NAZIONALE DI RIPRESA E RESILIENZA
UNIVERSITÀ DEGLI STUDI DI MILANO BICOCCA

INDEX

1. Introduction

In the last few decades, there has been an increase in public interest in air quality issues, partly due to the outbreak of the COVID-19 pandemic and increase health concerns in the population (Lou et al, 2022). However, there is still a lack of awareness among a large part of the population about the harmful and detrimental effects of air pollutants in the atmosphere. The World Health Organization (WHO) has linked over 6.7 million deaths per year to the combined effect of ambient and household air pollution exposure (WHO, 2024); similarly, in the scientific literature the exposure to $PM_{2.5}$ concentrations is linked to a global burden of disease of millions of deaths per year (Cohen et al., 2017; Burnett et al., 2018). This highlights the need for continuous action on air quality at a global level, with increasingly strict regulations and continuous, widespread monitoring of pollutants, especially in more critical environments. However, the impact of air pollution is not limited to human health. Air pollution is linked to climate-altering effects, as some pollutants are climate forcers, displaying both warming or cooling effect on the atmosphere (Unger, N., 2012; Maione et al., 2016); it also severely affects the global ecosystem (Mohapatra et al., 2014; Manisalidis et al., 2020; Özkara et al., 2018). Another significant damaging effect of air pollution concerns anthropogenic materials, as it has been observed how the interaction with atmospheric pollutants can affect electronic equipment (Ferrero et al., 2015) and promote degradative processes on cultural heritage materials and artworks (Matrali et al., 2023; Vidović et al., 2022). A more detailed assessment of the impacts of atmospheric pollutants is provided in the following sections of this dissertation.

At the present day, air quality monitoring activities are conducted in order to comply with existing local or international legislation or for scientific research purposes. At European level, air quality monitoring is outlined in the EU Directive 2008/50/EC, which establishes common methods and criteria for monitoring activities, as well as defining limit values and thresholds for each pollutant (PM_X, NO_X, SO_2, CO and O_3), in an effort to protect human health and vegetation. Recently, the EU Directive 2024/2881 revised the aforementioned directive, in an effort to align with the updated WHO Air Quality Guidelines (WHO, 2021), establishing stricter limit values for pollutants, aimed at

minimizing pollution to protect health and ecosystems, reducing premature deaths from PM ($PM_{2.5}$) exposure by over 55% and defining the need for monitoring of emerging pollutants like ultrafine particles (UFP), black carbon (BC), and ammonia (NH_3). However, as stated by the WHO, still over 99% of the world population is exposed to pollutants levels above the recommended guidelines levels, even more significantly in low- and middle-income countries. While monitoring air quality within urban and rural areas is now common practice, data coverage is still limited and restricted to official monitoring stations managed by local government authorities. This is mainly related to the fact that the reference instrumentation required for air quality measurements is often expensive, bulky, and is continuously subjected to maintenance and calibration processes to ensure the data accuracy and precision required by the legislation. This results in inadequate spatial and temporal data coverage, which often fail to provide sufficient information on emission sources and hotspots (Kumar et al., 2015). In response to this matter, in recent years there has been a significant surge, both in the market and in scientific research, into the development of low-cost technologies for monitoring air quality. The emergence of new technologies and miniaturization of electronics allowed for cheaper, smaller and publicly accessible devices that, since their introduction, started shifting the paradigm of air quality monitoring. These new devices overcome some of the limitations of traditional instruments, complementing their role in air quality measurements. Thanks to their affordability, these sensors can be implemented in dense networks, to gather high-resolution air quality data with increased spatial and temporal coverage. This also opens the door to the involvement of citizens and communities in the process air quality measurements, towards a scenario where the public is directly engaged in the monitoring process, gradually increasing awareness towards atmospheric pollution issues while contributing to data collection (Snyder et al., 2013; Jovašević-Stojanović et al., 2015). Thanks to their reduced bulk and portability, these sensors are suitable for applications in personal exposure studies, both in domestic and occupational environments (Morawska et al., 2018; Ruiter et al., 2023; Howard et al., 2022), as they can be directly paired to an individual for longer periods than traditional instruments and without the constant need for supervision.

Low-cost sensors (LCS) are seeing several applications also in indoor environments, where often air quality monitoring through traditional instrumentation is held back by their size, bulk and noise. Deployment of LCS for indoor studies could prove crucial in understanding these environments, complementing the limitations of research-grade sensors, providing site-specific information. As indoor environments are profoundly different from one another, extensive monitoring in different settings, even in the same building, is critical to understand and address potential risks to human health and materials. As of now, no indoor-specific regulation is in place for air quality at the European level, where indoor air quality (IAQ) is subject to general guidelines (i.e. WHO global air quality guidelines, figure 1.1) aimed at protection of human health or to improve the energy performance of buildings (Siddique et al., 2025).

Pollutant	Averaging time	Interim target				AQG level
		1	2	3	4	
$PM_{2.5}$, µg/m³	Annual	35	25	15	10	5
	24-hour[a]	75	50	37.5	25	15
PM_{10}, µg/m³	Annual	70	50	30	20	15
	24-hour[a]	150	100	75	50	45
O_3, µg/m³	Peak season[b]	100	70	–	–	60
	8-hour[a]	160	120	–	–	100
NO_2, µg/m³	Annual	40	30	20	–	10
	24-hour[a]	120	50	–	–	25
SO_2, µg/m³	24-hour[a]	125	50	–	–	40
CO, mg/m³	24-hour[a]	7	–	–	–	4

Figure 1.1. Recommended Air Quality Guidelines and interim targets as reported by the World health Organization (WHO, 2021).

However, as people tend to spend most of their time indoors (Bousiotis et al., 2023), there is still the need for proper monitoring of living spaces. Exposure to particulate and gaseous pollutants is generally higher in indoor spaces and has been linked to respiratory and cardiovascular diseases, as well as

possible carcinogenic effects depending on the chemical composition of the pollutant (Hoskins, 2003).

Given these premises, this work is aimed at the employment of low-cost devices for atmospheric pollutants monitoring, with the ultimate objective being to assess the role that these new technologies may play in addressing air quality. More detailed, this work is focused on the application, testing and analysis of low-cost, smart, and portable instrumentation for air quality monitoring, as powerful tools that can aid the scientific community, as well as the public, towards a more comprehensive understanding of the air we breathe.

Given the high variability of spaces, settings and conditions, this project aims to test low-cost sensors in different indoor and outdoor environments, from ambient air conditions in urban and sub-urban areas, to occupational and cultural heritage-related settings. As this technology is easily accessible and employed by the public and non-scientific community, this project is also greatly centred around the concept of *citizen-science* research, engaging citizens in the monitoring process, and the dissemination of air quality data to increase awareness and knowledge of environmental issues related to atmospheric pollution. However, these sensors display significant technical limitations, resulting in lower accuracy and precision in air quality measurements. This creates the need for a rigorous testing and calibration phase in comparison with reference instruments, both in laboratory and environmental conditions. Part of this work is therefore dedicated to a technical evaluation of the instruments employed in the conducted analyses, assessing their performance and their ability to establish themselves as a useful tool in atmospheric monitoring, while developing corrective algorithms where necessary to align the measurements with their reference counterparts.

This work was conducted within the MUSA – Multilayered Urban Sustainability Action – project, funded by the European Union – NextGenerationEU, under the National Recovery and Resilience Plan (NRRP) Mission 4 Component 2 Investment Line 1.5: Strengthening of research structures and creation of R&D “innovation ecosystems”, set up of “territorial leaders in R&D”. The MUSA project is an ecosystem of innovation born from the University of Milano-Bicocca, involving the other main universities of the city

(Politecnico di Milano, Bocconi University, and the University of Milan) and numerous public and private partners, aimed at proposing a new model of public-private collaboration that can be replicated at national and international level. The ecosystem was established in the metropolitan area of Milan in an effort towards the three dimensions of sustainability: environmental, economic and social. This project acted as part of Spoke 1 (Urban) of the MUSA ecosystem, focused on the development of strategies for urban regeneration, making cities more sustainable and responsive to the needs of today's citizens. At the University of Milano-Bicocca, this effort translated into the urban redevelopment plan of *Piazza della Scienza,* the university's science campus, where the whole architectural context of the square was renewed, offering better living spaces and green coverage. As the square was planned to be one of MUSA's living laboratories, it saw the collaboration of young researchers involved in several different scientific fields who collaborated to create a space dedicated to research and sustainability, where more than 50 sensors were installed to monitor numerous parameters, such as square temperature, *air quality*, noise impact of human activities and biomonitoring. As part of the project, this work covered the entire redevelopment plan of the square with air quality monitoring activities during the pre-construction, construction, and post-construction phases. This not only allowed for an environmental evaluation of the impact of the whole redevelopment plan on air quality, but it also proved to be an excellent testing ground for deploying and installing various low-cost monitoring devices.

All the work carried out will be presented in the following sections of this dissertation . Later in this chapter, we will introduce the main atmospheric pollutants and their impact on the environment, human health and materials. Chapter 2 will focus mainly on outlining the instrumentation, materials and methodologies common to all activities conducted, serving as a general reference for the following sections. Since all the activities share a common thread, but the studied environments and sensor applications are varied and different from one another, each chapter (apart from the chapters 1 and 2, serving as a common reference point for the entire work) has been structured to stand alone, similarly to a scientific paper with an introductory section and methodology specific to the type of work carried out. Chapter 3 describes all the activities carried out as part

of the MUSA ecosystem redevelopment plan of *Piazza della Scienza*. A detailed technical evaluation of the low-cost sensors used will be presented, including calibrations against reference instruments and the derivation of site-specific algorithms and correction factors. From the data obtained, a precise environmental assessment of the construction site is then presented, to highlight its impact on the overall air quality of the square and the adjacent university spaces. Finally, based on the data gathered in the first months following installation, the performance of the devices placed in fixed positions within the square is assessed compared to reference data, as the concluding legacy of the MUSA project. Chapter 4 presents work carried out with regard to an environmental monitoring campaign employing an innovative low-cost sensor for measuring atmospheric black carbon (BC), presenting data obtained during five months of sampling and comparison with a reference aethalometer in an urban background site in Mülheim-Styrum, Germany. Chapter 5 focuses on monitoring activities carried out within the "Grande Brera" museum complex in Milan (comprising the *Pinacoteca di Brera*, *Palazzo Citterio* and Leonardo da Vinci's *Last Supper*), conducted for the purpose of preserving the environments and cultural heritage within them. While the monitoring focused on an initial assessment of pollutant concentrations in the environment, the project also involved the use of low-cost sensors to complement traditional instruments. This allowed for greater spatial and temporal coverage of the environment, enabling a more comprehensive assessment of the analysed spaces than through standard monitoring. Chapter 6 discusses data obtained from two experimental campaigns monitoring particle emissions in occupational environments involved in the production of polyurethane (PU) foams, conducted as part of the BIOMAT project. Particle monitoring was carried out by combining reference instrumentation with medium- and low-cost devices, to assess the capability of these sensors to significantly detect process-related emissions. Finally, Chapter 7 focuses on *citizen science* initiatives carried out as part of this work, involving the use of different low-cost systems for air quality monitoring. A homemade , low-cost device for monitoring particulate matter and gaseous pollutants, developed by a group of local citizens as part of the Milano Smart Park project (Associazione Parco Segantini, Milan), was calibrated against a gravimetric sample in an

environmental campaign as planned by the F.AIR project. A low-cost, portable sensor for personal exposure monitoring (RESPIRO, Unimib) was developed and employed in pilot campaigns involving citizens and students in the data collection and dissemination phase.

Finally, conclusions are drawn from this entire study, providing an overview of the application of low-cost sensors as a complementing tool in air quality monitoring, highlighting the benefits that can be gained and the limitations that still persist.

1.1. Pollutants in the atmosphere

The following passage is primarily aimed at depicting the main pollutants found in the atmosphere. As atmospheric chemistry is a highly complex system involving numerous agents, this section will focus its attention on a limited selection of pollutants, highlighting those most relevant to the activities conducted in this work.

In urban environments, and primarily from the perspective of preserving human health and anthropogenic materials, one of the most significant pollutants is the particle phase, commonly referred to as particulate matter (PM). Other important pollutants are gaseous compounds, introduced into the atmosphere from direct sources or through chemical reactivity. Among the most relevant and essential for understanding this work and its implications are nitrogen oxides (NO_X), ozone (O_3), and carbon oxides (CO and CO_2). The next paragraphs will briefly introduce the mentioned pollutants, describing the main mechanisms of emission and formation, as well as their evolution and reactivity in the atmosphere.

1.1.1. Particulate matter

Atmospheric particulate matter (PM) is usually defined as a mixture of solid and liquid particles suspended in the atmosphere for different times (from seconds to weeks). This definition does not strictly refer to a single class of compounds but defines a highly heterogeneous set of particles with widely different chemical composition, shape, size and physical properties. These characteristics are

strongly dependent on emission sources, reactivity, and atmospheric evolution processes (EPA, 2019).

The origin of particles in the atmosphere can be direct, therefore mainly linked to emission sources, which can be divided into natural (i.e. mineral dust, sea spray, volcanic eruptions and biogenic sources) and anthropogenic (i.e. traffic emissions, industrial processes, domestic heating, agriculture) sources. However, a significant fraction of the particulate matter present in the atmosphere derives from secondary processes, linked to the chemical reactivity of compounds and ageing of particles capable of significantly altering their size and physio-chemical characteristics. New particle formation can occur from gaseous compounds in the atmosphere through a process called nucleation. As outlined in Figure 1.2, following formation by nucleation new particles can then grow through coagulation and condensation processes (Raes et al., 2000).

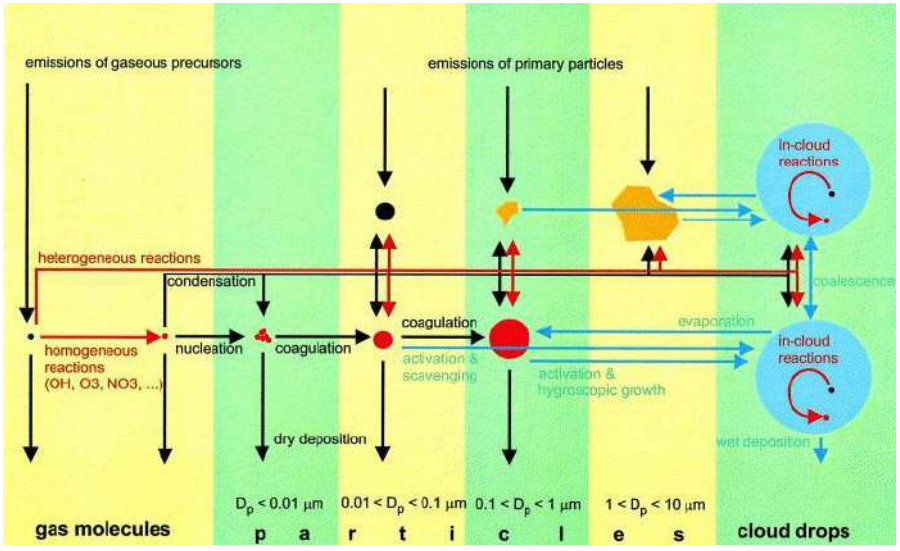

Figure 1.2. Schematics of reactions and processes in the atmosphere that influence particle size distribution and their physio-chemical characteristics (Raes et al., 2000).

The formation, ageing and deposition (dry or wet) processes therefore significantly influence the size distribution of particles in the atmosphere. This results in a number of modes that usually accurately depict particles in the atmosphere (Figure 1.3). The number size distribution is usually dominated by the nucleation mode (diameter less than 10 nm), characteristic of particles

generated via nucleation, and the Aitken mode (diameter comprised between 10 and 100 nm), dominated by condensation of secondary particles on primary nuclei (Seinfeld & Pandis, 2006). However, as the contribution in terms of number of particles with a diameter greater than 0.1 μm is negligible, the size distribution of particles in the atmosphere is different when mass concentration is considered. The accumulation mode, which consists of particles with diameters ranging from 0.1 to 2 μm, is predominantly dominated by particles of primary origin or those that have resulted from secondary coagulation and condensation processes; the coarse mode is characterized by particles with diameters between 2 to 50 μm, usually generated by mechanical processes, such as wind and erosion. These two modes generally dominate the volume and mass particle size distributions in most environments. Atmospheric particles are then further defined by their size in three different broad-size classes: the term *coarse* particles is generally used to describe particles with a diameter greater than 2.5 μm; particles with a diameter less than 2.5 μm are referred to as *fine* particles; additionally, particles with a diameter less than 0.1 μm are collectively referred to as *ultrafine* particles.

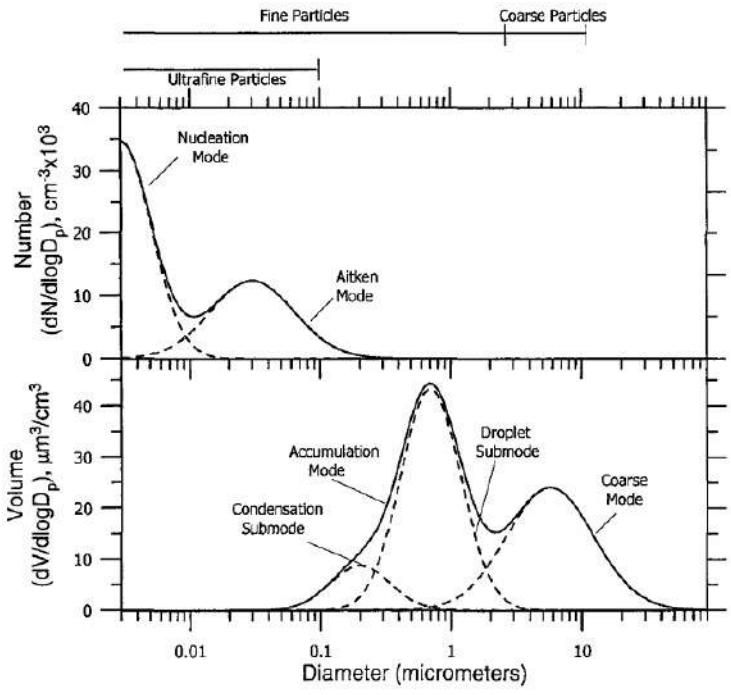

Figure 1.3. Number (up) and volume (down) size distribution with main modes highlighted (Seinfeld & Pandis, 2006).

The U.S. EPA (EPA, 2004) introduced a sampling convention for PM, defining two classes based on the efficiency of a sampling system and the equivalent aerodynamic diameter of atmospheric particles (Figure 1.4): PM_{10} and $PM_{2.5}$. The PM_{10} fraction is defined as the fraction of particulate matter collected by a sampling system with an efficiency of 55% for an aerodynamic diameter value of 10 μm following a well-defined sampling efficiency curve (Figure 3); the $PM_{2.5}$ is the fraction of particles collected by a sampling system with an efficiency of 48% for an equivalent aerodynamic diameter of 2.5 μm again following a well-defined sampling efficiency curve (Figure 3). As the sampling efficiency of a system is dependent on the flow geometry, different systems may employ different penetration efficiency. At the European level, PM is in accordance with UNI EN 12341, which defines PM_{10} as the fraction collected by a sampling system with an efficiency of 50% at 10 μm; similarly, $PM_{2.5}$ is defined as the fraction collected with an efficiency of 50% at 2.5 μm. These definitions allow the establishment of a parameter for assessing atmospheric particulate matter to simulate its ability to penetrate the human respiratory system, providing a useful index for health protection.

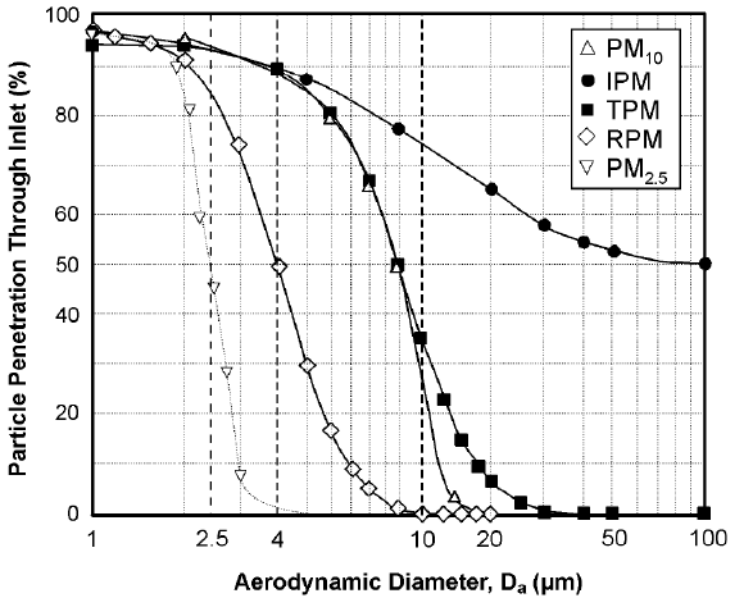

Figure 1.4. Sampling efficiency curves for atmospheric particulate matter measurement systems (EPA, 2004).

The chemical composition of atmospheric PM features site-specific and temporal variability, mainly related to differences in emission sources, in the chemical-physical processes undergone by the particles, as well as meteorological conditions and daily and seasonal cycles (Figure 1.5). Typically, the chemical composition of atmospheric PM is dominated by water-soluble compounds, primarily inorganic ionic species such as NH_4^+, NH_3^-, $SO_4^=$, derived mainly form secondary processes and accounts for almost 40% of atmospheric PM (Ferrero et al., 2013). A second important component is the carbonaceous fraction, consisting of a significant proportion of organic matter (OM), from both natural and anthropogenic sources, and elemental carbon (EC), also reported as *black carbon* (BC) and directly emitted by combustion processes; please note that EC is determined via a thermal method while BC from an optical method and therefore a recent publication reports the guidelines for reporting BC data (Savadkoohi et al., 2024). Finally, a less significant fraction of atmospheric PM is composed of mineral dust and metals (Zhang et al., 2020).

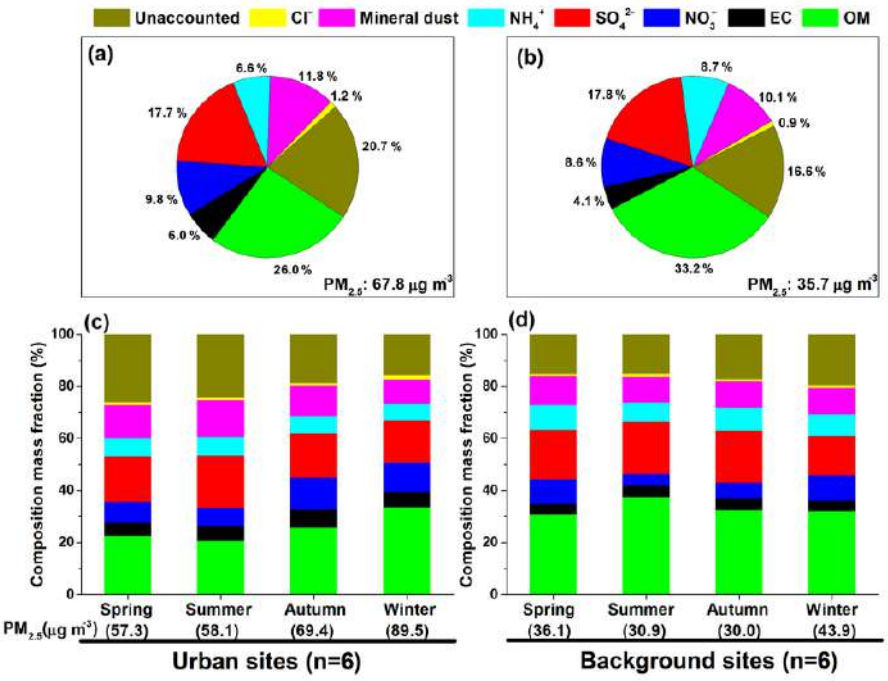

Figure 1.5. Average chemical composition and its seasonal variations of $PM_{2.5}$ at both an urban (left) and background (right) sites (Liu et al., 2018)

One of the most noteworthy properties of atmospheric particulate matter, in relation to its chemical composition, is its hygroscopicity. Some compounds, such as inorganic salts, can absorb water present in the atmosphere, thereby growing in size. When the ambient relative humidity (RH) is low, particles in the atmosphere are typically in a solid state. When particles reach a threshold RH value, defined as *deliquescence relative humidity* (DRH) and dependent on the chemical composition, they begin to spontaneously absorb water, transitioning to the aqueous phase and significantly increasing their mass. This phase transition is an equilibrium process, regulated by the Gibbs free energy. When the ambient RH decreases water evaporates; however, in the atmosphere the transition to solid state does not occur at the DRH and the solution remains supersaturated until a lower RH threshold is reached. This point is defined as *crystallization relative humidity* (CRH). The values (DRH and CRH) at which phase transitions occur are not constant but are determined by the chemical composition. Furthermore, not all species undergo a hysteresis cycle (Figure 1.6), but some highly hygroscopic species gradually absorb water in relation to RH values (Seinfeld & Pandis, 2006). Hygroscopicity plays a key role in both human health, influencing deposition in the respiratory tract, and climate, affecting properties and lifetime of clouds, as well as regulating the abundance of different species in the gas and particle phases (Shi et al., 2022). Additionally, aerosol hygroscopicity can heavily affect particle measurements conducted with optical particle counters, as particle can absorb water and grow in size in high RH conditions, thus influencing their refractive index light scattering (Nurowska & Markowicz, 2023). This process usually induces a mass overestimation in the particle measurement conducted with such devices.

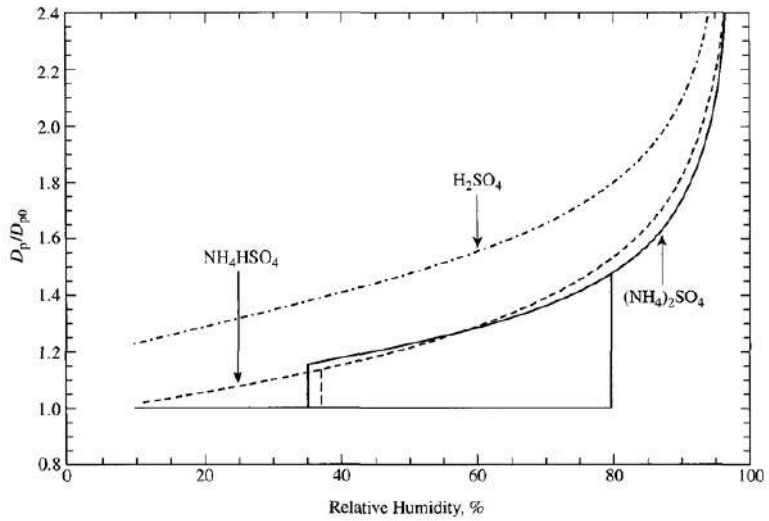

Figure 1.6. Hysteresis cycle of different chemical species, showed as change in particle diameter in relation to relative humidity levels (Seinfeld & Pandis, 2006).

The chemical composition, size distribution and hygroscopicity of atmospheric particulate matter determine a wide range of effects (Liu et al., 2018) that can significantly impact the climate, the environment, human health and anthropogenic materials. Section 1.2 provides a comprehensive overview of these impacts and their implications.

1.1.2. Nitrogen oxides

The chemistry of nitrogen-containing compounds in the atmosphere is complex and involves multiple chemical species. At the tropospheric level nitrogen oxides, mainly nitrogen oxide (NO) and nitrogen dioxide (NO_2), play a fundamental role in atmospheric chemistry. Nitrogen oxide (NO) is a colourless and odourless gas emitted primarily from combustion processes, both of biogenic and anthropogenic nature. Within urban centres NO is mainly emitted by vehicular exhaust emissions. Nitrogen dioxide (NO_2) is a gas characterised by a reddish-brown colour and a strong pungent odour. While NO_2 is also emitted as a primary pollutant through combustion processes, the main source is through reactivity in the atmosphere via the oxidation of NO. Given their reactivity and role in the atmosphere, it is usually convenient to define atmospheric nitrogen oxides as the sum of NO and NO_2, thus referred to as NO_X. Other nitrogen oxides present in

the atmosphere include nitrous oxide (N_2O), an inert gas that is emitted directly into the atmosphere from both biogenic and anthropogenic sources. This compound is a prominent greenhouse gas and, given its atmospheric lifetime of over 100 years, can therefore be transported into the stratosphere, where it acts as one of the most significant ozone-depleting substances of the present time. Other nitrogen oxides, like the nitrate radical NO_3 and dinitrogen pentoxide (N_2O_5), are crucial components of atmospheric chemistry, albeit being present in relatively low concentrations (Seinfeld & Pandis, 2006).

Considering only the NO_x, after NO is emitted in the atmosphere, it can rapidly be oxidized by ozone to nitrogen dioxide (Eq. 1). As NO_2 absorbs the solar radiation in the UV, it can then go through photodissociation forming NO and atomic triplet oxygen (Eq. 2). This step is critical, as the subsequent reaction (Eq. 3) with molecular oxygen (where M is a species capable of absorbing excess energy) is the only significant source of ozone in urban atmospheres. This series of reactions, known as the photolytic cycle of NO_2, is the main mechanism influencing NO_X and O_3 concentrations in the atmosphere at the steady state, a steady state that can be affected even by volatile organic compounds (VOCs) (Holland et al., 2024).

$$NO + O_3 \rightarrow NO_2 + O_2 \quad (1)$$

$$NO_2 + h\upsilon \rightarrow NO + O \quad (2)$$

$$O + O_2 + M \rightarrow O_3 + M \quad (3)$$

After its formation following the reaction described in Eq. 1, nitrogen dioxide can further react with ozone forming the nitrate radical NO_3 (Eq. 4). The concentration of NO_3, and its oxidative potential, is thus dependentent on the availability of ozone and concentration of NO_2 in the atmosphere. The nitrate radical is then quickly photolyzed by solar radiation (at wavelengths shorter than 630 nm), resulting in overall higher concentration during the night.

$$NO_2 + O_3 \rightarrow NO_3 + O_2 \quad (4)$$

Furthermore, NO_2 and the NO_3 radical can interact through a three-body reaction involving a compound able to absorb the excess energy (Ep. 5), resulting in the formation of dinitrogen pentoxide (N_2O_5) which acts as a short-term reservoir of

the NO_3 radical. Although N_2O_5 is easily degraded either thermally or photochemically, it is a crucial component of atmospheric chemistry as it can easily react with water to form nitric acid (Eq. 6), contributing to the rain acidification phenomenon and gas to particle conversion considering the affinity between HNO_3 and NH_3 in the atmosphere.

$$NO_2 + NO_3 + M \rightarrow N_2O_5 + M \quad (5)$$

$$N_2O_5 + H_2O \rightarrow 2\,HNO_3 \quad (6)$$

Nitric acid functions as a bridge between the gaseous phase and the particulate phase, as it reacts easily with basic compounds in the atmosphere, such as ammonia, to form the corresponding nitrate salts (Eq. 7).

$$NH_3 + HNO_3 \rightleftharpoons NH_4NO_3\,(s) \quad (7)$$

This process heavily impacts secondary particle formation through mainly heterogeneous reactions, especially in winter, due to high nitrate concentrations and generally high relative humidity levels.

1.1.3. Ozone

Ozone (O_3) is a highly reactive gas, and one of the most powerful oxidising species in the atmosphere. While most of the atmospheric ozone is found in the stratosphere (about 90%), a significant portion, between 10% and 15% dependent on latitude, is present in the troposphere (Fishman et al., 1990). In the stratosphere, ozone plays a fundamental role, absorbing almost all ultraviolet solar radiation at wavelengths between 240 and 290 nm (UV-C) and part of the radiation between 290 and 320 nm (UV-B). At the tropospheric level, however, high concentrations of ozone can pose harmful effects on human health, resulting in damage and inflammation to the respiratory system, and vegetation (Seinfeld & Pandis, 2006). A significant part of tropospheric ozone is exchanged from the stratosphere through the Stratosphere-Troposphere Exchange (STE); however, most of ozone found in the troposphere is formed directly from photochemical reactions in the atmosphere involving other gaseous pollutants like NO_X and

volatile organic compounds (VOCs), methane and carbon oxides (Guicherit & Roemer, 2000).

Ozone in the troposphere plays a critical role in atmospheric chemistry as it contributes to the formation of the hydroxyl radical (OH), which rules the oxidative processes in the atmosphere (Lelieveld & Dentener, 2000). After photodissociation, the ground-state atomic oxygen produced (Eq. 8) can react with water vapour resulting in the hydroxyl radical OH (Eq. 9):

$$O_3 + h\upsilon \rightarrow O(1D) + O_2 \quad (8)$$

$$O(1D) + H_2O \rightarrow 2OH \quad (9)$$

Among anthropogenic sources, ozone is primarily generated in the atmosphere by sunlight-induced photodissociation of NO_2 (Finlayson-Pitts & Pitts, 1993), as already highlighted by Eq. 2 in section 1.1.2. In a setting where no side reactions occur, the overall concentration of O_3 in the atmosphere is regulated by the photolytic cycle of NO_2, thus depending on generation by photodissociation of NO_2 and removal by the subsequent oxidation of NO to NO_2. In reality, however, the cycle is perturbed by other chemical species, like hydrocarbons or volatile organic compounds (VOC), that compete in the oxidation of NO to NO_2, thus preventing the removal of O_3 and promoting its accumulation in the atmosphere.

1.1.4. Carbon oxides

Carbon monoxide (CO) is a colourless, odourless gas and one of the most prevalent gaseous pollutants in the atmosphere. CO is usually formed as a product of incomplete combustion processes of carbonaceous materials. Although CO can originate from natural sources, most of its emission in the atmosphere (around 90%) comes from combustion processes linked to anthropogenic activities, like motor vehicle exhaust, industrial processing and domestic heating (Jaffe, 1968). While vehicle emissions are one of the main sources of CO in urban centres and heavily populated areas, the introduction of catalytic converters in exhaust systems has led to a significant reduction in emissions of this pollutant over the years (Twigg, 2011). As demonstrated by Mott

et al. (2002), CO concentrations in the U.S. have fallen by over 70% since the introduction of catalytic converters in 1975.

In the atmosphere, the main reaction that carbon monoxide undergoes is oxidation by the hydroxyl radical to form carbon dioxide and a hydrogen atom in its ground electronic state:

$$CO + OH \rightarrow CO_2 + H \tag{10}$$

This reaction is one of the main pathways in which OH radicals are removed from the troposphere (Bjork et al., 2016). The oxidation from CO to CO_2 can also occur in the presence of molecular oxygen (Eq. 11), although this reaction is kinetically much slower:

$$CO + O_2 \rightarrow CO_2 + O \tag{11}$$

Through interaction, and subsequent depletion, with the hydroxyl radical, carbon monoxide acts as an indirect greenhouse gas, favouring the accumulation in the atmosphere of other greenhouse gases that would otherwise be removed by OH, like methane (CH_4) (Daniel & Solomon 1998).

Carbon dioxide is a chemically inert gas, whose overall concentration in the atmosphere is influenced by the carbon-cycle through photosynthesis and respiration, decomposition of organic matter, carbon fixation, geological and combustion processes, as well as the atmosphere-ocean exchange. Atmospheric concentrations of CO_2, however, have been increasing significantly in the past decades driven by anthropogenic emissions, with over 70% resulting from the combustion of fossil fuels and industrial activities (IPCC, 2013). While its concentrations in the atmosphere are of particular interest due to their climate-changing effect as a greenhouse gas, CO_2 is also widely studied with regard to indoor air quality monitoring. In indoor environments, where carbon dioxide concentrations can be strongly influenced by release through human respiration, high concentrations of CO_2 can severely impact cognitive function (Du et al., 2020).

In the following section the impacts on human health, climate and ecosystems, and anthropogenic materials of the aforementioned pollutants will be detailed in greater depth, with particular regard to the activities carried out in this work.

1.2. Impact and effects of atmospheric pollutants

The study and monitoring of atmospheric pollutants in different environments is of fundamental importance in understanding the impact they can have on our world and thus guiding the decision-making processes to promote their mitigation and prevention. Scientific literature highlights how these compounds and their interaction in various atmospheric processes can significantly influence the Earth's climate and the entire ecosystem. Furthermore, these pollutants have a negative impact on human health, being often linked to increased human mortality, respiratory and cardiovascular diseases (Orellano et al., 2020), and the onset of cancer and other conditions. Finally, it is important to underline the link between atmospheric pollutants and various detrimental effects on materials of anthropogenic origin, potentially resulting in significant economic, social and cultural implications.

The following subsections will address the individual impacts of these pollutants on climate change, ecosystems and the natural environment, as well as on human health, and materials of anthropogenic origin and use. Given the focus of this work, special consideration will be given to the effects regarding human health and man-made materials.

1.2.1. Impact on climate, environment and ecosystem

The impact of atmospheric particulate matter (PM) on the climate is mainly caused by changes in the Earth's radiation budget, thus leading to warming or cooling of the atmosphere. Atmospheric particulate matter can have two effects in terms of radiative forcing: a direct effect, due to interaction with the solar radiation through absorption or refraction; or an indirect effect, interacting with cloud formation, changing certain characteristics such as persistence in the atmosphere or reflectivity (Bellouin et al., 2020). Overall, the effect of atmospheric particulate matter on the Earth's radiation budget is negative, as an increase in aerosol concentrations has been linked to a net cooling at the top of the atmosphere (Charlson et al., 1992; Levy et al., 2013). The radiative forcing of atmospheric aerosols is therefore able to offset part of the positive forcing caused

by greenhouse gases, having a substantial influence in concealing a significant portion of atmospheric warming caused by anthropogenic emissions. However, the role of atmospheric aerosol is double: from one side can cool the surface and the top of the atmosphere while on the other side it can warm the atmosphere, thus bringing to an energy redistribution (both in space and time). In this respect, one of the main components of atmospheric particulate matter influencing radiative forcing is the black carbon (BC), whose absorption of light radiation leads to atmospheric warming. Conversely, some compounds such as inorganic salts (mainly sulphates and nitrates) as well as some organic aerosols can scatter solar radiation, thus leading to a significant net cooling effect .

Atmospheric particulate matter also has profound effects on soil, vegetation and marine ecosystems. Plant leaves are one of the major sinks for atmospheric PM via deposition. It has been observed that atmospheric particulate matter can adversely impact vegetation, altering physiological (photosynthesis rate) and biochemical (i.e. pH, water content) parameters and affecting morphology, through reduction in plant development and growth (Singh & Verma, 2023). After deposition, atmospheric PM can penetrate deep into the soil leading to various detrimental effects based on its chemical composition, such as accumulation of chemical components, changes in nutrients, alteration of species diversity and population, disruption of biogeochemical cycles and soil acidification. (Zuhara & Isaifan, 2018; Grantz et al., 2003).

As detailed in the case of PM, the impact on the Earth's climate linked to nitrogen oxides (NO_X) present in the atmosphere is twofold. These compounds present a net warming effect on the atmosphere as they interact with volatile organic compounds (VOCs) to form ozone, a well-known greenhouse gas (Tan et al., 2018); in an equivalent way, nitrogen oxides in the atmosphere can be converted into nitrous oxide (N_2O), another potent greenhouse gas (Forster et al, 2007). The negative forcing of nitrogen oxides, in contrast, is the result of their reactivity in the atmosphere, where they play a role in the creation of the OH radical thus reducing the lifetime of methane (CH_4) in the atmosphere. Furthermore, as NO_X can undergo nucleation processes to form particulate matter, they can consequently contribute to the formation of compounds capable of reflecting light and increase the Earth's albedo, thus leading to a net cooling

effect on the atmosphere. In addition, nitrogen oxides are one of the main compounds leading to acidification of rain. This decrease in rain pH levels can have profound implications on soil, leading to a decrease in plant growth and a loss in nutrients, on marine ecosystems, directly harming marine fauna, and on plants, leading to leaf alterations or reduction in crop yields (Singh & Agrawal, 2008).

Stratospheric ozone plays a fundamental role, as detailed in section 1.1.3, in blocking ultraviolet solar radiation, contributing marginally towards cooling Earth's surface. Tropospheric ozone, on the other hand, has the opposite effect on the climate, acting as a greenhouse gas comparable to CH_4 and N_2O resulting in a net positive radiative forcing of about 0.3 W m^{-2} (Mohnen et al., 1993; Sudo, 2023). Furthermore, tropospheric ozone has been identified as one of the most toxic gaseous pollutants for plants and is linked to adverse effects on the entire ecosystem (Fuhrer et al., 2016).

Carbon dioxide (CO_2) is widely known as one of the main greenhouse gases in the atmosphere, responsible for a net positive radiative forcing of 1.826 ± 0.19 W m^{-2}, with an estimated increase per decade, between 2000 and 2010, of 0.2 W m^{-2} (Feldman et al., 2015).

While carbon monoxide (CO) has a direct, albeit very limited, positive forcing effect on the Earth's climate, its major effect is indirect, as CO competes to remove the OH radical from the atmosphere (forming CO_2), thereby increasing the lifetime of methane (CH_4), a powerful greenhouse gas (Daniel & Solomon, 1998).

1.2.2. Impact on human health

The effects of air pollution on human health have been extensively studied and described in scientific literature, mainly linked to respiratory, cardiovascular and neurological morbidity, damage to the reproductive system and the incidence of cancer. This translates into an increase in early mortality, hospitalization, as well as an increase in total healthcare cost.

Atmospheric particulate matter is one of the most studied pollutants from a human health perspective. The main factor influencing the adverse health effects of PM is particle size, thus their ability to penetrate the respiratory system: *coarse* particles (diameter higher than 2.5 μm), usually identified as the PM_{10} fraction,

can reach the upper respiratory tract; *fine* particles (diameter less than 2.5 µm, usually identified as the $PM_{2.5}$ fraction), however, can penetrate deeper, reaching the alveoli and, in some cases, entering the bloodstream (Kampa & Castanas, 2008). Moreover, ultrafine particles (UFP, diameter less than 100 nm), thanks to their smaller size, can easily spread from the lungs to the circulatory system, contributing to adverse health effects also in extrapulmonary organs (Oberdörster et al., 2005; Oberdörster et al., 2004).

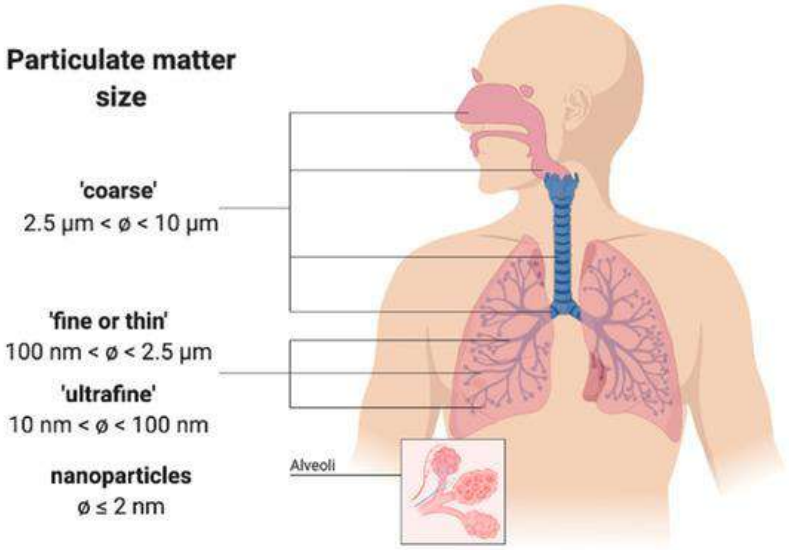

Figure 1.7. Permeation of atmospheric PM in the respiratory tract (Sanità di Toppi et al., 2020).

Exposure to fine PM concnetrations has been extensively linked to increased cardiovascular mortality, accounting for nearly 80% of pollution-related deaths (Basith et al., 2022). Moreover, it is the leading cause for increase in cardiovascular morbidity, such as myocadial infarction, strokes, hearth failures and arrhythmias (Krittanawong et al., 2023). Exposure, both short- and long-term, to high PM concentrations has been linked to a higher incidence of chronic respiratory diseases, such as asthma and chronic obstructive pulmonary disease, and a loss in lung function (Bentayeb et al. 2013; Kyung & Jeong, 2020; Guillam et al., 2013). These PM-related diseases are particularly severe for the most vulnerable groups of the population, such as the elderly and children (Gao et al., 2014). Given its variability of chemical species and relative toxicity, atmospheric PM has been classified as a Group I carcinogen by the International Agency for

Research on Cancer (IARC), as its relation with lung cancer, as its relationship with the insurgence of lung cancer is widely documented in scientific literature (Sahu et al., 2014; Raaschou-Nielsen et al., 2016; Hamra et al., 2014). Overall, exposure to atmospheric PM has been linked to an increase in mortality rate (Pope & Dockery, 2006).

Ozone is a highly oxidising gas in the atmosphere which, upon inhalation, can lead to oxidative stress and inflammation of the respiratory tract (Nuvolone et al., 2018). Short-term exposure to high ozone concentrations can lead to worsening of respiratory symptoms, while long term exposure to ozone is often linked to exacerbation of pre-existent respiratory diseases, to chronic lung diseases and an overall increase in respiratory and cardiovascular mortality rate (Bell et al., 2004; Liu et al., 2018; Jerret et al., 2009; Wang et al., 2020).

Similarly, exposure to high concentrations of nitrogen oxides, especially NO_2, can lead to respiratory symptoms, inflammation of the respiratory tract or aggravate pre-existing respiratory conditions. Longer exposure to high concentrations of NO_2 can result in the development of chronic respiratory diseases, such as asthma, respiratory symptoms and an increase in respiratory and cardiovascular mortality (Theodorakidou & Lambrou, 2017; Tao et al., 2011; Belanger et al., 2005).

Once inhaled, carbon monoxide (CO) can easily diffuse from the lungs into the bloodstream, where it binds to hemoglobin with an affinity 200–250 times stronger than oxygen. This can cause a significant decrease in oxygen supply in the blood, leading to cellular hypoxia (Abelsohn et al., 2002). The health implications of exposure to low concentrations of CO have been recognised for several decades, with evidence highlighting possible cardiovascular and neurobehavioural effects, as well as complications on fetuses and newborns (U.S. EPA, 1984). CO poisoning is a widely documented phenomenon, linked to an increase in mortality even at low concentrations and short-term exposure (Ernst & Zibrak, 1998; Chen et al., 2021). Carbon dioxide (CO_2), while not considered one of the major atmospheric pollutants, is nevertheless regarded as an excellent indicator of indoor air quality and proper ventilation in buildings (Dimitroulopoulou et al., 2023*)*. Exposure to high CO_2 concentrations was shown to cause cognitive decline and fatigue, dizziness and respiratory symptoms

(Samudro et al., 2022). Moreover, CO_2 is one of the pollutants considered, as an indicator for poor ventilation, regarding the Sick Building Syndrome (SBS), a condition involving a plethora of symptoms and health issues due to poor air quality inside indoor environments.

1.2.3. Impact on anthropogenic materials

While the effects of air pollution on human health have been extensively studied in scientific literature, the impact that certain pollutants can have on anthropogenic materials has been less explored. However, it is now clear how atmospheric pollutants can impact our daily lives, affecting every material that is exposed to the air. This section will focus on addressing some of the most significant effects the discussed pollutants have on anthropogenic materials, from damage and soiling of civil structures and cultural heritage sites to effects on electronic equipment and printed circuits.

The materials most susceptible to degradation over time due to exposure to atmospheric pollutants are those used in the construction of buildings and civil structures, which are predominant in every urban context. While the degradation rate for most employed materials has been decreasing in recent years thanks to anti-pollution policies (Brimblecombe & Grossi, 2010), the effect on buildings and infrastructure is still significant and capable of causing socio-economic damage, as well as potential harm to people's lives. Damage to building materials is mainly caused by the interaction of certain pollutants with the material, which can lead to degradation, corrosion, erosion and soiling of surfaces. One of the main contributors to surface degradation is the phenomenon of acid rain, mainly linked to the presence of compounds such as sulphur and nitrogen oxides in the atmosphere. These compounds, emitted directly from anthropogenic sources or reactivity in the atmosphere, can react further to form acid compounds, such as nitric acid (HNO_3) and sulphuric acid (H_2SO_4). These acids can then, through dry or wet deposition, settle on surfaces causing corrosion and degradation, leading to material loss and structural failings in buildings (Rao et al., 2014, Sharma et al., 2023; Ruffolo et al., 2023). Among the main targets of this type of process are stone materials, especially carbonate-based materials such as marbles and limestones, as detailed by Ruffolo et al., (2023) through equations 12 and 13:

$$2HNO_3 + CaCO_3 \rightarrow Ca(NO_3)_2 + H_2O + CO_2 \quad (12)$$

$$H_2SO_4 + CaCO_3 \rightarrow CaSO_4 + H_2O + CO_2 \quad (13)$$

A further mechanism of degradation of limestone surfaces occurs through natural dissolution by rain, naturally acidified by CO_2 in the atmosphere, in what is known as the karst effect (Eq. 14).

$$CaCO_3 + H_2O + CO_2 \rightarrow Ca(HCO_3)_2 \quad (14)$$

This reaction leads to the formation of calcium bicarbonate, about a hundred times more soluble than calcium carbonate, thus leading to a loss of material (Cardell-Fernández et al., 2002). Metal surfaces in contact with outdoor air may undergo a corrosive phenomenon known as atmospheric corrosion, defined as a corrosive process of material degradation following exposure to air. Corrosion usually occurs as a result of water vapour condensation on metal surfaces exposed to air, where a thin liquid layer is formed and acts as an electrolytic solution, allowing dissolution of gaseous or particulate pollutants. The actual corrosion process is activated by the presence of this aqueous layer on metal surfaces and the dissolution of molecular oxygen (O_2) in it, acting as an electron acceptor. Atmospheric pollutants can influence the kinetics of this process, influencing the corrosion rate, which is usually dependent on the metal, air temperature and relative humidity, as well as the chemical composition and concentration of atmospheric gaseous and particulate pollutants involved. Metal corrosion can therefore lead to material deterioration, resulting in a loss of structural integrity for building and thus in lower longevity, while also posing a safety risk for occupants.

The degradation, corrosion and soiling of surfaces are particularly critical for cultural heritage materials such as historic buildings, paintings and sculptures, exposed to atmospheric pollutants. Most cultural heritage sites and artworks are usually made of materials that are easily degraded and are located in highly anthropized areas, making them particularly susceptible to the effects of ageing and degradation caused by atmospheric agents and pollutants through some of the processes mentioned above (Sablier & Garrigues, 2014). As detailed by Vidović et al. (2022), atmospheric particulate matter (PM), nitrogen oxides (NO_X), sulphur dioxide (SO_2) and ozone (O_3) are the main contributors to

pollution-induced deterioration of cultural heritage objects, as they can lead to acidification thus deterioration and corrosion of materials. While the effect of ozone on cultural heritage material is generally less explored in the scientific literature, its role in deterioration of plastic, rubber, paints and coatings has been recognized. Sulphur dioxide has a leading role in the corrosion processes of metal exposed to air contaminants; however, its impact on cultural heritage materials has been decreasing due to recent anti-pollution policies in most countries. Atmospheric particulate matter has been identified as one of the pollutants with the greatest impact on cultural heritage materials. Given its high variability in terms of size and chemical composition, PM can cause physical, chemical and biological damage to surfaces. Atmospheric PM is one of the main agents causing surface *soiling*, defined as the accumulation of materials on surfaces, which can lead to their deterioration and visual impairment of the object. In the context of cultural heritage, soiling can lead to blackening of surfaces due to the deposition of carbonaceous material (elemental and organic carbon) as well as the formation of gypsum ($CaSO_4 \cdot 2H_2O$) from the interaction between sulphur dioxide in the atmosphere and calcium carbonate (Barca et al., 2014; Comite & Fermo, 2018). Deterioration linked to atmospheric pollutants is not a process that only affects cultural heritage exposed to outdoor air, but also artworks confined in indoor environments, such as museums, exhibitions and historical sites. Fine particulate matter (PM2.5) is one of the main agents of deterioration in indoor environments, leading to surface soiling (Grau-Bové & Strlič, 2013). Soiling of indoor surfaces can lead to two different effects: a visual impairment or modification of the surface due to deposition of dust, and degradation due to chemical interaction at surface level. Moreover, particles in indoor environments are subjected to wet-dry cycles of dissolution and crystallization due to their interaction with ambient relative humidity and temperature, thus potentially leading to cracking, detachment of materials, scaling and discolorations (Motta et al., 2022). In indoor cultural heritage environments, visitors are an important source of pollutants, such as carbon dioxide (CO_2) and ammonia (NH_3), mainly from the respiration. Monitoring of these pollutants is of great importance as they can lead to formation of secondary particles, as well as degradation and discoloration of surfaces. To prevent damage to paintings, artworks and

sculptures contained within these environments, it is therefore essential to monitor pollutant concentrations, as well as environmental parameters such as temperature and relative humidity. The fine tuning of these parameters, especially RH levels, and the control of ventilation, air circulation and conditioning systems in museum environments are some of the key measures required to preserve cultural heritage.

An additional category of anthropogenic material negatively impacted by atmospheric pollutants are both the electric and electronic infrastructure. Atmospheric PM, especially its inorganic fraction, can increase the risk of flashover events on insulators of the power grid systems after interaction with water (Gini et al., 2023). Atmospheric particulate matter has also been demonstrated to cause damage to electrical circuits and printed circuit boards (PCBs), resulting in short-circuits and electrical failures. Once deposited on the electrical surfaces, PM can reach the DRH, enabling the dissociation of water-soluble ionic compounds, thus becoming both electrically conductive and corrosive (Ferrero et al., 2013). For this reason, as highlighted by Ferrero et al. (2015), monitoring pollutant concentrations and environmental parameters within high-risk environments, such as data centers, can lead to significant economic, energy and environmental savings.

2. Materials & methods

As described in the previous section, this work is aimed at the employment of several low-cost instrumentation for monitoring pollutants in the atmosphere. The devices used in the present work are characterized by different operating principles and applications, suitable for very specific aims and usages in various environments, as detailed in the next sections of this work. In addition, since low-cost sensors require comparison and calibration with reference instruments, the research-grade devices employed are described as well. Therefore, this chapter focuses on providing a detailed description of each device and equipment used. Since most of the equipment discussed here is the one used in the environmental applications outlined in the following sections, the information reported below provides a common foundation for the materials and methods used in all the activities described hereinafter this chapter. In fact, each of the following chapters will contain a more detailed description of the methodology specific to each application, referring to this section where necessary.

2.1. Gravimetric system: HYDRA Dual Sampler

The Low Volume Gravimetric PMx sampler used during this work was an HYDRA Dual Sampler (FAI Instruments s.r.l.) system: a sampling system for atmospheric particulate matter collection on filter membranes (either teflon or quartz, 47 mm diameter) with two independent sampling lines (figure 2.1). The system is fully automated and allows the management of particulate matter sampling according to the time specifications defined during the sampling setup. Once blank filters are loaded into the container, the instrument automatically manages their loading, PMx accumulation and unloading of the sampled filter for recovery by the operators.

Figure 2.1. HYDRA Dual Sampler system. On the right the HYDRA system with a cabinet for outdoor applications.

The device is designed to work with an operating flow rate in the range 0.8 – 2.5 m^3/h, with a relative uncertainty of 2% of the measured value and a reproducibility of 1% of the measured value. The flow rate is controlled automatically and regulated by a valve moved by a step motor with a relative precision of about 1% of the set nominal value. The airflow is regulated by two pump units, located downstream of the sampler unit, which draw air from the environment through the sampling heads, the sampling lines and the two filter membranes. Automatic flow rate adjustment is conducted independently on the two sampling lines. The instrument is equipped with an external air compressor (200–300 kPa) necessary to manage the movements of the servomechanisms that control the loading and unloading of the filters. The sampling method adopted by the HYDRA Dual Sampler complies with the European technical standard EN 12341 "*Ambient air - Standard gravimetric measurement method for the determination of the PM_{10} or $PM_{2.5}$ mass concentration of suspended particulate matter*". Additionally, the device is equipped with PM_{10} Low Volume sampling heads (model LVS-PM10, FAI Instruments) designed in compliance with the sampling requirements set out by the Italian Ministerial Decree no. 60 of 2 April 2002 "*Procedure operative ai fini della certificazione di equivalenza*

dei metodi e dei sistemi per il campionamento e la misura del PM_{10} da parte dei laboratori primari di riferimento". Given these specifications, the HYDRA Dual Sampler instrumentation can be defined as a reference PMx monitoring system. For compliance with regulations, the sampler must be employed at a specific constant airflow (2.3 m^3/h), over a nominal sampling period of 24 hours. In addition, the instrument must provide specific environmental and instrumental parameters, including ambient temperature and pressure, total sampled volume and pressure drop at the filter membrane.

When employed for applications relevant to this work, the HYDRA Dual Sampler was equipped with low-volume sampling heads for PM_{10} and $PM_{2.5}$ in compliance with EN 12341 and EN 14907. This sampling heads are based on the principle of inertial classification, where particles with inertia under a specific threshold value (corresponding to a specific equivalent aerodynamic diameter) follow the airflow and are sampled on the filter, whereas particles with sufficient inertia can escape the flow and are captured on the impaction plate (figure 2.2).

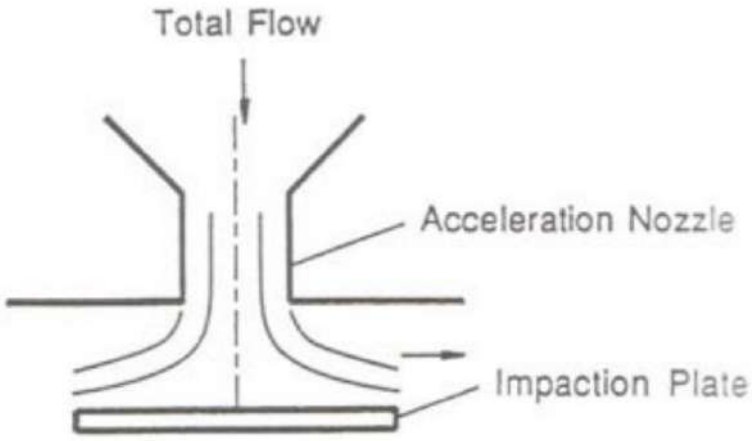

Figure 2.2. Schematics of an inertial classifier.

The inertial impactor must be designed to allow sampling in a wide range of environmental conditions, protecting the filter from rain, insects and other foreign objects from entering the system, thus compromising the representativeness of the sampled PM fraction. Additionally, the temperature of the sampling lines must not exceed the ambient temperature by 5°C and no obstructions or flow impairments must be present, in order to prevent losses on the PM sample.

In all the activities reported in this work where a gravimetric PM measure was applied, the HYDRA Dual Sampler was equipped with standard EU low-volume sampling heads for PM_{10} and $PM_{2.5}$, compliant with the EN 12341 and EN 14907 standards respectively. Each measure was conducted with a constant flow of 2.3 m^3/h over a sampling period of 24 hours. To ensure compliance with the European standard and an accurate mass quantification, sampled filter weighing was conducted, after conditioning for 48 hours in a desiccator, in a room with controlled environmental conditions.

2.2. Optical particle counters

2.2.1. Environmental Dust Monitor – model 1.107

The Environmental Dust Monitor model 1.107 (GRIMM Aerosol Technik GmbH) is a compact and portable aerosol spectrometer, generally defined as optical particle counter (OPC), built for real-time assessment of airborne atmospheric particles and their size distribution (figure 2.3). To simplify further discussions, throughout this document the device will be referred to as OPC Grimm. The device measures the numeric particle size distribution (unit particles/litre) in the range 0.25 - 32 μm. Additionally, the device is designed to classify the sampled particles into 32 separate size channels (unit particles/litre), thus providing an accurate deternibation of the particle size distribution in terms of equivalent optical particle diameter (Howell et al., 2006). Through a specific calculation algorithm, the instrument also reports the particle mass concentration, expressed as $\mu g/m^3$, in the three main PM fractions, namely PM_{10}, $PM_{2.5}$ and PM_1. The standardized dust mass fractions in terms of occupational health (respirable, thoracic and alveolic) according to EN 481, are also reported. To ensure an accurate and reproducible particle concentration assessment, the OPC Grimm operates with a constant and stable airflow set at 1.2 litre/minutes. Data can be reported at different time resolutions, from a minimum of 6 seconds to a maximum of 60 minutes. Thus, the Grimm OPC is an excellent tool for real-time particulate matter measurement in various environments and contexts where high temporal resolution is required, enabling short-lived emission events to be detected. Finally, the instrument is equipped with a sensor for monitoring

ambient parameters such as relative humidity, temperature and pressure, necessary for subsequent data analysis.

Figure 2.3. The Environmental Dust Monitor model 1.107

The Environmental Dust Monitor detection principle is based on the light scattering phenomenon, as detailed in figure 10. Each device is equipped with a laser diode as a monochromatic light source, at a specific wavelength of 655 nm. As airborne particles are sampled, they are led directly in the measuring cell and focused aerodynamically in a way that statistically ensures only one particle in the measuring volume at a time. Particles are then hit by the laser source, perpendicular to the airflow, and the resulting scattered light is detected by a receiving mirror at an angle of 90° and focused onto a receiver diode (figure 2.5). The manufacturer explains that the 90° position of the mirror allows to minimize the influence of the refractive index of aerosol particles in the determination of particle size. The opening angle of the detector optics was selected to compensate for uncertainty of the scattering light intensity due to MIE scattering undulations caused by monochromatic illumination. This setup enables the detection of the particle size in distinct and sufficiently narrow dimensional classes. The number concentration outputted by the device results from the number of particles detected divided by the flow rate. The particle size is directly proportional to the intensity of the detected scattering light signal. However, the intensity of this

signal can be influenced by different factors, such as the particles' refractive index, shape, and orientation.

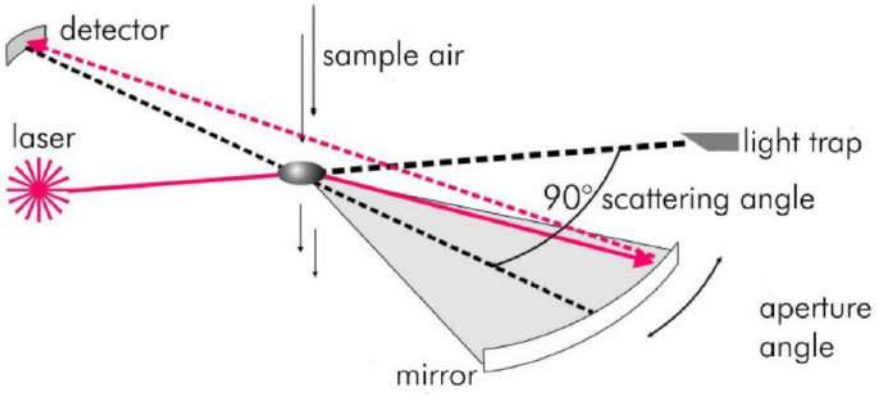

Figure 2.4. Measuring principle of the Environmental Dust Monitor model 1.107 as reported by the manufacturer.

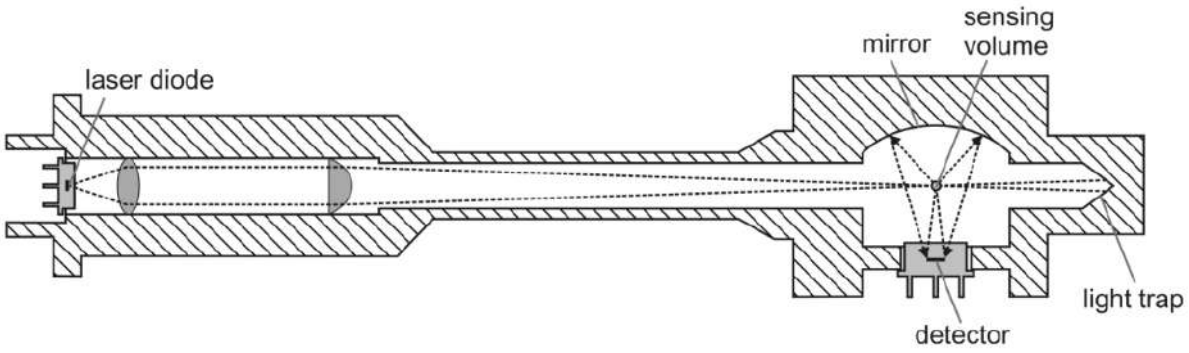

Figure 2.5. Schematics of the measuring chamber for the Environmental Dust Monitor model 1.107 as reported by the manufacturer.

Given these specifications, the OPC Grimm proves to be a useful tool in monitoring atmospheric PM, providing great accuracy and reproducibility in the measurements. As reported by Grimm & Eatough (2009), the device shows strong agreement with results obtained with a filter dynamic measurement system (FDMS) and tapered element oscillating microbalance (TEOM) monitors. Additionally, the conversion from number size distribution to mass size distribution was robust when compared with FDMS results, as highlighted by the authors.

Thanks to its ease of use, compact size, and ability to provide real-time measurements at high temporal resolutions, this instrument is a valuable tool for

monitoring indoor environments or mobile sampling, where the use of a gravimetric sampler would not be possible.

2.2.2. OPC-N3

The OPC-N3 (Alphasense) is a low-cost (~ 500€), small, and portable optical particle counter, developed for applications in highly polluted urban environments. The sensor provides a real time measure of particle number concentration and mass concentration, expressed as µg/m^3, in the three main PM fractions: PM_{10}, $PM_{2.5}$ and PM_1. While available at a slightly higher price than other low-cost sensors on the market, this device stands out for its ability to also provide accurate measurements of the particle size distribution, with 24 dimensional channels in the size range 0.35 – 40 µm.

Figure 2.6. Outer case of the OPC-N3 sensor.

The OPC-N3 operates through the same principle as traditional optical particle counters, measuring the scattered light from a monochromatic laser source (with a wavelength of 658 nm) after interaction with individual particles carried in the entering air stream. Particle number concentration can then be obtained, while particle size is calculated from the intensity of the scattered light based on the Mie scattering theory at the refractive index of polystyrene latex sphere. The PM mass concentration is calculated via an algorithm in compliance with the European Standard EN 481. To convert from number size distribution to mass

distribution, the sensor applies a default fixed particle density value of 1.65 g/cm^3 and an average refractive index (RI) of 1.5 + i0. These assumptions are made based on factory calibrations and testing and are suitable for most environmental applications. However, since it is well known that particle refractive index and density vary greatly depending on emission sources, environmental conditions and particle size, it is often necessary to set actual experimental density values within the algorithm in order to improve the accuracy of the sensor. To enable a more accurate estimate of PM concentrations, the OPC-N3 allows for different particle density values to be set for different dimensional channels. The device is also equipped with a temperature and relative humidity sensor. However, as this sensor is mounted directly on the PCB, the reported values are affected by heating of electronic components and thus do not represent the ambient conditions. The OPC-N3 manages the airflow by means of a small fan positioned on the opposite side to the inlet, which allows the sampled particles to pass directly into the measuring chamber. The device is then susceptible to sudden variations in the fan speed and to any obstruction to the inlet or fan outlet. To solve this issue, the OPC-N3 is equipped with a patent-pending correction algorithm capable of dynamically compensating moderate flow variations, thus ensuring stability in PM measurements.

Given its small size, ease of use, and ability to obtain a good estimate of PM concentrations and their size distributions at a lower cost, the OPC-N3 has seen a wide variety of applications. The scientific literature concerning this device shows good correlation with reference instruments, while highlighting the need for site-specific calibrations and correction factors. Sousan et al. (2021) evaluated the OPC-N3 in laboratory conditions comparing performance in environmental and occupational exposure, obtaining strong correlation with reference instrumentation, while highlighting differences between studied settings. Kaur & Kelly (2023) found strong correlation ($R^2 > 0.9$) for PM_{10} with FEM-monitors, during monitoring of dust events. DeSouza et al. (2023) employed the OPC-N3 during mobile monitoring in the urban area of Boston; after calibration with reference data, the proposed correction worked best for stationary measurements but showed limitations in correcting the data obtained from mobile monitoring. Dupont et al. (2025) managed to obtain strong correlation with reference devices

and good estimates of dust emission fluxes employing the OPC-N3, after correcting for variations due to ambient conditions. Nurowska et al. (2023) demonstrated the application of the OPC-N3 as a tool to monitor fog droplets. Schneiders et al. (2025) detailed the application of the OPC-N3 in Arctic regions, highlighting the significant aging and soiling of the sensor due to extreme events.

2.3. Purple Air Flex (and integrated OPC)

The Purple Air Flea air quality monitor (PurpleAir, Inc.) is a low-cost (~300$) real-time device developed for air quality assessment in indoor and outdoor environments. The Flex monitor was designed not strictly for scientific applications, but also for use by the general public. The device therefore features a compact design and a user-friendly interface.

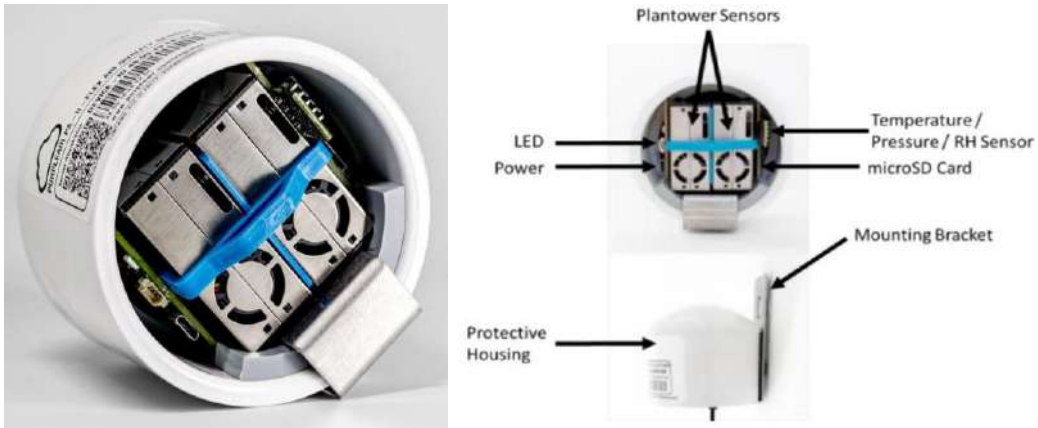

Figure 2.7. Purple Air Flex air quality monitor (left) and schematics of the device (right)

The Purple Air Flex monitor is equipped with two separate low-cost PM sensors (PMS-6003, Plantower Technology), working in tandem to provide duplicate PM measures to the device, thereby increasing the overall accuracy. The PMS-6003 is a low-cost optical particle counter, capable of providing an estimate of number particle concentration in the range 0.3 – 10 μm over five separate size channels (0.3, 0.5, 1.0, 2.5, 5.0 and 10 μm), with a counting efficiency of 50% at 0.3 μm and 98% at ≥0.5 μm. While these sensors can provide estimate of PM mass concentrations in the three main fractions (PM_{10}, $PM_{2.5}$ and PM_1), the device is marketed solely as a $PM_{2.5}$ monitor, as the manufacturer can guarantee a

reliable measure (maximum consistency error: ±10% at 100 to 500 µg/m³ and ±10 µg/m³ at 0 to 100µg/m³, as reported by the manufacturer) only for this fraction. Additionally, the Flex device is equipped with a sensor (BME688, Bosch) for monitoring environmental parameters (pressure, temperature and relative humidity) and atmospheric concentration of volatile organic compounds (VOC).

The device manages the measured environmental output both locally (via SD memory) and online via Wi-Fi connection. An online platform (figure 2.8), public and easily accessible via smart devices, allows remote access to the sensor data, providing a clear, real-time overview of PM concentrations and trends over time. This is a major advantage of the Purple Air devices, providing an excellent resource not only for the scientific community, but also for citizens concerned with air quality issues, promoting public knowledge and awareness of environmental topics.

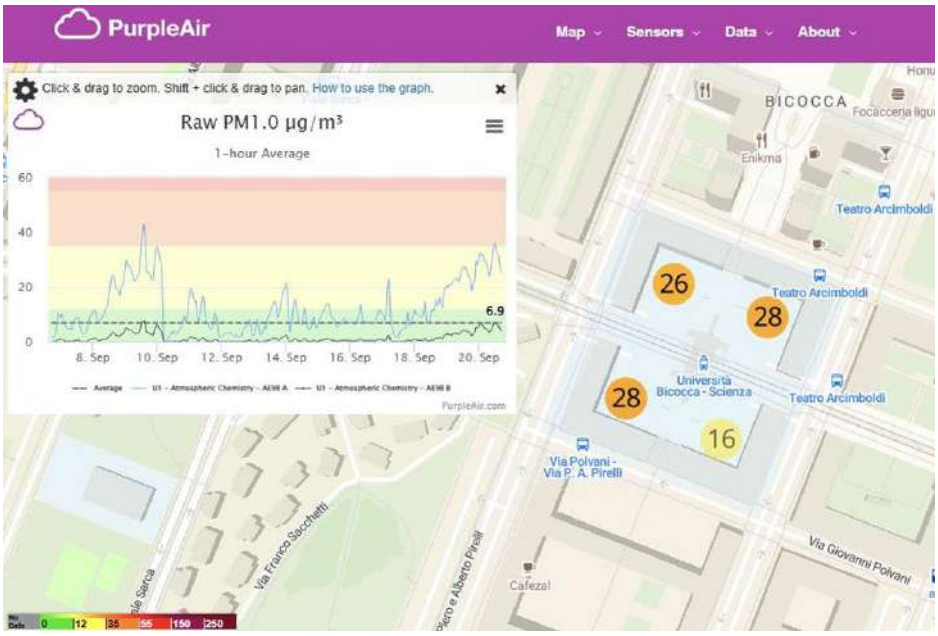

Figure 2.8. Online Purple Air platform for data visualization.

The Purple Air devices are now widely studied in the scientific literature regarding low-cost air quality sensors and are extensively evaluated in different environments and settings. The U.S. South Coast Air Quality Management District (AQMD) has evaluated the sensor correlation with reference instrumentation as part of their Air Quality Sensor Performance Evaluation Center (AQ-SPEC) program, in both laboratory and field conditions. The Purple

Air Flex monitor showed strong correlation (R^2 > 0.9) and precision when compared to FEM monitors for all PM fractions; field evaluation showed moderate to strong correlation for PM_1 and $PM_{2.5}$, while PM_{10} poorly correlated (R^2 = 0.2-0.4) with reference instrumentation. Numerous studies reported a strong correlation for $PM_{2.5}$ between the Purple Air and reference instrumentation, highlighting however a significant overestimation of concentrations and linking deviations to influence of aerosol properties and environmental conditions (Tryner et al., 2020; Stavroulas et al., 2020; Johnson et al., 2020; Heintzelman et al., 2023). Kaur & Kelly (2023) tested the PMS6003 sensor with monodisperse dioctyl sebacate particles, highlighting a limitation in detecting coarser particles, which were categorized in the lowest size bin. Ouimette et al. (2022) demonstrated how the PMS sensor employed inside Purple Air devices appears to behave as an imperfect reciprocal integrating nephelometer rather than an OPC, deriving PM concentration from a near-constant normalized number distribution converted from the scattering signal through an unknown algorithm.

Multiple studies developed correction factors for $PM_{2.5}$ Purple Air measurements, effectively improving the sensor agreement with reference monitors (Barkjohn et al., 2021; Barkjohn et al., 2022; Nilson et al., 2022). Wallace et al. (2022) developed a calibration factor for correcting $PM_{2.5}$ estimates after comparing 182 outdoor Purple Air monitors with 47 regulatory monitors in the U.S., showing good agreement after data correction. The derived correction factor (CF = 3.4) is now directly employed in the official Purple Air platform for data visualization and analysis.

2.4. Polludrone Pro (integrated multi-sensor monitoring station)

The Polludrone Pro (Oizom Instruments) is a multiparameter air quality monitoring system devised for environmental and industrial applications, capable of providing accurate, real-time measurements of various pollutants in the atmosphere. The device is designed for fixed and continuous monitoring over time, allowing for a proper evaluation of the overall air quality, as well as a

comprehensive assessment of environmental parameters such as noise, weather and radiation. While this device is not marketed as scientific-grade equipment designed for research, it is positioned as a mid-range tool above standard low-cost sensors thanks to the strong support of machine learning in the process of correcting and calibrating environmental data.

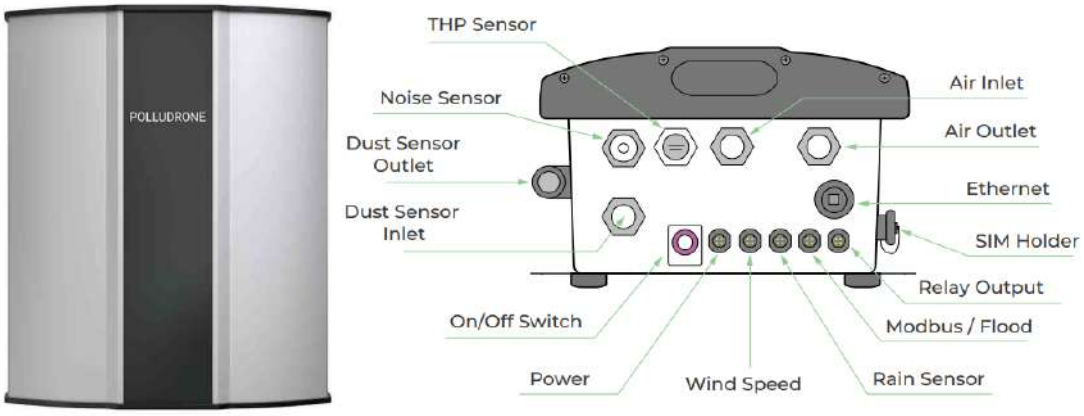

Figure 2.9. Outer case of the Polludrone system (left) and schematics of sensors' inlets (right), as reported by the manufacturer.

The device consists in a single, compact, and corrosion-proof case enclosing a wide array of low-cost sensors. The Polludrone device is equipped with a standard optical particle counter, based on the laser scattering principle, for assessment of PM concentration. This provides an estimate of the mass concentration of the main PM fractions, namely PM_{10}, $PM_{2.5}$ and PM_1. While the manufacturer does not provide the actual model of the optical counter installed in the unit, the sensor is able to measure airborne particles from a minimum detection limit of 1 $\mu g/m^3$ up to 5000 $\mu g/m^3$, with a resolution of 0.1 $\mu g/m^3$. The installed OPC is the set to sample with a flow rate of 1 litre/minute. Additionally, the device provides a measurement of total suspended particles (TSP) in the atmosphere, outputted as PM_{100}. The Polludrone monitoring unit features a wide array of NDIR, electrochemical, and semiconductor sensors for the assessment of gaseous pollutants, allowing a direct measure of carbon monoxide (CO), carbon dioxide (CO_2), nitrogen dioxide (NO_2), nitrogen monoxide (NO), ozone (O_3) and total volatile organic compounds (TVOC). Table 2.1 list the specifications of the mounted gas sensors.

Parameter	Range	Resolution	Minimum detection	Error / Drift	Working Principle
CO_2	0-5000 ppm	1 ppm	20 ppm	< ±5 ppm/yr	NDIR
CO	0-100 ppm	100 ppb	100 ppb	< ±100 ppb/yr	Electrochemical
NO_2	0-20 ppm	1 ppb	10 ppb	< ±20 ppb/yr	Electrochemical
NO	0-20 ppm	1 ppb	10 ppb	< ±50 ppb/yr	Electrochemical
O_3	0-20 ppm	1 ppb	10 ppb	< ±20 ppb/yr	Electrochemical
TVOC	0-20 ppm	1 ppb	5 ppb	N.A.	PID

Table 2.1. Specifications of the gas sensors mounted on the Polludrone, as detailed by the manufacturer.

To enable a comprehensive assessment of ambient conditions and complement air quality data, the device is designed to measure different environmental parameters, such as temperature, humidity, pressure, wind speed and direction, environmental noise, light intensity and UV radiation index.

To ensure the best accuracy in the output data, the device goes through three levels of calibration procedures, in factory, laboratory and ambient conditions, carried out by the manufacturer. Moreover, each device is equipped with an innovative and proprietary suction-and-exhaust system ("Micro Active Sampling", e-breathing technology) that manages air sampling to minimise the impact of external factors on measurement accuracy, leading to a 13% increase over industry standards. Furthermore, the output environmental data are readily accessible through the proprietary online platform (Envizom). This system allows for immediate and real-time data visualization and analysis, as well as the setup of automated operations and alerts.

As this device is relatively new on the market, the scientific literature regarding its application is still limited. Some studies saw the application of the Polludrone device in both environmental and occupational settings, successfully assessing targeted pollutants concentrations (Subramaniam et al., 2023; Shankar et al., 2023). Gulia et al. (2020) analyzed PM_{10} and $PM_{2.5}$ data of ten Polludrone unit in the city of Delhi (India) against a calibrated PM monitor (GRIMM) and found a similar trend with correlation coefficient (R^2) values of 0.73 and 0.85,

respectively. Kurtenbach et al. (2022) found the Polludrone device significantly overestimated PM concentrations when the relative humidity exceeded a value of 85% and derived a potential correction factor. Overall, the Polludrone monitoring system is an effective tool in monitoring atmospheric pollutants; however, there is still need for proper in-situ calibration to effectively assess real pollutant levels.

2.5. Milano Smart Park (integrated homemade multi-sensor monitoring unit)

The Milano Smart Park air quality monitoring unit (henceforth referred to as MSP), is a low-cost and do-it-yourself device for air quality monitoring, developed by the citizen-based initiative "Associazione Parco Segantini" e.t.s. (APS) in the urban area of Milan, Italy. The development of the device is aimed at raising awareness of urban environmental protection issues, while disseminating knowledge on the complexity of air pollution in order to adapt behaviour and protect health.

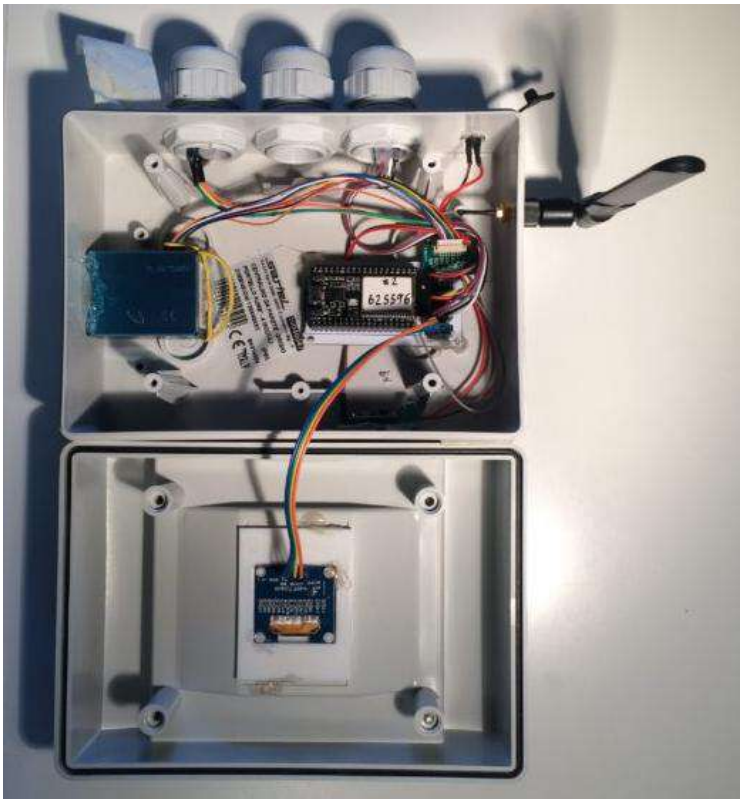

Figure 2.10. Milano Smart Park monitoring unit (milanosmartpark.it).

The device is equipped with a low-cost optical particle counter (PMS5003, Plantower Technology), working via the laser scattering principle, as already detailed in the previous sections. This sensor allows the detection of PM mass concentration in the range 0.3 - 10 μm, allowing the determination of three different size classes: PM_{10} ($d_{ae} \leq 10$ μm), $PM_{2.5}$ ($d_{ae} \leq 2.5$ μm) and PM_1 ($d_{ae} \leq 1$ μm). The MSP device also houses a multi-channel sensor (Grove – Multichannel Gas sensor) for measuring gaseous pollutants, based on the metal oxide semiconductor sensing unit MiCS-6814 (SGX Sensortech). This unit is comprised of three fully independent sensing elements: RED (reduction), OX (oxidation) and NH_3 (ammonia), whose combination allows for the measurement of a wide range of polluting gases, like carbon monoxide (CO), nitrogen dioxide (NO_2), ethanol (C_2H_6OH), hydrogen (H_2), ammonia (NH_3), methane (CH_4), propane (C_3H_8) and isobutane (C_4H_{10}). The sensor however, as stated by the manufacturer, is not able to determine the exact gas concentration, only reflects the approximate trend in concentration within a permissible error range. Additionally, the monitoring unit hosts a sensor (BME680, Bosch) for monitoring environmental parameters (pressure, temperature and relative humidity) and atmospheric concentration of volatile organic compounds (VOC). The MSP device operates by acquiring data every 30 minutes, storing both locally (via SD memory) and online through Wi-Fi connection. Data acquired by every MSP unit is publicly available on the Milano Smart Park Website (https://www.milanosmartpark.it/).

2.6. bcMeter

The bcMeter is a small, do-it-yourself, and low-cost (< 300€ for the total bill of materials) black carbon monitoring device, recently released as an open-source tool targeted at tackling the issue of black carbon concentrations in environmental and industrial fields. This device is based on the same principle as conventional aethalometers, where an LED light source in the infrared spectrum (880 nm) is targeted at the attenuation (referred to as ATN) of the radiation through a filter membrane after particle deposition. From the data obtained, the sensor can extrapolate the atmospheric BC concentration, employing standard

equations already established in the scientific community, as outlined by Ferrero et al. (2024). The device consists in a 3D-printed outer housing, which houses an LED source, the filter compartment, an airflow controller, a small 5V pump, and a PCB for software management, as shown in figure 2.11.

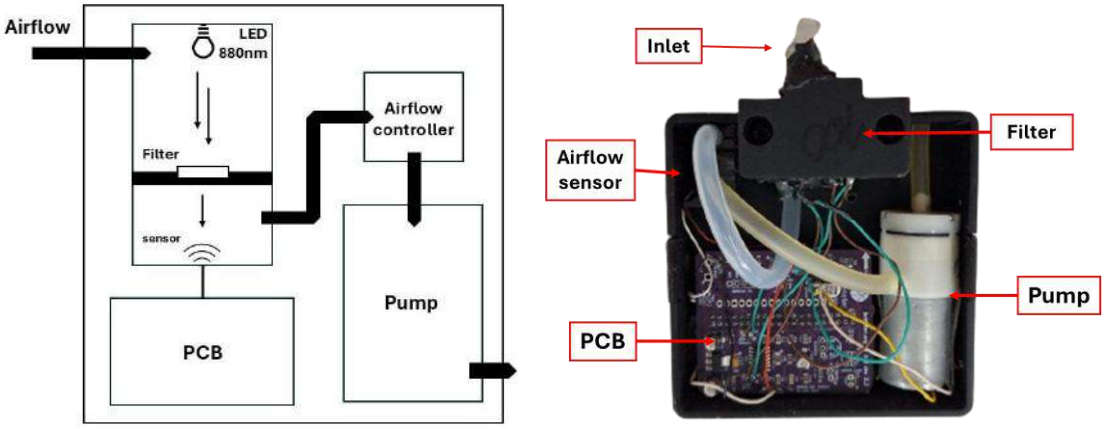

Figure 2.11. Schematic of the bcMeter (left) and sensor with top case removed, with main components highlighted (right), as reported by Doldi et al., (2025).

The airflow controller allows the device to work at a constant airflow, which can be modified by the user. The main difference between the bcMeter and traditional aethalometers is the management of the filter loading effect. The continuous accumulation of particles on the filter membrane can lead to a change in the sensor's sensitivity. As detailed by Virkkula et al. (2007), this can result in two main effects on the determination of BC mass concentration: as the ATN value increases the BC concentration is underestimated; on the other hand, scattering of aerosol can lead to an overestimation of BC. Traditional research-grade aethalometers solve this issue by sampling on two different spots at different flow rates, correcting for the filter loading effect via specific algorithms. Due to technical constraints and cost-effectiveness, the bcMeter is limited to sampling on a single spot. For the same reason, while standard aethalometers are usually equipped with a self-advancing filter tape, the bcMeter can allocate a single filter at a time that needs to be manually changed once the ATN threshold is reached.

2.7. Nanoscan SMPS Model 3910

The Nanoscan SMPS (Scanning Mobility Particle Sizer) model 3910 (TSI Instruments Ltd.) is a portable instrument aimed at measuring atmospheric nanoparticles concentration (as particles/cm^3) and size distribution, mainly designed to for air quality assessment in indoor/outdoor environments and workplace exposure monitoring. The Nanoscan SMPS consists of two main units for particle monitoring: a patented Radial Differential Mobility Analyzer (RDMA), allowing for particle size classification, and a Condensation Particle Counter (CPC), an optical detector for nanoparticle counting. The device operates in a dimensional range from 10 up to 420 nm, in 13 size channels. The Nanoscan SMPS is able to detect nanoparticle concentrations from 100 to a maximum of 10^6 particles/cm^3. While the time resolution for particle concentration is 1 second, size distribution on atmospheric nanoparticles is outputted at a maximum resolution of 1 minute.

Figure 2.12. The Nanoscan SMPS model 3910, TSI.

The detection of particles is carried out by the instrument in four main components: a cyclon, the patented unipolar charger, the patented compact Radial Differential Mobility Analyzer (RDMA) and a condensation particle counter (CPC), as detailed in figure 2.13. After sampling, larger particles are removed by the cyclone with a cutoff diameter of 550 nm. Then an inlet conditioner removes large particles with multiple charges per particle, as these

can result in an inaccurate measure. Afterwards, the sampled particles are moved through a unipolar charger and collide with a stream of unipolar ions. This collision improves the mixing of the sampled particles ensuring that most of them reach a consistent charge state within the time spent inside the mixing chamber. Then the flow of charged particles passes through the compact Radial Differential Mobility Analyzer (RDMA). This component consists of an upper ground plate and a lower negative voltage plate, generating an electric field. Particles subjected to this electric field and to a drag force from an opposite airflow show different electrical mobility (equated using Stokes' law) allowing for size classification (figure 2.14). The size-classified aerosol exits through a monodisperse outlet and are directed to an internal Condensation Particle Counter (CPC), where the particles are increased in size by condensation of a supersaturated vapor (isopropyl alcohol, IPA), allowing detection by a laser detector.

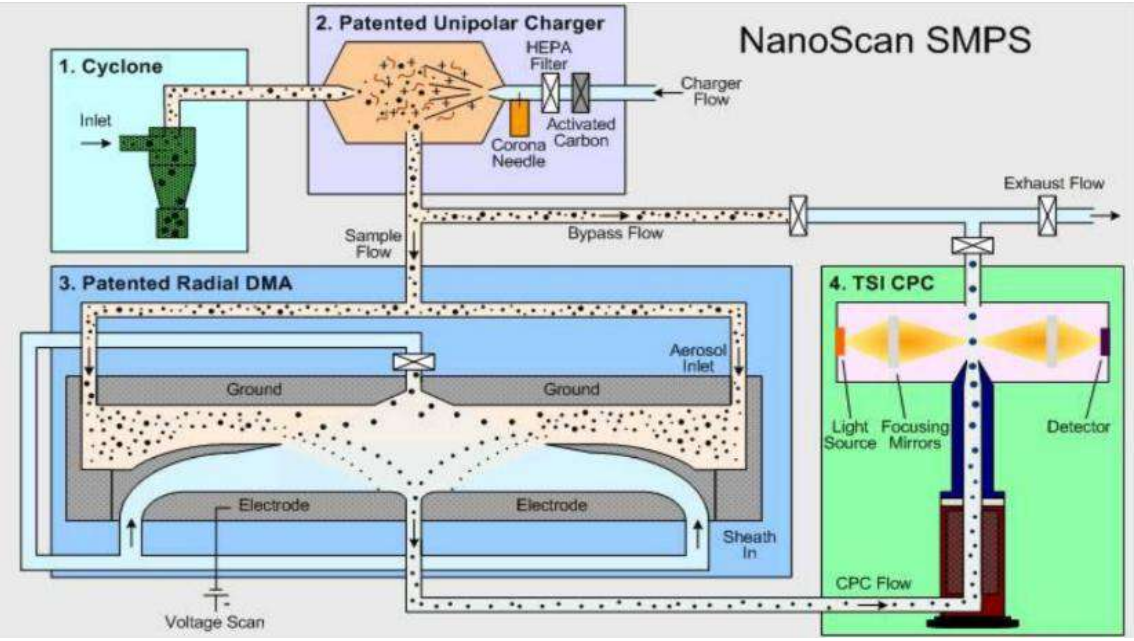

Figure 2.13. Schematics and main components of the Nanoscan SMPS. Source: TSI.

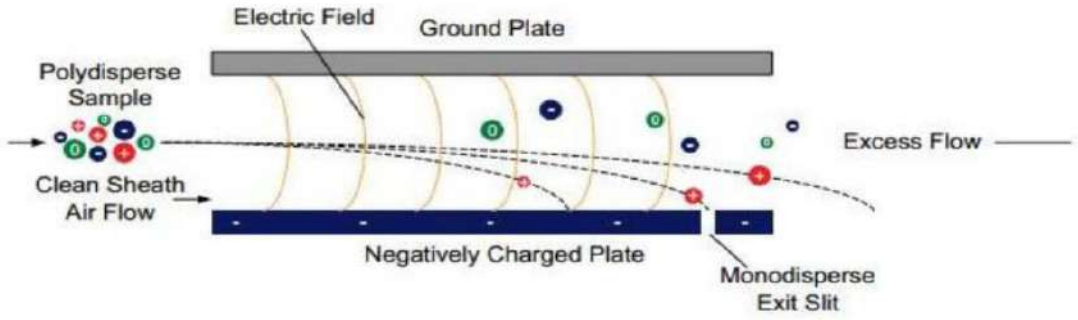

Figure 2.14. Schematics and working principle of the patented Radial Differential Mobility Analyzer. Source: TSI.

As detailed by Tritscher et al. (2013), the Nanoscan SMPS proved to be a reliable tool for assessing nanoparticle concentrations and size distribution, showing good correlation with reference SMPS systems and concentration linearity up to 10^6 particles/cm^3 with reference CPCs. Given its compact size, portability and easiness-of-use, the device can be an ideal solution for environmental applications in contexts where the use of bigger and not battery supplied reference instrumentation is impractical.

2.8. Aerosol Dosimeter Partector-2

The Partector-2 (naneos particle solutions gmbh) is a small, hand-held aerosol dosimeter specifically designed for the assessment of personal exposure to airborne nanoparticles in occupational environments and ambient air. The device allows for real-time measurements (1 second time resolution) of nanoparticle number concentration up to 10^6 particles/cm^3, in the range from 10 – 300 nm. Additionally, the Partector-2 is able to measure the average particle diameter and total surface area of sampled particles, as well as the lung deposited surface area (LDSA). LDSA is a crucial indicator of nanoparticle exposure at lung level, quantifying the total surface area of inhaled particles able to reach the alveolar region. As nanoparticles are thus able to diffuse into the bloodstream, and therefore causing adverse effects even to extrapulmonary systems, as described in chapter 1, LDSA emerges as a key parameter for safeguarding human health. The Partector-2 is set to detect LDSA in the range 0 – $1.2 \cdot 10^4$ μm^2/cm^3.

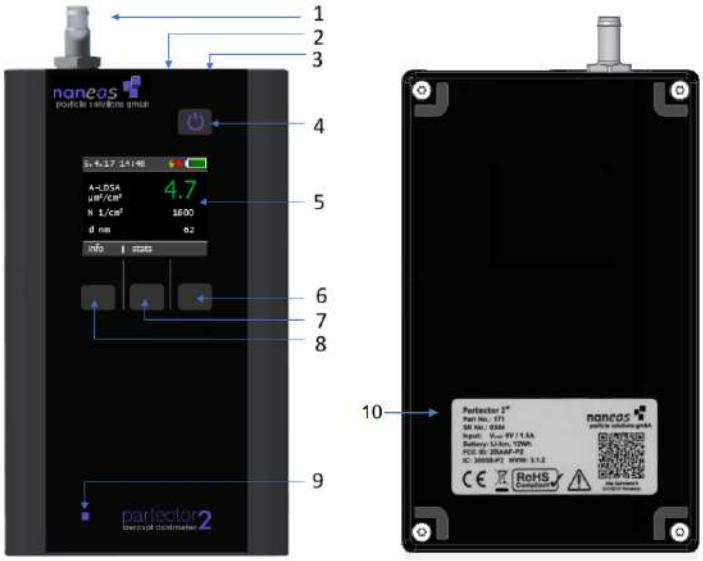

Figure 2.15. Partector-2 device.

The air inlet, located at the top of the instrument, is regulated by an internal pump that sets a constant flow rate of approximately 0.5 litre/minute. Additionally, the device is equipped with integrated sensors for measuring environmental parameters such as relative humidity, pressure, and internal temperature, essential for ensuring performance within the recommended operational limits (0-40 °C, 10-90% RH). The Partector-2 is a device that offers an innovative method for particle counting. The working principle of the Partector-2 is similar to that of conventional diffusion chargers (DC), already widely used in the development of aerosol measuring instrumentation, with the main difference being the absence of a particle filter to capture particles and measure the deposited current. The Partector devices apply a novel technique based on induced currents (figure 2.16), as detailed by Fierz et al. (2014) and Fierz et al. (2015).

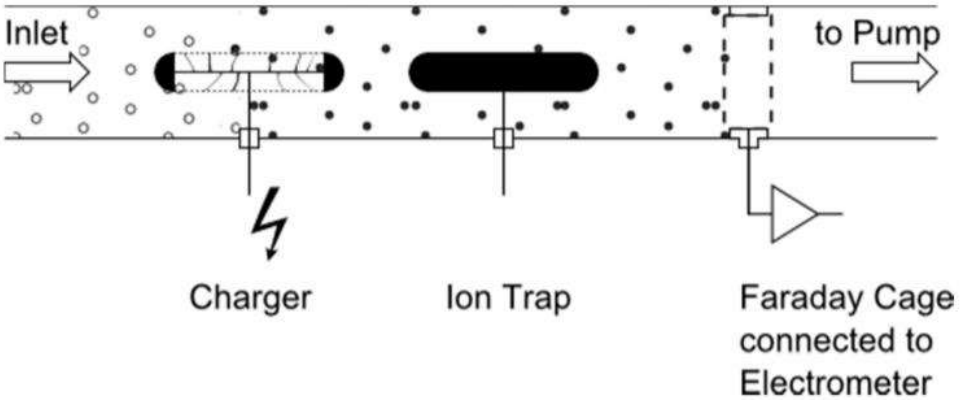

Figure 2.16. Scheme of an induced current detector, as described by Fierz et al. (2015).

In the Partector-2, a grounded Faraday cage (that prevents any electric field lines from escaping) replaces the particle filter stage. Then, the device measures the current flowing to or from the cage as time derivative of the charge (dQ/dt). In order to maintain a detectable signal, as a constant charge in the cage cannot be measured this way, the charge must undergo temporal variation. Thus, the measurement is obtained by pulsing the unipolar charger (frequency of 0.5 Hz), which enables an oscillating signal to be detected at the electrometer. The amplitude of the obtained signal is proportional to the charge transferred to the aerosol. The applied method is also more robust than traditional DC, reducing the zero-offset drifting over time or due to changes in the environmental conditions, removing the need for warm-up time or zeroing procedures.

2.9. AC32M - Chemiluminescent Nitrogen Oxides Analyzer

The AC32M (Environnement S.A.) analyzer is designed to monitor low nitrogen oxides (NO_2 and NO) concentrations (in the range 0 – 50 ppm) in ambient air. The device operates according to the principle of chemiluminescence, measuring radiation emitted by nitrogen monoxide (NO) in the presence of high concentrations of ozone molecules with strong oxidizing capacity. Outdoor air is sampled by means of an external pump through a Teflon tube (d = 6 mm) associated with a dust filter to prevent atmospheric particles from entering the system. The sampled air is directed inside three main units necessary for the

measurement: the pre-reaction chamber, the reaction chamber, and a converter. The converter consists of a thermally isolated molybdenum oven, with a controlled temperature equal to 340°C. An enclosure containing a photomultiplier, the radiation detector, is adjacent to the reaction chamber separated by an optical filter.

Figure 2.17. AC32M analyzer

Chemiluminescence is obtained through oxidation of nitrogen monoxide (NO) by ozone (O_3):

$$NO + O_3 \rightarrow NO_2^* + O_2 \quad (15)$$

The excited NO_2* molecules produced can then return to the fundamental electronic state by emitting radiation with wavelength in the range 600-1200 nm:

$$NO_2^* \rightarrow NO_2 + h\nu \quad (16)$$

Part of the energy can be lost by quenching, the interaction with other molecules present in the sampled air. As this can influence the accuracy of the measurement, this phenomenon is prevented by reducing the pressure inside the reaction chamber thus lowering the quenching probability. To remove interferences due to hydrocarbons, an optical filter removes radiation with a wavelength greater than 610 nm. Finally, a photomultiplier detects and converts the signal into the concentration output. As nitrogen dioxide (NO_2) cannot be measured this way, it must be reduced to NO by a molybdenum oven:

$$2NO_2 + Mo \rightarrow 2NO + O_2 \quad (17)$$

The measuring procedure is thus comprised of three mains steps, referred to as *reference cycle*, *NO cycle* and *NOX cycle*. During the *reference cycle*, the sampled air is directed into a pre-reaction chamber, where the photomultiplier acquires a signal without chemiluminescence, considered as zero reference. Afterwards, the sample is directed into the measurement chamber, where it undergoes the reactions described in equations 15 and 16 (*NO cycle*). Ozone in the measurement chamber is generated by a discharge ozone generator. Finally, the acquired signal is proportional to the number of NO molecules in the air sample. Finally, the sample goes through the molybdenum oven, where all NO_2 is reduced to NO (eq. 17); then, it goes through a second cycle of oxidation by ozone (*NOX cycle*). During this final cycle, the measured signal is proportional to the total number of NO and NO_2 in the sample.

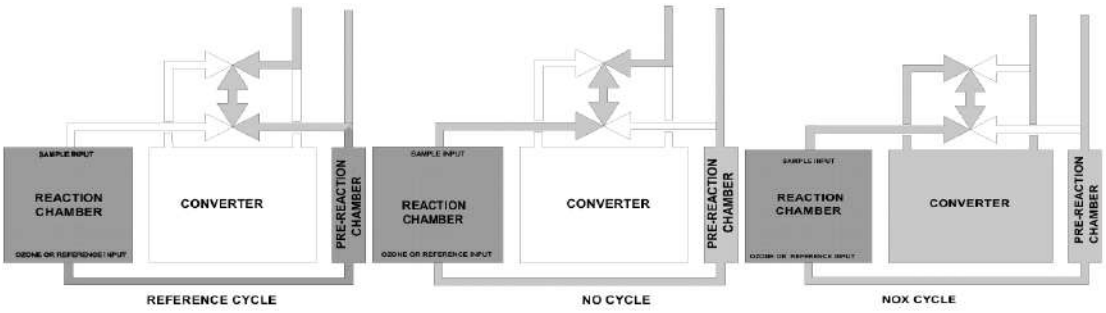

Figure 2.18. Schematics of the main component in the AC32M analyzer and main detection cycles. Source Environnement S.A.

3. MUSA Open-air laboratory: low-cost sensors as a tool for air quality monitoring during urban regeneration activities

3.1. Introduction

As already extensively detailed in chapter 1, air pollution poses a significant risk to human health, to the entire ecosystem and environment, as well as to materials of anthropogenic origin. These impacts are obviously more severe in areas where human impact is greater. These environments include urban areas, which are characterized by higher population density and the presence of major sources of emissions, such as road traffic, industrial processes, biomass burning and agricultural production. As over 90% of the global population lives in areas with air pollutant concentrations higher than suggested guidelines (WHO, 2021), this poses a major health risk. Thus, air pollution control has become increasingly crucial in most urban areas aiming to safeguard the health and well-being of citizens. To tackle this issue, most cities are now employing a comprehensive approach in the design of urban spaces which focuses not only on environmental concerns, but also on addressing social and economic inequalities. For this reason, the principle of urban regeneration is now one of the main drivers of development in most cities, facing urbanization as an opportunity to drive sustainability and citizen-based decisions (Opoku & Akotia, 2020). Atmospheric pollutant control has therefore become one of the key aspects of urban regeneration projects, aiming to improve public health and mitigate climate change effects. To achieve this, large-scale monitoring of pollutants at high temporal resolutions is required. An emerging trend is this application to see the rise of smart and low-cost technologies that can provide real-time air quality data, enabling a rapid response and swift implementation of adaptive strategies (Nazari, 2025). While traditional instrumentation employed in air quality monitoring often limits spatial and temporal resolution of data due to the high cost required, low-cost sensors are proving to be a valuable asset for complementing conventional measurements, increasing real-time data coverage across the territory and thus promoting the implementation of effective control strategies (Kumar et al., 2015).

In the urban area of Milan, this concept was introduced by the MUSA (Multilayered Urban Sustainability Action) ecosystem, in an effort to bring together universities, research institutions and public and private entities towards a replicable model aimed at sustainability and citizen's well-being. Acting through one of its main branches (Spoke 1 – Urban), the ecosystem conducted a major urban regeneration effort at the University of Milano-Bicocca, renewing the architectural context of the university science campus of *Piazza della Scienza*. While the urban redevelopment of the area brought better living spaces and green areas for the community, technological innovations and energy savings, the newly renewed square acted also as a fertile ground for scientific research, involving researchers and students of diverse scientific fields in the decision-making process, monitoring and pursuit of new strategies for sustainable development. As the project demanded air quality monitoring during each phase of the urban regeneration effort, this work covered monitoring activities of both outdoor and indoor spaces involved. To effectively carry out the environmental monitoring of spaces, while taking into account the state of the art and technological innovations in the field of air quality assessment in urban regeneration contexts, this work employed different low-cost sensors available on the market for monitoring of pollutants during the pre-construction, construction and post-construction phases of *Piazza della Scienza*. These sensors, along with research-grade instrumentation, were employed for mobile monitoring of particle concentrations, such as PM mass concentration and nanoparticles number concentrations, during the three redevelopment phases of the square. The activities carried out during the work phase mainly involved removing the previous flooring (dry-laid mineral slabs on sand and gravel), excavation of soil and excess materials, laying of insulation layer, installation of new flooring, and planting of new green areas. To properly assess the particle emission related to these processes, PM and nanoparticles concentrations were monitored during the entire construction process, allowing for the quantification of the whole construction site impact on air quality. The post-work phase involved monitoring particle concentrations after completion of the work, following the inauguration of the square. The renovated spaces mainly saw an increase in green space, with the addition of flower beds and trees; in addition, the entire walkable surface was

modified with the new paving and walkable areas. PM and nanoparticles concentrations were assessed through the same methodology and experimental setup applied for the pre-construction and construction phases. This allowed a comprehensive evaluation of the overall impact of the urban regeneration plan enacted in *Piazza della Scienza* in terms of particle emission.

Finally, as the MUSA ecosystem envisioned a long-term monitoring of air quality in the square towards students' and workers' well-being, low-cost sensors were installed in fixed positions throughout the outdoor spaces. A multiparametric unit (OIZOM Polludrone) for monitoring of PM and gaseous pollutants, and four low-cost PM sensors (Purple Air Flex) were installed in the four corners of the square, ensuring continuous and permanent monitoring of pollutants in the environment, while also serving as a source of air quality information and awareness among users of university spaces. To ensure greater data accuracy, the deployed sensors were evaluated against reference data, assessing their overall performance, highlighting their limitations and computing a correction algorithm.

This chapter will focus on detailing each part of the monitoring activities conducted under the MUSA urban regeneration plan in *Piazza della Scienza*. To achieve a more accurate measurement of PM concentrations, the low-cost OPC-N3 (Alphasense) sensors were first corrected by applying density-based correction factors, derived by calculating apparent density values based on experimental data from comparison with the reference OPC Grimm. Furthermore, an environmental analysis of the urban regeneration work on the square will be carried out by first estimating the impact in terms of particle emissions resulting from the construction site and working activities, and then evaluating the entire urban regeneration project, assessing how the interventions carried out may affect the air quality of the square. The final section of this chapter will focus on the first evaluation of data acquired from the recently installed sensors in fixed positions in the renovated outdoor environments of *Piazza della Scienza*.

3.2. Materials and methods

3.2.1. Mobile monitoring

To evaluate the entire urban regeneration project for *Piazza della Scienza* proposed by the MUSA ecosystem in terms of air quality, three sampling campaigns were carried out: one campaign prior to the start of construction (hereinafter referred to as the *pre-construction phase*), which served as a baseline following data analysis; one campaign during construction (referred to as the *construction phase*); and finally a monitoring campaign carried out at the end of the project and after the official inauguration of the square to the public (referred to as *post-construction phase*). A fixed route (adapting to construction site closures as far as possible), common to each campaign, was established selecting eleven sampling locations throughout the outdoor and indoor environments of the university science campus of *Piazza della Scienza* (figure 3.1). Four outdoor points were selected near the access ramps to the underground parking lots of each building (U1, U2, U3, and U4), one for each corner of the square. Four indoor points were selected in the classroom corridors on the basement floor of each building. An additional indoor sampling location was selected in the central corridor that connects all four main buildings that presents mixed characteristics of both indoor and outdoor environments. Finally, the Atmospheric Chemistry laboratory (Piazza della Scienza, Building U1, third floor) acted as the starting and end point of each measurement.

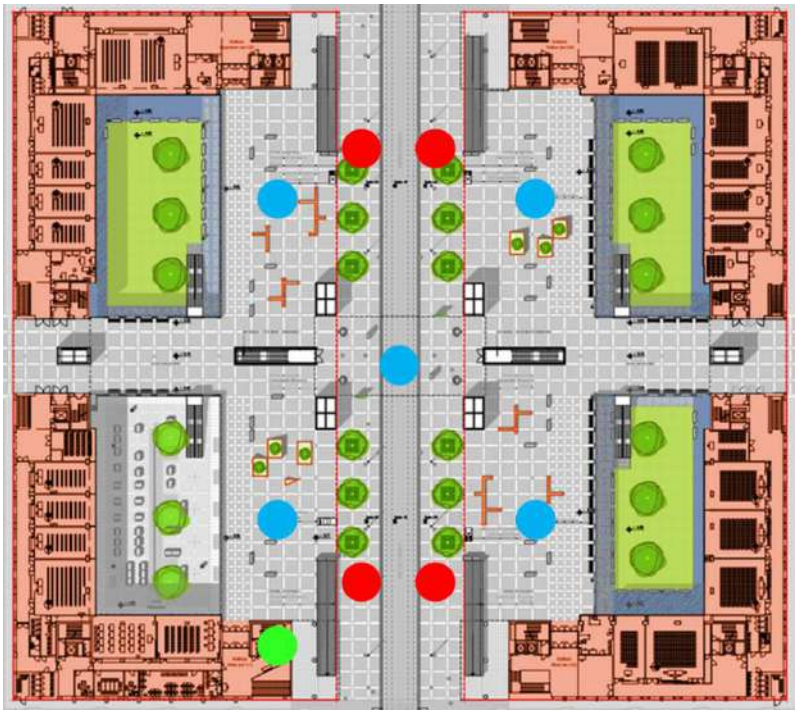

Figure 3.1. Map of the Bicocca campus in Piazza della Scienza and related sampling points. Outdoor environments in red, indoor environments in blue, in green the atmospheric chemistry laboratory, reference point (start and end) for each measurement.

The square's air quality was evaluated in terms of particle concentration, monitoring particulate matter (PM) mass concentrations as well as nanoparticles number concentration. Monitoring was carried out by combining portable scientific-grade sensors and low-cost sensors. PM mass concentration was determined by employing an optical particle counter, specifically an Environmental Dust Monitor (GRIMM), coupled with its low-cost counterpart comprising four OPC-N3 (Alphasense) devices. The selection of these instruments was driven by the necessity to obtain an estimate of the mass of PM in the three primary fractions (PM_{10}, $PM_{2.5}$, PM_1) as well as their size distribution. Nanoparticles concentrations and size distribution were acquired through the employment of a Nanoscan SMPS (TSI), coupled with the portable Partector-2 (Naneos). The detailed technical specifications of each instrument used are extensively described in Chapter 2. All instruments were mounted on a cart for easier movement between the sampling locations (figure 3.2), sampling for five minutes in each location. A single measurement consisted in monitoring each of

the indoor and outdoor environments one at a time moving through a fixed route. Each single measurement was conducted between one and two times a day at fixed times, at 12:00 and 15:00. The time slots were selected to ensure the least amount of external influence due to the presence of large numbers of students in the areas studied, which could have affected the results.

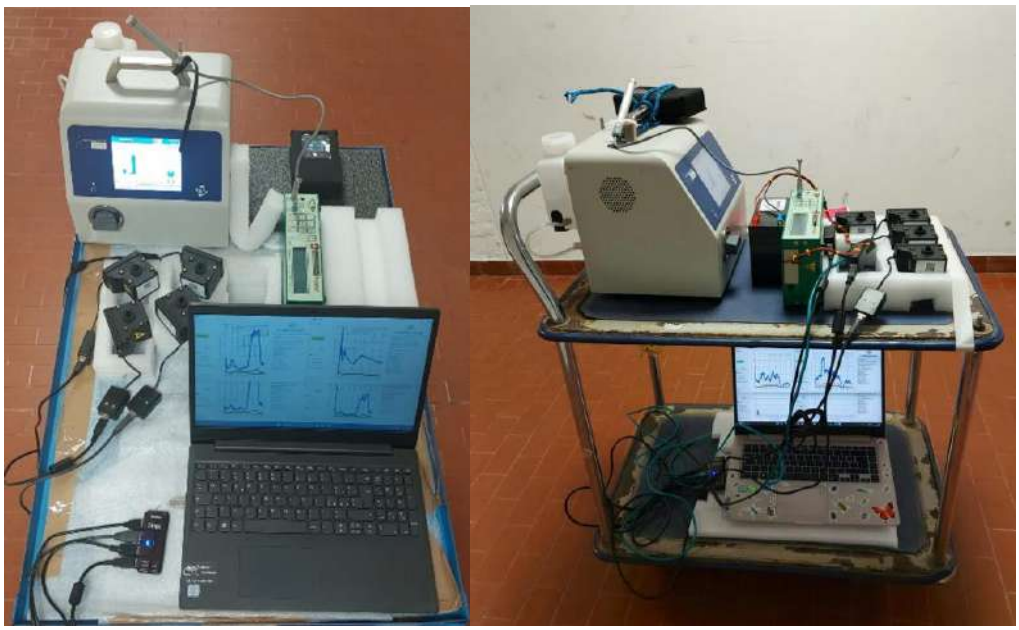

Figure 3.2. Instrument setup for air quality monitoring on the campus.

The sampling campaign for the pre-construction phase was conducted during the month of May 2023 and consisted of 16 sampling rounds. As previously mentioned, data collection during pre-construction was mainly aimed at identifying the environmental conditions prior to the urban regeneration effort, to act as a baseline for subsequent analysis. The sampling campaign for the construction phase was conducted from the month of July 2023, start of construction works in the square, until December 2023, for a total of 12 sampling rounds. The selection of sampling timeframes for the construction phase was subjected to certain technical and practical requirements: on the one hand, monitoring was subject to the time and space constraints imposed by the construction site, where access was limited for safety reasons; on the other hand, the progress of the work on the square was heterogeneous, with different types of interventions overlapping at different points in Piazza della Scienza. For this reason, this work features an overall evaluation of the construction site, not

referring to individual operations as it was not possible to match the data collected to the individual activities carried out by the workers. The sampling campaign for the post-construction phase was conducted from July 2025 up until October 2025, for a total of 13 sampling rounds. Pollutant monitoring at this phase was carried out once all work on the square had been completed and the spaces had been opened to the public, in order to obtain a representative measurement of the renovated environments.

3.2.2. Fixed monitoring

Following completion of the construction work on *Piazza della Scienza*, air quality monitoring continued through the installation of sensors in fixed positions within the regenerated spaces of the square. The permanent installation of these instruments took place in February 2025, at the end of the scheduled construction work on the square and following the official inauguration and opening. Four Purple Air Flex monitors, one for each corner of the square, were installed in front of the entrance to the four buildings facing the square (figure 3.3). The sensors were mounted on poles at a height of approximately 4 meters above the ground, in order to ensure a good estimate of the concentrations in the square while also protecting the devices from external interferences. The installed Purple Air monitors allow this way a continuous and real-time evaluation of PM concentration in the square, with publicly available data through the Purple Air Real-Time Interactive map (https://map.purpleair.com/air-quality-standards-us-epa-aqi?opt=%2F1%2Flp%2Fa10%2Fp604800%2FcC0#17.17/45.513469/9.211707), ensuring that air quality data is easily accessible to the public. In one of the four corners of the square (in front of building U1), the multiparametric monitoring unit Polludrone (OIZOM) was also installed. This device allows continuous monitoring of PM concentrations, as well as an assessment of gaseous pollutants concentrations (CO, CO_2, NO_2, NO, O_3 and TVOC). Moreover, this air quality monitoring unit is equipped with sensors to monitor environmental parameters (temperature, humidity, pressure, wind speed and direction, environmental noise, light intensity and UV radiation index), which are essential for

contextualizing air quality data obtained in the correct environmental setting. A more in-depth description of these devices is reported in Chapter 2 of this work.

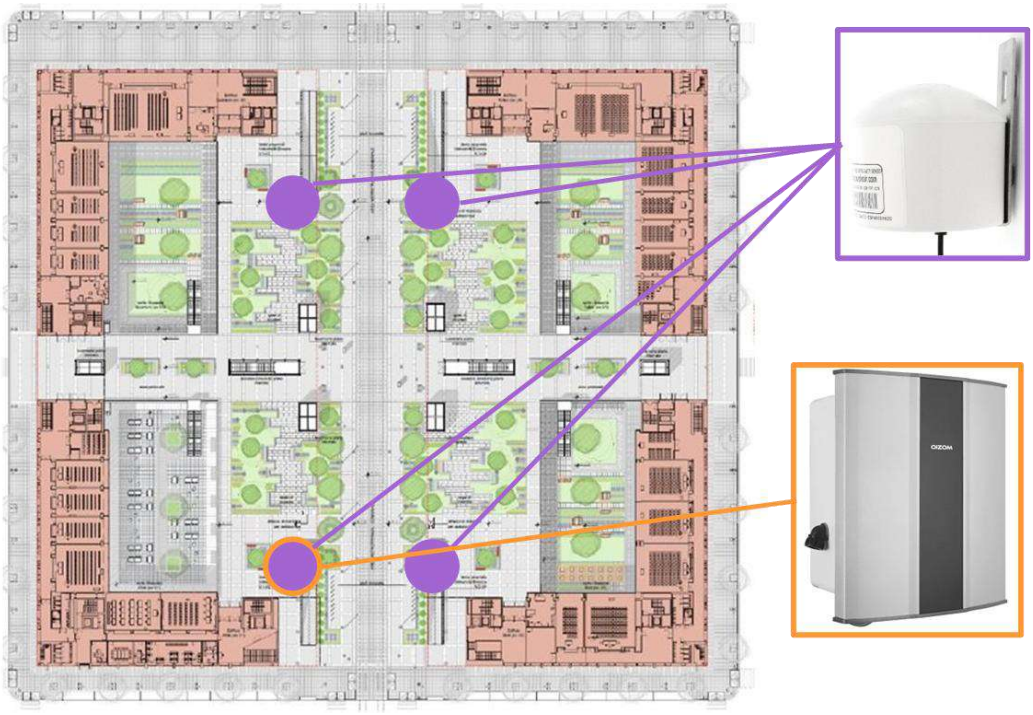

Figure 3.3. Layout of the renovated environments of Piazza della Scienza, with position of the installed sensors. In purple the four Purple Air devices, in orange the OIZOM Polludrone air quality monitoring unit.

3.3. Results

As previously stated, the monitoring activities carried out during the urban regeneration project for *Piazza della Scienza*, planned by the MUSA ecosystem, focused on the use of low-cost and smart air quality sensors. The instruments employed, the PMx monitor OPC-N3 and the Partector-2 (Naneos), were therefore an integral part of the monitoring activities. The sensors were utilized in all monitoring phases, coupled with reference sensors to allow for data comparison, ultimately leading to the assessment of the impact of the urban regeneration project of the square.

3.3.1. Performance analysis and calibration of low-cost and smart devices

The scientific literature, as reported in chapter 2 of this dissertation, concerning the low-cost OPC-N3 (Alphasense) and, in general, all low-cost devices employed in air quality research, agrees that this class of sensor provides less accuracy than reference and research-grade instrumentation, highlighting the need for site-specific comparison and calibration prior to any monitoring activity. During the monitoring of the *Piazza della Scienza* redevelopment project, the assessment of the impact of the construction site in terms of air quality was preceded by a comprehensive analysis of the performance of the instruments used and the derivation of specific correction factors. In this case, the calibration phase was not carried out prior to monitoring the activities in the square, but rather after all the data collection had been completed as the reference OPC Grimm 1.107 was concomitantly running. Low-cost, smart, and portable instruments were used alongside their scientific counterparts during all monitoring phases (pre-construction, construction and post-construction), thus allowing for a field comparison under very different environmental conditions and particle emission sources. Data obtained from the OPC-N3 during the first two phases of redevelopment (figure 3.4), namely pre-construction and construction, averaged for each of the sampling locations selected, highlighted how the device consistently underestimated PM concentrations.

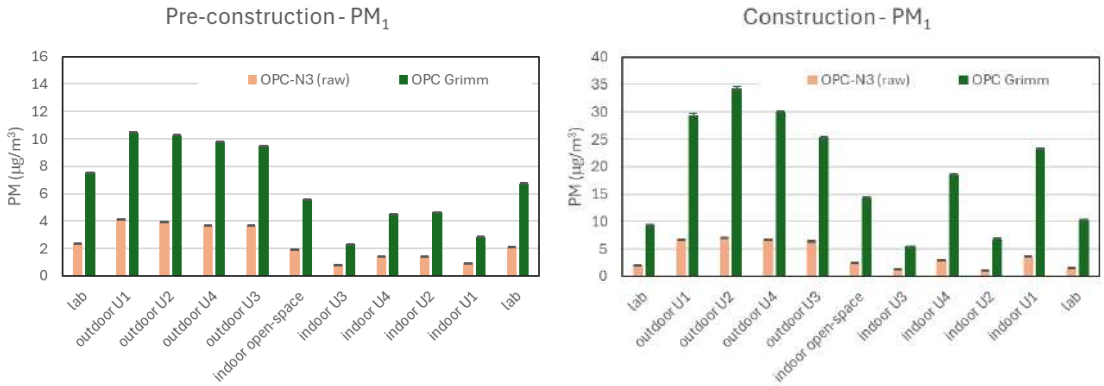

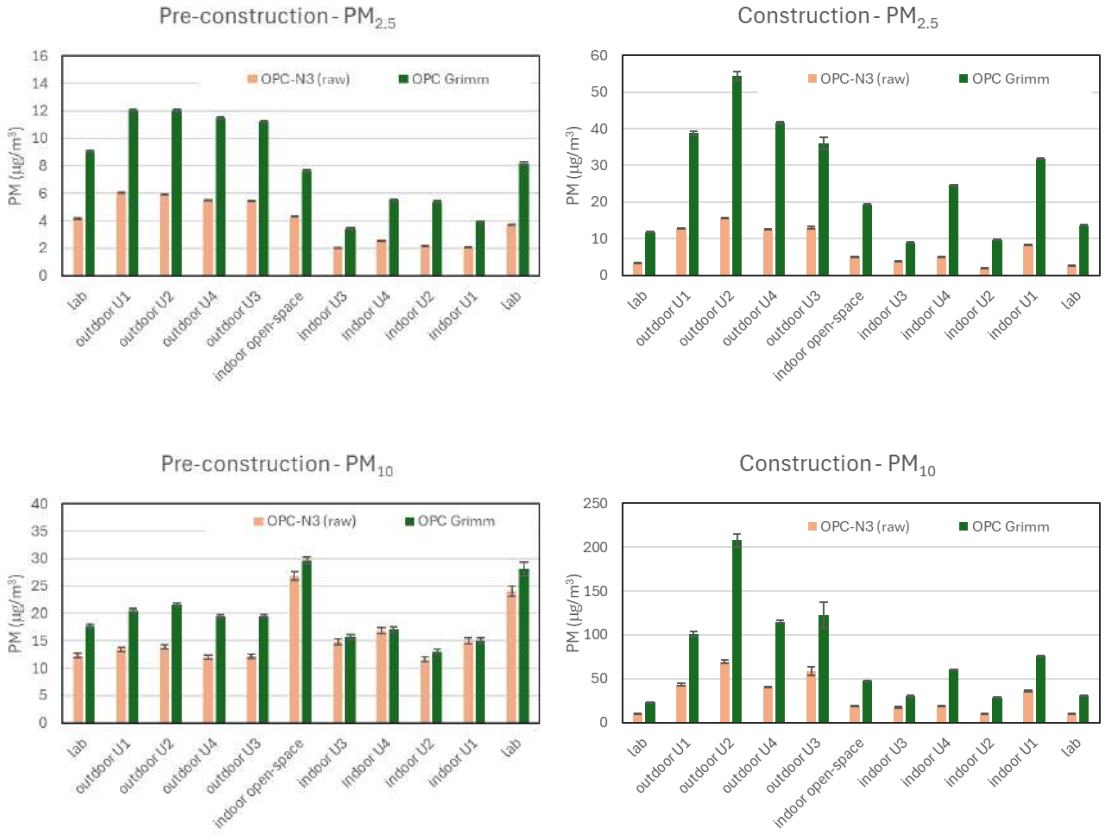

Figure 3.4. PMx concentrations in the three main fractions (PM_1, $PM_{2.5}$ and PM_{10}) for the OPC-N3 (reported as average of the four employed devices) and the OPC Grimm. Data is reported as average for each sampling location, divided for each phase of work on the square.

Table 3.1 reports the slope and coefficient of determination (R^2) values obtained after linear correlation fit between OPC Grimm and OPC-N3 (as average of the four sensors deployed) data, averaged for each of the sampling locations. Low slope values (0.23 – 0.81) for all three PMx fractions confirms how the OPC-N3 strongly underestimated PM concentrations throughout all monitoring, particularly in the finer fractions. The R^2 coefficients obtained through linear correlation fit, however, show strong correlation between the low-cost device and the reference OPC Grimm.

	pre-construction		
	PM_1	$PM_{2.5}$	PM_{10}
slope	0.42	0.48	0.81
R^2	0.98	0.97	0.67

	construction		
	PM_1	$PM_{2.5}$	PM_{10}
slope	0.23	0.31	0.35
R^2	0.92	0.93	0.92

Table 3.1. Coefficient of determination (R^2) and slope of linear correlation fit between OPC-N3 and OPC Grimm, reported for the pre-costruction (left) and the construction (right) phases.

As one of the main causes of this underestimation in PM concentration could be traced to the constant density (1.65 g/cm^3) the OPC-N3 applies to each size bin, a density-based correction factor was derived from experimental data. A new apparent density value was then calculated for the three main fractions (<1 µm, 1-2.5 µm, 2.5-10 µm) and introduced in the PMx calculation algorithm, replacing the constant value applied by the manufacturer (table 3.2). Moreover, the apparent density also accounts for the truncation effect typical of each OPC.

OPC-N3 density factor (g/cm^3)	Derived density factor (g/cm3)		
PM_1, $PM_{2.5}$, PM_{10}	PM_1	$PM_{1-2.5}$	$PM_{2.5-10}$
1.65	4.40	1.43	1.76

Table 3.2. First derived apparent densities for the OPC-N3 from experimental data, compared to the constant value employed by Alphasense.

While this first derived apparent density proved to be particularly effective in correcting data collected during the pre-construction phase (May 2023) and for the first part of the construction phase (Jul-Oct 2023), the correction was inadequate for data obtained during the month of December 2023, where the corrected PM values still deviated significantly from the reference OPC Grimm. By analyzing the PM concentrations obtained during the construction phase via

linear correlation fit between OPC-N3 and OPC Grimm, there is a clear difference in data distribution between the period between July and October 2023 and the month of December 2023, as reported in figure 3.5.

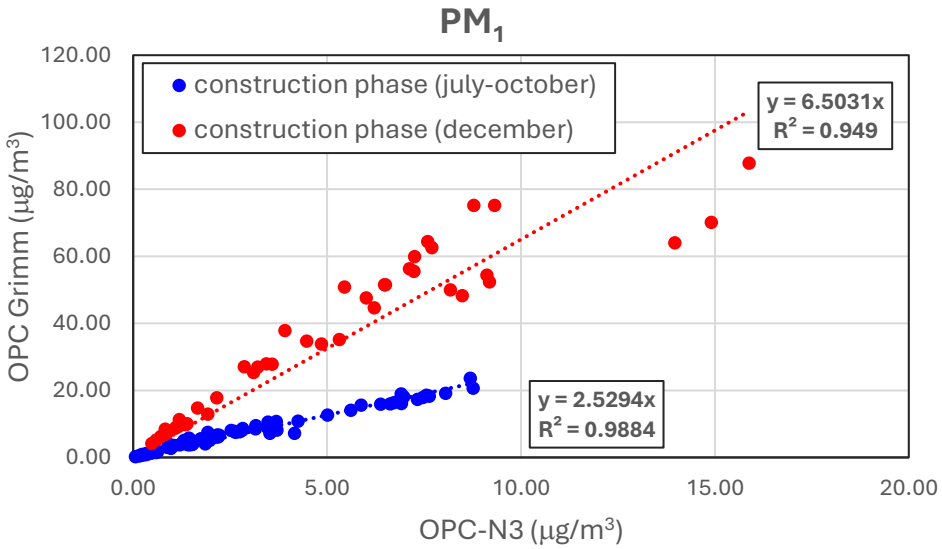

Figure 3.5. Linear correlation fit for OPC-N3 and OPC Grimm during the construction phase.

The observed difference can be traced to the marked differences in ambient conditions and construction-related emissions that characterized the month of December. During this period, characterized by typical winter weather conditions (such as lower mixing layer height, high atmospheric pressure and low temperatures), an intensification of construction site activities was also observed, with the simultaneous presence of depaving activities and handling of building material and soil, which led to an increase in particle emissions, especially in the coarse fraction leading to an airborne PMx with complete different chemical and physical features compared with the typical Milan urban PMx. Comparing the numeric (figure 3.6) and volumetric (figure 3.7) size distributions of both OPC-N3 and OPC Grimm for data obtained from May to October (pre-construction and first part of the construction phase) and for the month of December, two important factors can be highlighted regarding the overall performance of the low-cost sensor in assessing atmospheric particles. First, the size range of the OPC-N3s denotes a clear cut off at a minimum diameter of 0.35 µm, while the OPC Grimm cuts at a particle diameter of 0.25 µm. Additionally, the OPC Grimm

compensates for this cut-off by employing a higher apparent density for lower size bins, while the OPC-N3 applies a constant density factor to all channels. This can strongly affect the number concentration (significantly impacting the accumulation mode) but result in a minor loss when converted to mass concentrations, as smaller particles contribute less to the overall mass. Additionally, a marked discrepancy between the size distribution of the two devices can be observed in the range between 0.5 and 10 µm. This difference is particularly marked in the volumetric distribution (up to a factor of 10) which, as a proxy for mass distribution, accounts for the heavy mass loss in OPC-N3 measurements. These two factors therefore highlight two important technical limitations of the OPC-N3 in accurately detecting atmospheric PM concentrations, especially in the case of coarse particle emissions, such as those observed during the intensification of construction works on *Piazza della Scienza*.

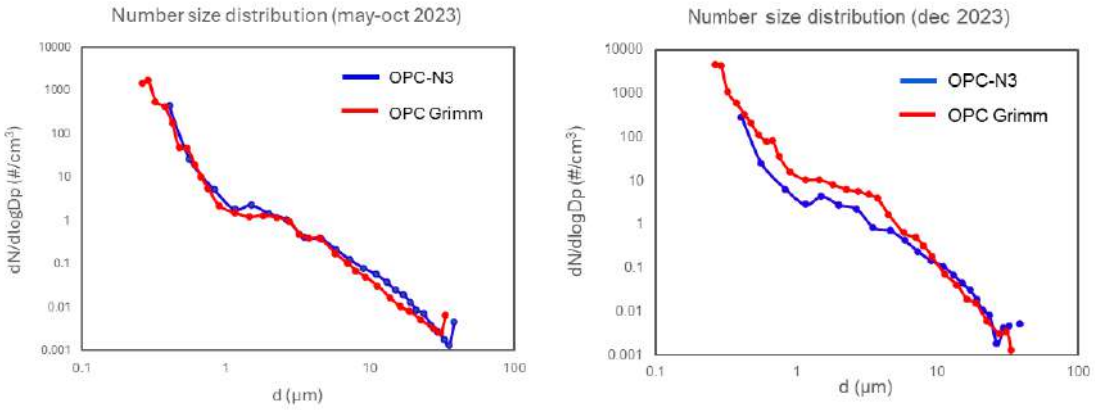

Figure 3.6. Number size distributions of OPC-N3 and OPC Grimm for the two periods under analysis.

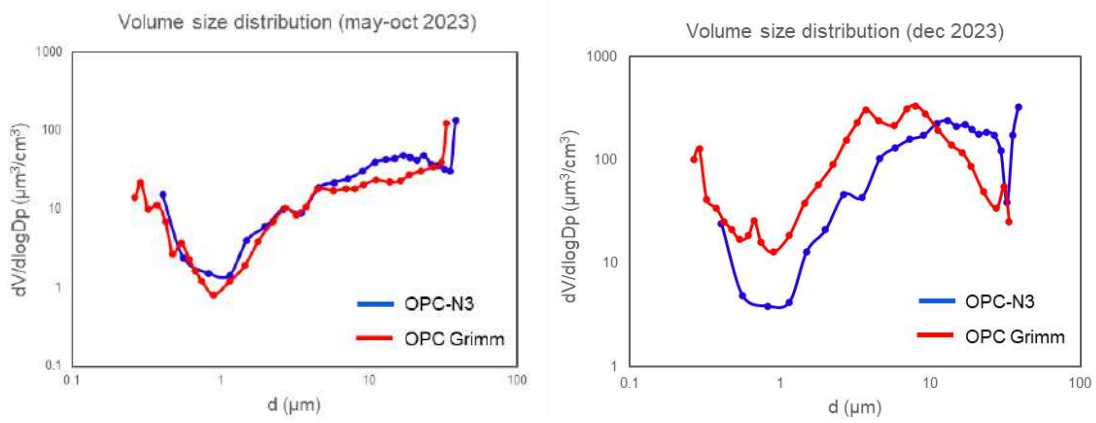

Figure 3.7. Volume size distributions of OPC-N3 and OPC Grimm for the two periods under analysis.

In order to obtain greater accuracy and, consequently, a more precise assessment of the impact of the urban regeneration project, and to resolve the underestimation observed for December 2023, new density-based correction factors were derived. To take into account all factors affecting PM concentrations and the type of construction work on the square, new apparent densities were calculated, specific to each phase of the project (Table 3.3).

density	PM_1	$PM_{2.5-1}$	$PM_{10-2.5}$
pre-construction	4.56	1.44	1.67
construction (july-october)	4.17	1.71	2.26
construction (december)	10.73	5.47	5.79
post-construction	5.17	1.84	2.14

Table 3.3. New derived apparent densities applied to the OPC-N3 for data correction, for each different construction phase.

The new derived apparent densities were computed in the PM calculation algorithm used by the OPC-N3 to obtain corrected PM concentrations for all construction phases. Figure 3.8 to 3.11 report average PM concentrations (as PM_1, $PM_{2.5}$ and PM_{10} fractions) for all construction phases considered. OPC-N3 data is reported before and after the correction, to allow for direct comparison with the OPC Grimm.

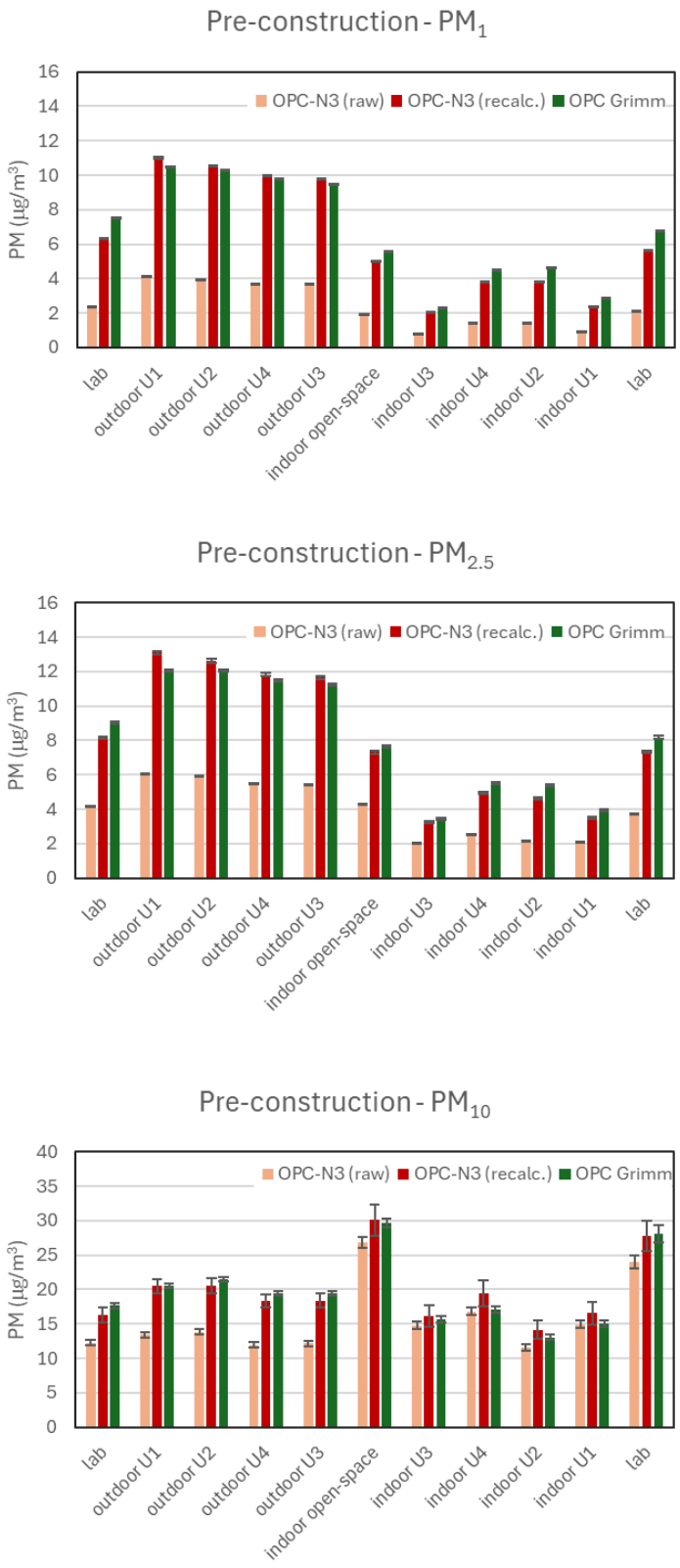

Figure 3.8. Average PM concentrations in the three main PM fractions for the pre-construction phase.

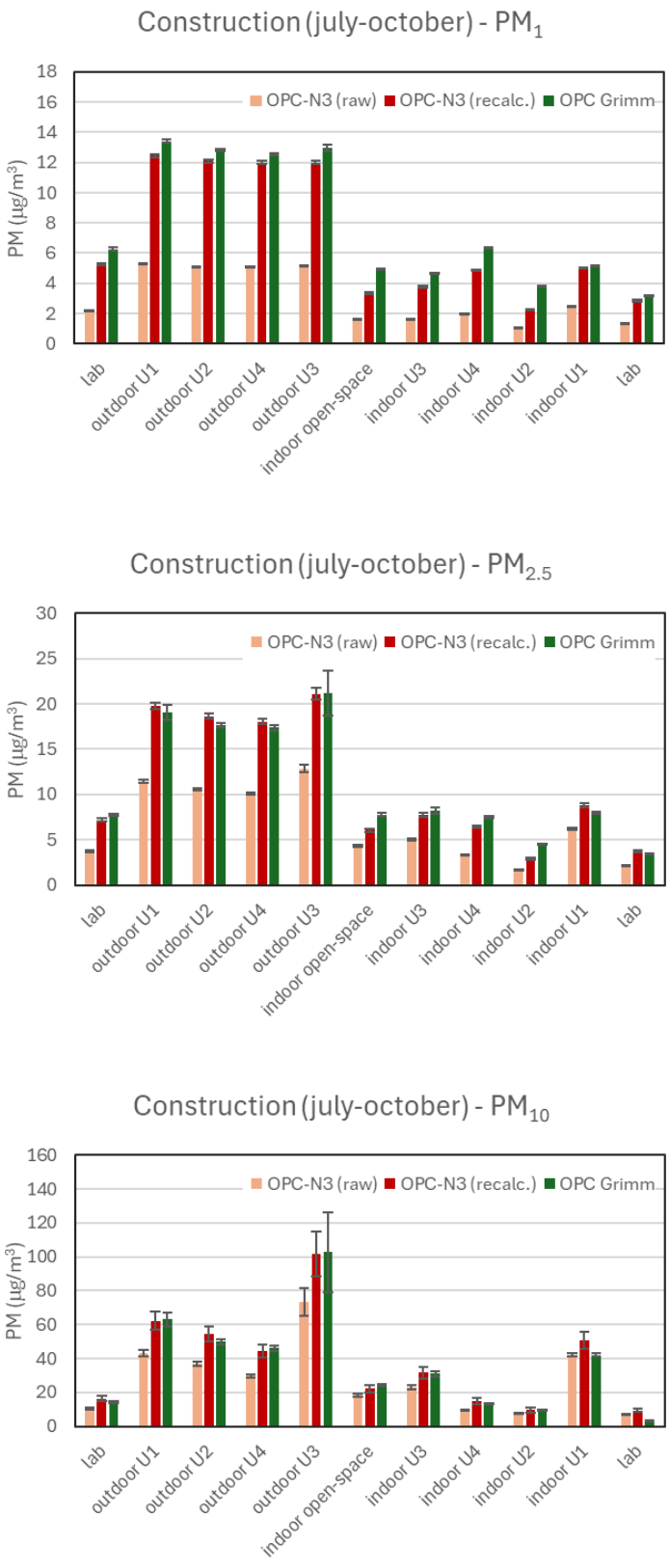

Figure 3.9. Average PM concentrations in the three main PM fractions for the construction phase (from July to October).

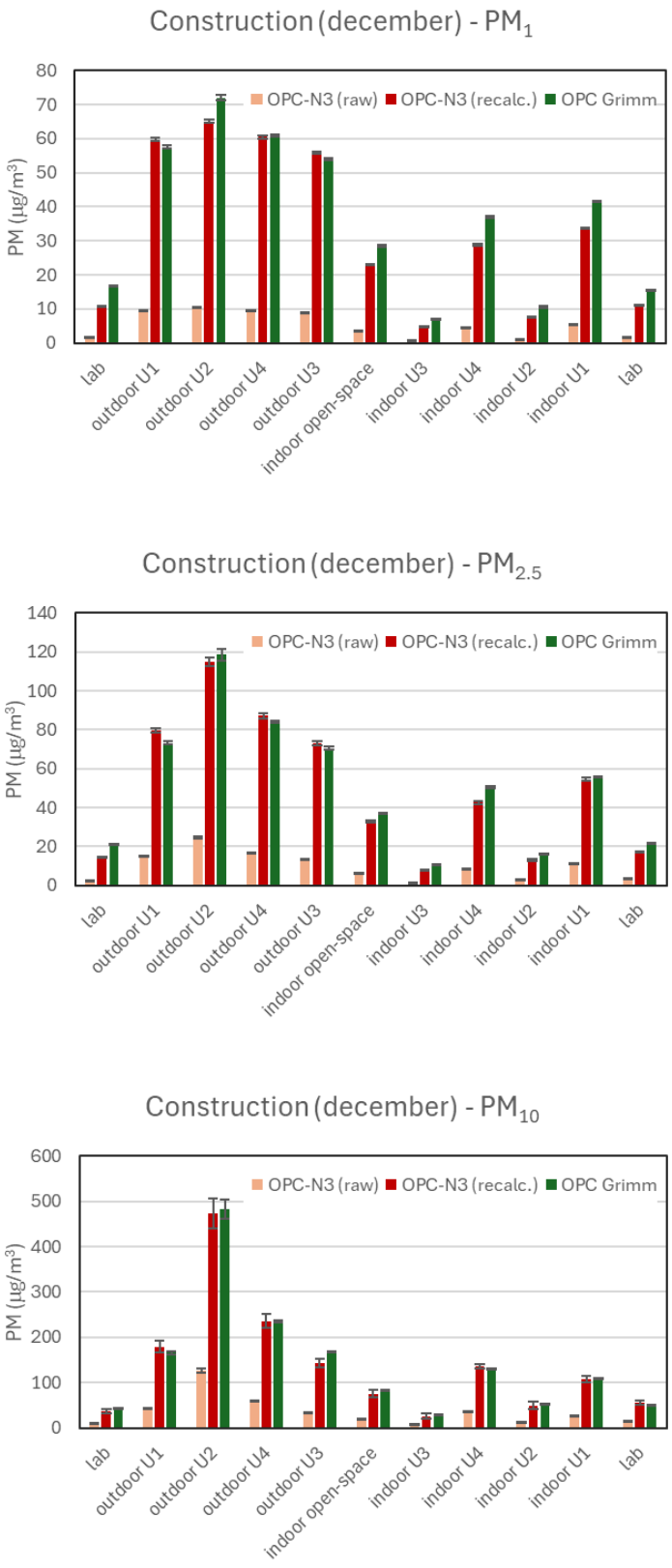

Figure 3.10. Average PM concentrations in the three main PM fractions for the construction phase (for the month of December).

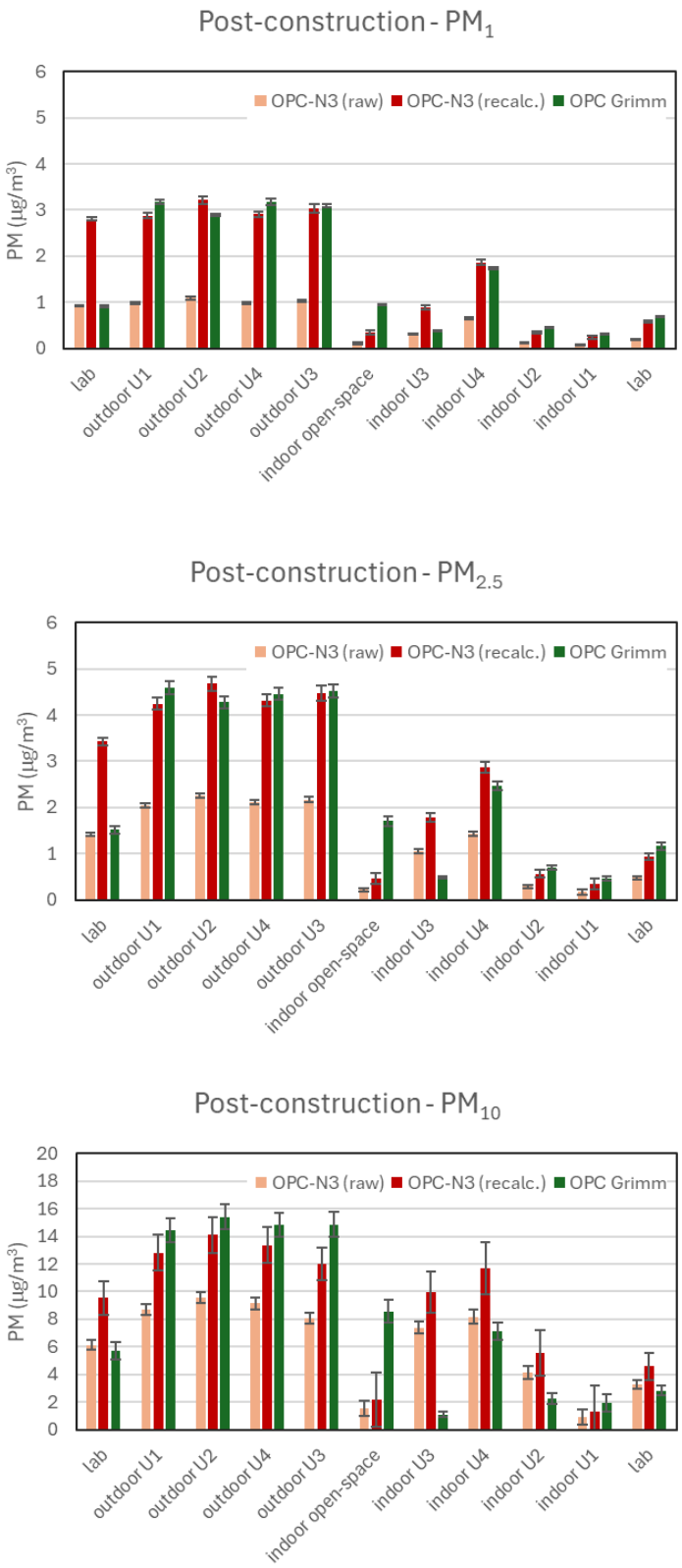

Figure 3.11. Average PM concentrations in the three main PM fractions for the post-construction phase.

BEFORE CORRECTION

pre-construction

	PM_1	$PM_{2.5}$	PM_{10}
slope	0.42	0.48	0.81
R^2	0.98	0.97	0.67

construction (july-october)

	PM_1	$PM_{2.5}$	PM_{10}
slope	0.41	0.62	0.69
R^2	0.98	0.97	0.96

construction (december)

	PM_1	$PM_{2.5}$	PM_{10}
slope	0.17	0.21	0.26
R^2	0.98	0.99	0.99

post-construction

	PM_1	$PM_{2.5}$	PM_{10}
slope	0.30	0.43	0.35
R^2	0.75	0.79	0.44

AFTER CORRECTION

pre-construction

	PM_1	$PM_{2.5}$	PM_{10}
slope	1.12	1.13	0.93
R^2	0.98	0.98	0.95

construction (july-october)

	PM_1	$PM_{2.5}$	PM_{10}
slope	1.02	1.08	0.97
R^2	0.99	0.99	0.99

construction (december)

	PM_1	$PM_{2.5}$	PM_{10}
slope	1.03	1.06	0.98
R^2	0.98	0.99	0.99

post-construction

	PM_1	$PM_{2.5}$	PM_{10}
slope	0.88	0.90	0.55
R^2	0.74	0.78	0.49

Table 3.4. Coefficient of determination (R^2) and slope of linear correlation fit between the OPC-N3 and OPC Grimm, reported before and after the proposed correction.

As reported in table 3.4, the corrected PM concentrations for the OPC-N3 showed strong correlation with the OPC Grimm ($R^2 > 0.9$) for data collected during the pre-construction and the construction phases. Data correlation for the post-construction phase showed only minor improvements after the correction, with good correlation ($R^2 > 0.7$) for the finer fractions (PM_1 and $PM_{2.5}$), while PM_{10} proved to be only moderately correlated with reference OPC after the implementation of the new apparent densities ($R^2 = 0.5$). Moreover, the applied corrections proved to be capable of effectively correcting the underestimation of

PM concentrations detected by the OPC-N3 for the entirety of the pre-construction and the construction phases (slope ~ 1). For the post-construction phase, the applied correction factor able to adequately correct the underestimation for PM_1 and $PM_{2.5}$ fractions (slope ~ 0.9) yet showed limitations in effectively correcting the underestimation for the coarse fraction (PM_{10}), showing only a slight improvement compared to the uncorrected data (slope = 0.5). The reason for this limitation in the proposed correction factor can be traced back to a lack of reference data considered in the derivation of the correction algorithm during the post-construction phase as, due to technical limitations, during this phase the Grimm OPC could only be employed in two monitoring days. Given the strong correlation with the OPC Grimm obtained as a result of the calibration process, the OPC-N3 data corrected through the new apparent densities were then employed in assessing the impact on air quality of the entire urban regeneration project for *Piazza della Scienza*.

The emission of particles in the nanometric fraction was evaluated through the application of the portable Partector-2 (Naneos), coupled with research-grade particle counter Nanoscan SMPS model 3910 (TSI). Figures 3.12 to 3.14 report average particle number concentration (PNC) in the nanometric fraction for the three phases of the urban redevelopment of the square, as reported by the employed sensors. The Partector-2 was able to correctly estimate nanoparticle concentrations throughout the entire monitoring, showing strong correlation (R^2 > 0.96) with the Nanoscan SMPS and a linear fit slope value ranging from 0.8-1 during all three phases. The highest deviation from the reference Nanoscan SMPS was observed during the construction phase, where the Partector-2 showed a slight underestimation of particle number concentrations, with a slope of linear fit of 0.85. This is in line with other studies involving the Partector device. Asbach et al. (2024) evaluated the Partector-2 Pro against a reference mobility particle size spectrometer (MPSS) at an urban background site in Mülheim-Styrum (Germany), showing strong agreement with the MPSS with a slope of the linear fit of 0.998 and a regression coefficient of R^2=0.996. Todea et al. (2017) tested the Partector with generated polydisperse aerosols against a reference ultrafine condensation particle counter (UCPC), showing an overall comparability of ± 50% for particle number concentration, and highlighting how particles with a

diameter particles > 400 nm can drastically influence the measurement results. Bezantakos et al. (2024) proved how the accuracy of the Partector remains in the range ±30% reported by the manufacturer even when tested at reduced pressure and temperature conditions that are typical of higher altitudes. In this study, the Partector-2 showed a higher uncertainty (confidence interval at 95% confidence level) in the averages of some of the selected sampling locations. This is mainly due to the difference in time resolution between the two instruments: the Nanoscan SMPS operates at a maximum time resolution of 1 minute, while the Partector-2 is capable of measuring at a frequency of 1 second. This allows the Partector-2 to more optimally detect short-lived emission events. Given the positive results achieved with Partector-2, the device was employed in the subsequent impact assessment analysis of the *Piazza della Scienza* regeneration project.

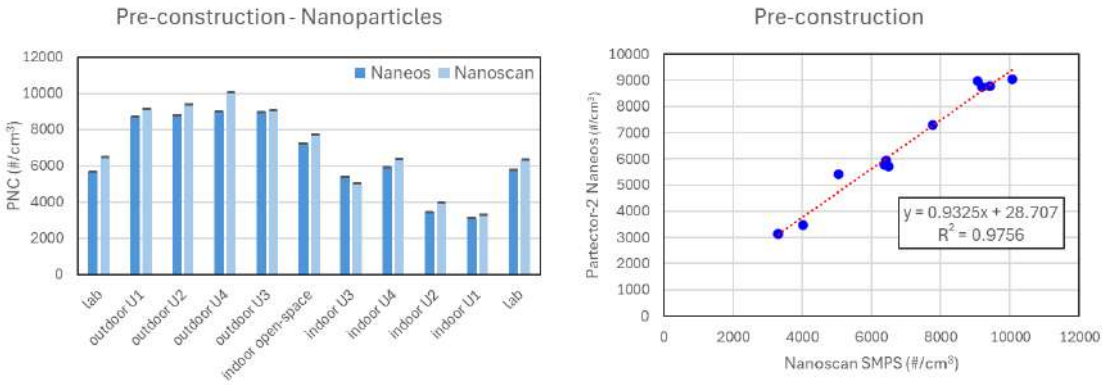

Figure 3.12. Particle number concentration (PCN) in the nanometric fraction reported for the Partector-2 (Naneos) and the Nanoscan SMPS (TSI) as average for each sampling location for the pre-construction phase (left). On the right linear correlation fits between the two devices.

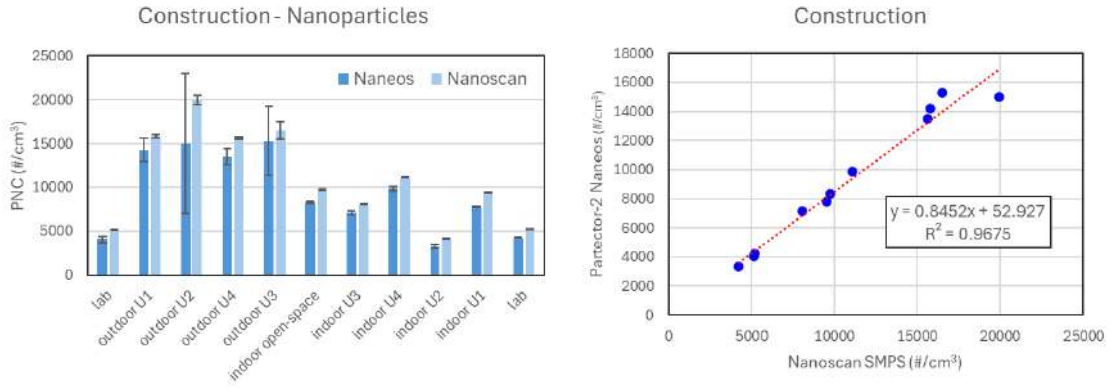

Figure 3.13. Particle number concentration (PCN) in the nanometric fraction reported for the Partector-2 (Naneos) and the Nanoscan SMPS (TSI) as average for each sampling location for the construction phase (left). On the right linear correlation fit between the two devices

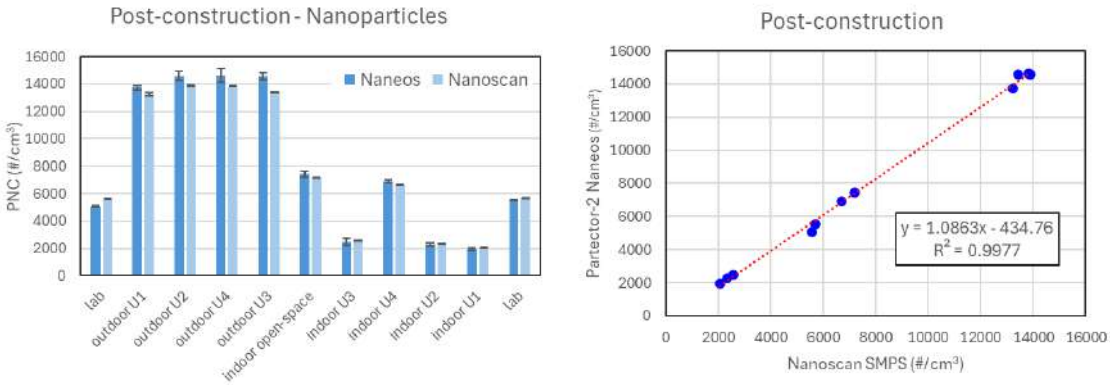

Figure 3.14. Particle number concentration (PCN) in the nanometric fraction reported for the Partector-2 (Naneos) and the Nanoscan SMPS (TSI) as average for each sampling location for the post-construction phase (left). On the right linear correlation fit between the two devices.

3.3.2. Impact of the construction phase on air quality

For a comprehensive assessment of the entire urban regeneration project for *Piazza della Scienza*, the impact on air quality was evaluated in terms of particle emissions as PM mass concentration and number concentration in the nanometric fraction. Two different impact assessments will be discussed in this work. The first assessment will focus solely on the construction phase, calculating

the particle emissions resulting from the working activities conducted during the urban redevelopment of the square. A second assessment will concern the entire *Piazza della Scienza* renovation project carried out by the MUSA ecosystem, evaluating the effectiveness of the technological and architectural changes in terms of air quality, by comparing particle concentrations in the pre-construction phase and post-construction phase.

During the construction phase, a series of activities and works were carried out on the square, as envisaged by the MUSA ecosystem, to renovate the architectural context and offer new green spaces and gathering places. These activities first involved removing the old paving covering the square (figure 3.15), mainly mineral flooring laid on sand and gravel, and replacing it with new paving consisting of Luserna stone blocks surrounded by granite frames. This phase was characterized by heavy handling of materials such as stone, sand, and gravel, resulting in significant dust release into the air. A second important phase in the work involved the installation of insulating material on the square surface, through the use of open flames (figure 3.16). Soil excavation and movement, for the removal of the previous flower beds in favor of the creation of new and more extensive spaces dedicated to the green coverage of the square, saw the resuspension of coarse material into the atmosphere. Another significant source of particles throughout the construction phase was the process of removing and transporting excavated materials, including stone, sand, gravel, and soil, utilizing heavy-duty vehicles (figure 3.17).

Figure 3.15. Overview of part of the square during the depaving work.

Figure 3.16. Overview of part of the square during the positioning of the insulating material.

Figure 3.17. Overview of part of the square during the removal of materials, where dust resuspension becomes clearly visible.

In order to estimate the overall impact on PM concentrations, both indoors and outdoors, data from low-cost sensors OPC-N3 was utilised, previously corrected through the density-based correction factors described in section 3.3.1. To evaluate the impact on PNC in the nanometric fraction, data from the Partector-2 was employed. To address seasonal variability in particle concentrations that could otherwise heavily influence the results, the obtained data was first normalized on data from the reference monitoring station of the regional environmental protection agency (ARPA, *Agenzia regionale per la protezione ambientale*) of Milano Pascal. While not directly collocated with *Piazza della Scienza*, the Milano Pascal reference station provides PM concentrations representative of an urban background site comparable to the area under examination, thus ensuring an accurate comparison. PM data form the ARPA Milano Pascal reference station from the pre-construction and construction phases allowed to determine expected concentrations for the OPC-N3 in the construction phase, providing an estimated concentration value based on an ideal scenario without any work being carried out in the square. As ARPA reference data could only be obtained for $PM_{2.5}$ and PM_{10} fractions, $PM_{2.5}$ reference data was employed in the impact assessment for PM_1 and PNC in the nanometric fraction. The derived concentrations allowed an estimate of the impact, in terms of particle concentration, of the construction site in its entirety (figure 3.18). Confidence interval (at 95% confidence level) is reported to quantify

the uncertainty in the calculation. The calculated impact for the entire construction phase for PM mass concentrations was 11.1 ± 23.8 μg/m^3 for PM_1, 33.6 ± 53.0 μg/m^3 for $PM_{2.5}$ and 82.1 ± 79.4 μg/m^3 for PM_{10}. For PNC in the nanometric fraction, the calculated impact was -3318.3 ± 3825.6 cm^{-3}. Overall, PM concentrations showed a positive impact throughout the construction phase; however, the reported values for PM_1 and $PM_{2.5}$ showed uncertainty (as confidence interval at 95% confidence level) higher than the actual increase in concentration derived. Thus, it is not possible to claim the construction site had a statistically significant positive impact on the square air quality for these fractions. The same considerations can be drawn for the PNC in the nanometric fraction, where a general negative impact is observed for the entire construction phase, although statistically the assumption that the actual variation is null cannot be excluded, as the confidence interval associated with this estimate is wide and includes the zero value. For PM_{10}, however, the reported positive impact is statistically significant. This highlights how the construction site of the urban regeneration plan carried out in *Piazza della Scienza* impacted the monitored environments with significant particle emission particularly in the coarse fraction. The calculated impact on the PM_{10} fraction show an increase higher than both EU issued limit values and WHO Air Quality Guidelines, resulting in a potential health risk increase.

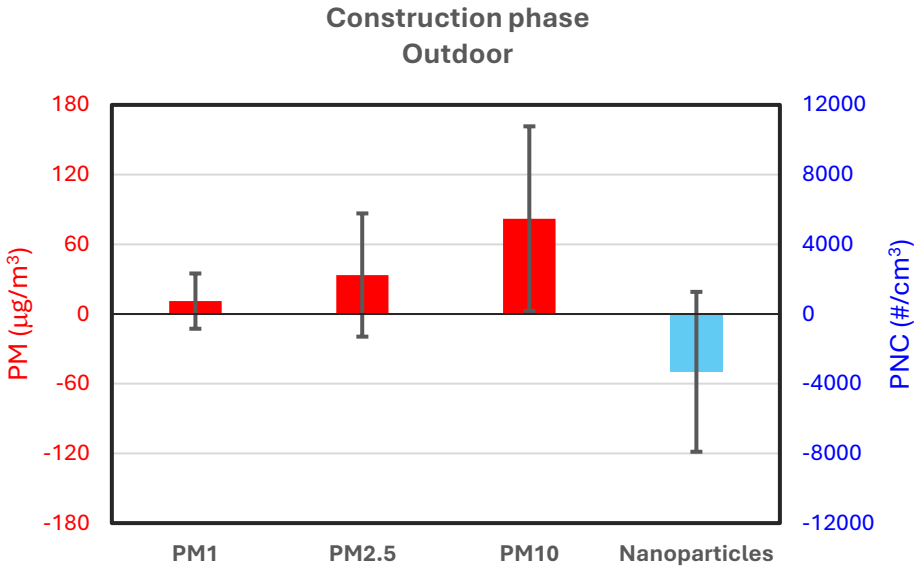

Figure 3.18. Calculated impact on outdoor environments of Piazza della Scienza linked to the construction activities.

The analysis of construction site impact on indoor environments followed the same methodology applied for the outdoor case study. However, particulate matter in indoor environments is not independent of the external context but can be influenced by three main factors: any existing internal source, the resuspension of deposited particles and, crucially, infiltration of outdoor air. To provide an estimate of the expected indoor concentrations, a linear equation is widely applied in the scientific literature (Hänninen et al., 2004; Hoek et al., 2008; Sangiorgi et al., 2013):

$$C_{in} = F_{INF} \cdot C_{out} + C_{ig}$$

where C_{in} and C_{out} are, respectively, the indoor and outdoor particle concentrations; F_{INF} is the infiltration factor and C_{ig} is the concentration of indoor generated particles. From this relationship, F_{INF} and C_{ig} can be respectively derived as the slope and the intercept of a linear regression fit between outdoor and indoor concentrations. For the university environments of *Piazza della Scienza* examined in this work, F_{INF} and C_{ig} values were derived from a linear correlation fit of OPC Grimm data for both the pre-construction and the construction phase. The obtained values were then applied to outdoor reference data from ARPA Milano Pascal to derive estimates of indoor reference

concentrations, then employed in the impact calculation as described for the outdoor evaluation. The calculated impact (figure 3.19) on indoor environments for the entire construction phase for PM mass concentrations was 0.3 ± 6.9 $\mu g/m^3$ for PM_1, 3.9 ± 12.6 $\mu g/m^3$ for $PM_{2.5}$ and 2.3 ± 29.2 $\mu g/m^3$ for PM_{10}. For PNC in the nanometric fraction, the calculated impact was -8056.3 ± 2418.4 cm^{-3}. Overall, indoor PM concentrations showed a minor positive impact throughout the construction phase, however statistically the assumption that the actual variation is null cannot be excluded, as the confidence interval associated with this estimate includes the zero value. Conversely, PNC in the nanometric fraction showed a substantial and statistically significant decrease for indoor environments. This result is consistent with effective dilution and reduction of external contributions on indoor air, achieved by the university's ventilation and filtration system in place for indoor environments. We should also speculate that, as the coarse fraction increases, nanoparticles can more easily coagulate on bigger particles, resulting in an overall decrease in PNC. Overall, a general positive impact in terms of particle emissions has been observed for outdoor environments monitored during the construction phase, specifically for the coarser fraction. In contrast, in indoor environments the infiltration of particles from the outdoor was minimal and was largely offset by the ventilation, air conditioning, and air recirculation systems present in the indoor environments of the university campus of *Piazza della Scienza*.

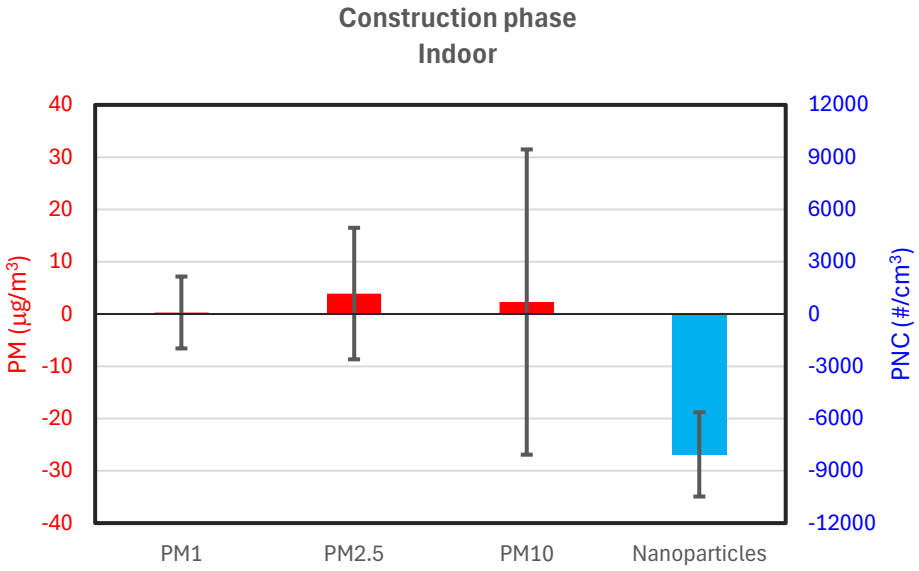

Figure 3.19. Calculated impact on indoor environments of Piazza della Scienza linked to the construction activities.

3.3.3. Overall impact of the urban regeneration project of Piazza della Scienza on air quality

In order to carry out a comprehensive assessment of the air quality of the entire urban regeneration project carried out in Piazza della Scienza, the context of the square was evaluated following the completion of the works and activities envisaged by the MUSA ecosystem. The project saw a 40% increase in green coverage, soil de-impermeabilization to manage rainwater and mitigate extreme weather events, and depaving, reducing mineral flooring in favor of a new surface consisting of Luserna stone blocks surrounded by granite frames. The impact on air quality was therefore quantified by monitoring particle concentrations during the post-construction phase, compared with data obtained during the pre-construction phase. To keep the results consistent, the same methodology and calculation applied and described in chapter 3.3.2 for the construction phase were employed. The calculated impact on outdoor environments in the post-construction phase for PM mass concentrations was -5.2 ± 5.5 µg/m^3 for PM_1, -5.6 ± 6.4 µg/m^3 for $PM_{2.5}$ and -5.9 ± 8.6 µg/m^3 for PM_{10}. For PNC in the nanometric fraction, the calculated impact was 5640.1 ± 4588.5 cm^{-3} (figure

3.20). PM concentrations during the final phase of the project showed overall a negative impact, with a decrease in concentrations through all three fractions compared to the pre-construction phase. Analogous to the case study of the construction phase, the reported confidence interval (at 95% confidence level) for all three PMx fractions is higher than the actual decrease in concentration. Thus, statistically the assumption that the actual variation is null cannot be excluded, as the confidence interval associated with this estimate includes the zero value. To further assess the square outdoor air quality, the impact on PMx emissions in the post-construction phase was calculated with the same methodology employing data from the Polludrone (OIZOM) monitoring unit, installed in a fixed position on the square (U1 corner) following the completion of the redevelopment works. The impact calculation derived from the Polludrone data (figure 3.21) showed comparable results to the OPC-N3 calculation, resulting in -4.1 ± 4.2 μg/m^3 for PM_1, -5.1 ± 4.7 μg/m^3 for $PM_{2.5}$ and -5.0 ± 7.6 μg/m^3 for PM_{10}. In contrast to the calculation made using OPC-N3 data, in this case a significant decrease in $PM_{2.5}$ was observed. Overall, while a decreasing trend in concentration can be observed for all PM fractions in the post-construction phase, no definitive conclusions can be drawn regarding a statistically significant decrease in PM concentrations. Conversely, for PNC in the nanometric fraction a statistically significant increase in concentrations compared to the pre-construction phase was observed. A possible explanation for this result could reside in increased emissions of biogenic volatile organic compounds (VOCs) following the higher vegetation cover of the square envisioned by the MUSA ecosystem, resulting in the formation of secondary organic aerosols (SOA) from nucleation and condensation processes in the atmosphere. Plants are among the main sources of biogenic volatile organic compounds (bVOC), accounting for over 90% of total emissions (Guenther, 1995). These compounds can lead to the formation of SOA in the atmosphere, following reaction with oxidising chemical species such as O_3, OH radicals and NO_3 radicals (Joutsensaari et al., 2005; Holopainen et al., 2017). This process is one of the most significant for the formation of aerosols in the atmosphere, with a greater impact during the summer season (Wu et al., 2020). This may partially explain the increase in nanoparticle concentrations observed during the post-construction phase, as this

fraction of particulate matter is specifically linked to the formation of secondary aerosols from nucleation and coagulation processes. Furthermore, the coincidence of post-construction monitoring with the summer season may have played a key role in amplifying this effect.

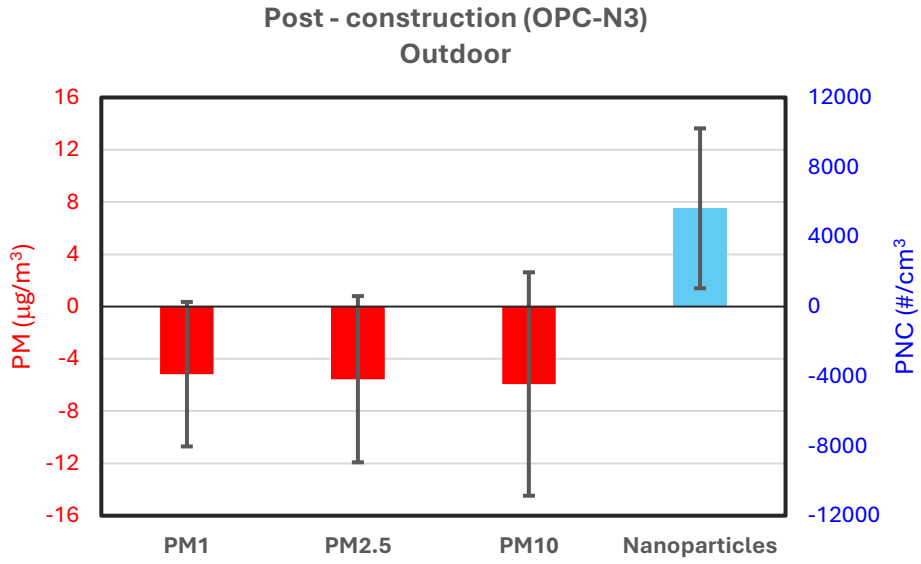

Figure 3.20. Calculated impact on outdoor environments of Piazza della Scienza linked to the entire urban regeneration process enacted by the MUSA ecosystem.

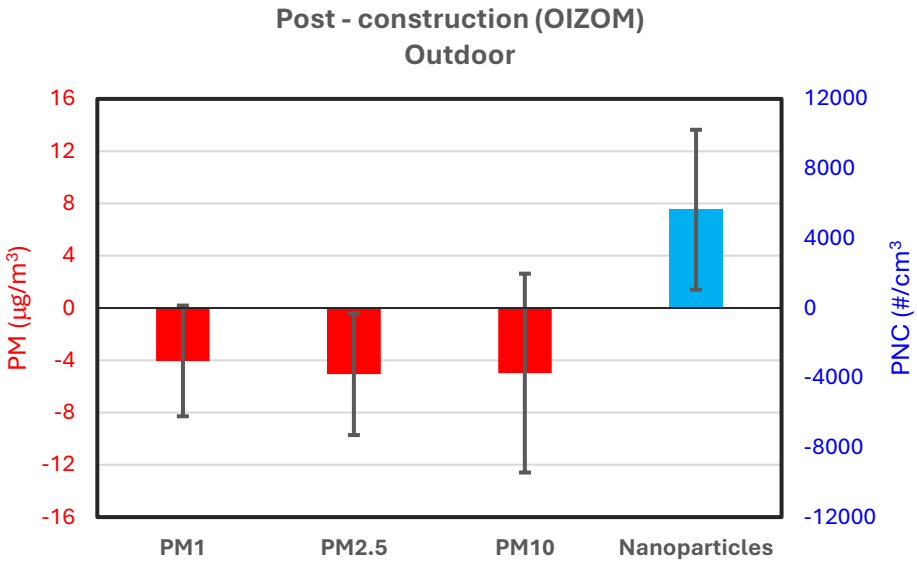

Figure 3.21. Calculated impact, employing Polludrone (Oizom) PM data, on outdoor environments of Piazza della Scienza linked to the entire urban regeneration process enacted by the MUSA ecosystem.

For indoor environments, the calculated impact in the post-construction phase for PM mass concentrations was -1.3 ± 1.4 µg/m³ for PM_1, -0.8 ± 2.0 µg/m³ for $PM_{2.5}$ and -2.5 ± 8.7 µg/m³ for PM_{10}. For PNC in the nanometric fraction, the calculated impact was -286.9 ± 1227.3 cm^{-3} (figure 3.22). A decreasing trend is observed for both particulate matter, in line with what is reported for outdoor environments, and for PNC in the nanometric fraction, in contrast to the corresponding outdoor case. Nevertheless, even in this instance, the confidence intervals (at 95% confidence level) obtained do not allow the observed decrease to be considered statistically significant, and therefore the possibility of negligible impact on concentrations in the square cannot be ruled out.

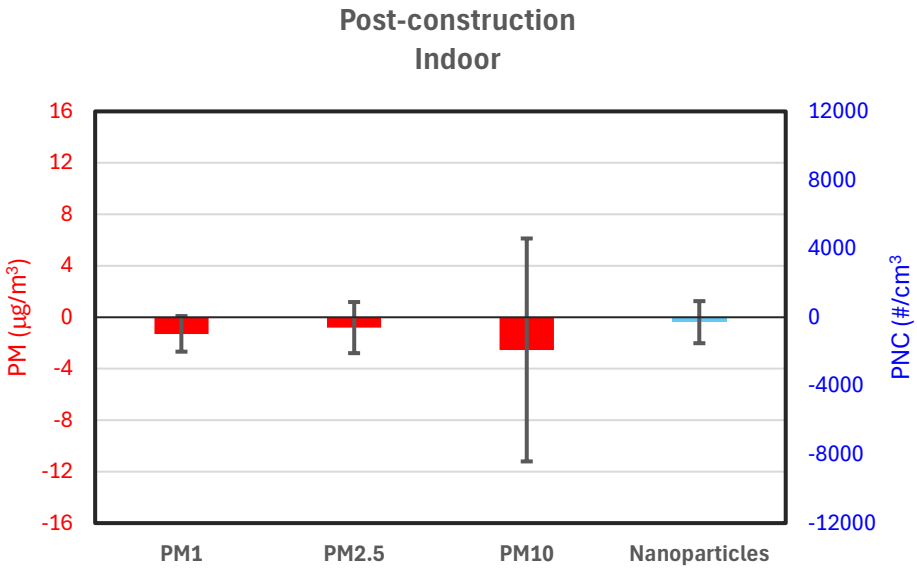

Figure 3.22. Calculated impact on indoor environments of Piazza della Scienza linked to the entire urban regeneration process enacted by the MUSA ecosystem.

3.3.4. Evaluation of low-cost fixed sensors – a look into the future of Piazza della Scienza

At the end of the urban regeneration project carried out in Piazza della Scienza, the MUSA ecosystem envisaged the transformation of the new spaces in the square into a fully-fledged scientific hub dedicated to research and dissemination. The final phase of the project therefore saw the creation of the MUSA Open-air Laboratory, with the spaces in Piazza della Scienza becoming a testing ground for the study and monitoring of numerous environmental parameters. Thanks to the installation of multiple sensors (four Purple Air Flex, one Polludrone OIZOM air monitoring unit), continuous, real-time monitoring of atmospheric pollutants is carried out in the outdoor environments of *Piazza della Scienza*, enabling a constant flow of data aimed at atmospheric research and an excellent tool for disseminating and raising awareness of environmental issues among university students and citizens. After installation (in January 2025) and the first months of data acquisition, the sensors' performance was evaluated against reference data obtained from the reference monitoring station of ARPA Pascal. Given the

technical impossibility of conducting a calibration campaign with reference instruments in the square during the first months of monitoring, the ARPA data provide a valid comparison for an initial assessment of the installed sensors.

As detailed beforehand, the Polludrone (OIZOM) multiparametric monitoring unit allows for continuative monitoring of PM and gaseous pollutants. Analysis of the data obtained from the first month of monitoring after installation showed that the pollutant data returned by the Polludrone unit showed no correlation with the ARPA data for most pollutants, as reported in Table 3.5.

	$PM_{2.5}$	PM_{10}	NO	NO_2	O_3
Slope	0.037	0.073	1.038	0.544	0.454
R^2	0.001	0.001	0.198	0.569	0.120

Figure 3.5. Coefficient of determination (R^2) and slope of linear correlation fit between the Polludrone (Oizom) monitoring unit and reference data from the ARPA monitoring station of Milan Pascal

The observed discrepancy in data was mainly due to Oizom's proprietary correction algorithm. In fact, the Polludrone device is equipped with a machine learning algorithm based on factory calibration data provided by the manufacturer, which corrects the pollutant data returned based on environmental conditions, most notably air temperature. After an initial testing phase, we found that the Polludrone control unit installed in *Piazza della Scienza* was still calibrated according to the environmental conditions of the manufacturing region (Ahmedabad, India). Updating these parameters to the actual data for the square resulted in an instant improvement in the environmental data obtained by the control unit. The following analysis will provide data acquired after the detailed correction. Overall, the Polludrone follows the reference concentration trend over time reasonably closely, for both $PM_{2.5}$ and PM_{10} fractions (figure 3.23 and 3.24). Polludrone data showed good correlation with reference concentrations, with coefficients of determination equal to $R^2 = 0.74$ for PM_{10} and $R^2 = 0.71$ for $PM_{2.5}$ (figure 3.25). A slight overestimation in PM concentrations can be observed for the Polludrone data, more marked for the PM_{10} fraction, highlighted by the slope of linear fit derived

(s = 1.59 for PM_{10} and s = 1.11 for $PM_{2.5}$). A first explanation of this overestimation can be explained by the influence of relative humidity (RH) on the light scattering sensors, influencing the PM measurements. As highlighted in figure 3.23 and 3.24, the majority of the observed PM overestimation by the Polludrone unit occurs during episodes with relative humidity > 80%. However, this effect is limited to a few isolated episodes and does not extend to the entire monitoring period, possibly indicating a dependence on the variability of the chemical composition and hygroscopic properties of the particulate matter in the square at a given time. Moreover, the machine learning correction algorithm employed by Oizom is able to compensate to some extent for changes in ambient relative humidity and temperature.

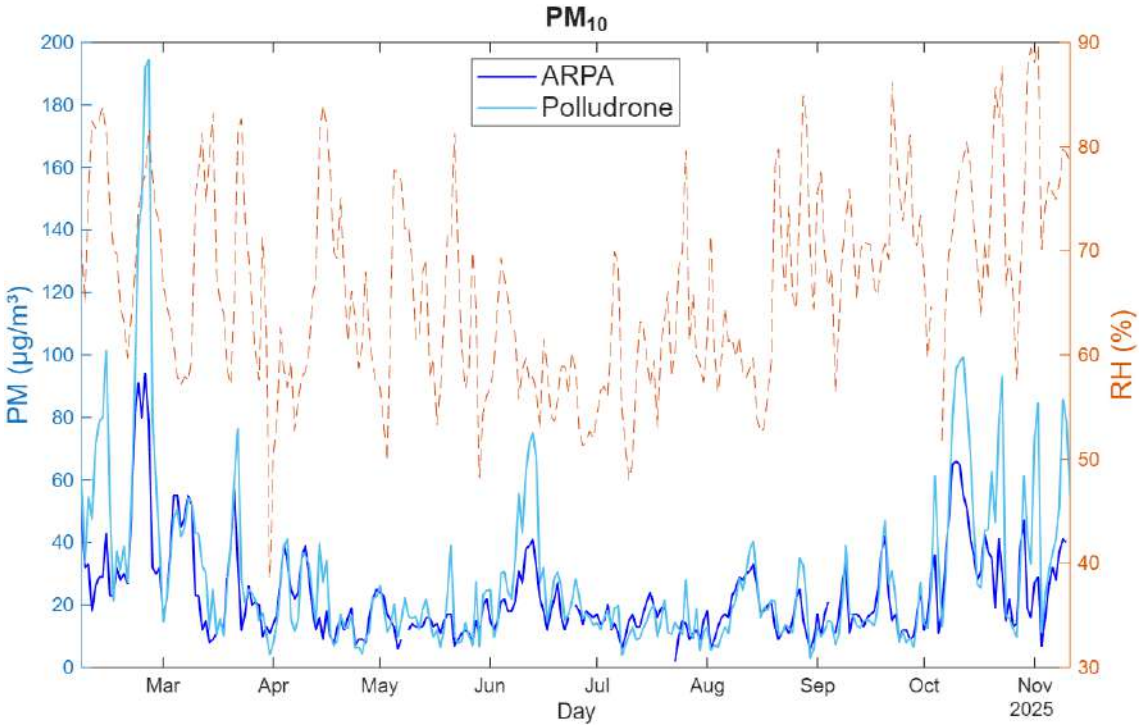

Figure 3.23. PM_{10} concentration trend over time as daily averages for the Polludrone and reference ARPA data. The orange dashed line represents relative humidity levels measured by the Polludrone in the square.

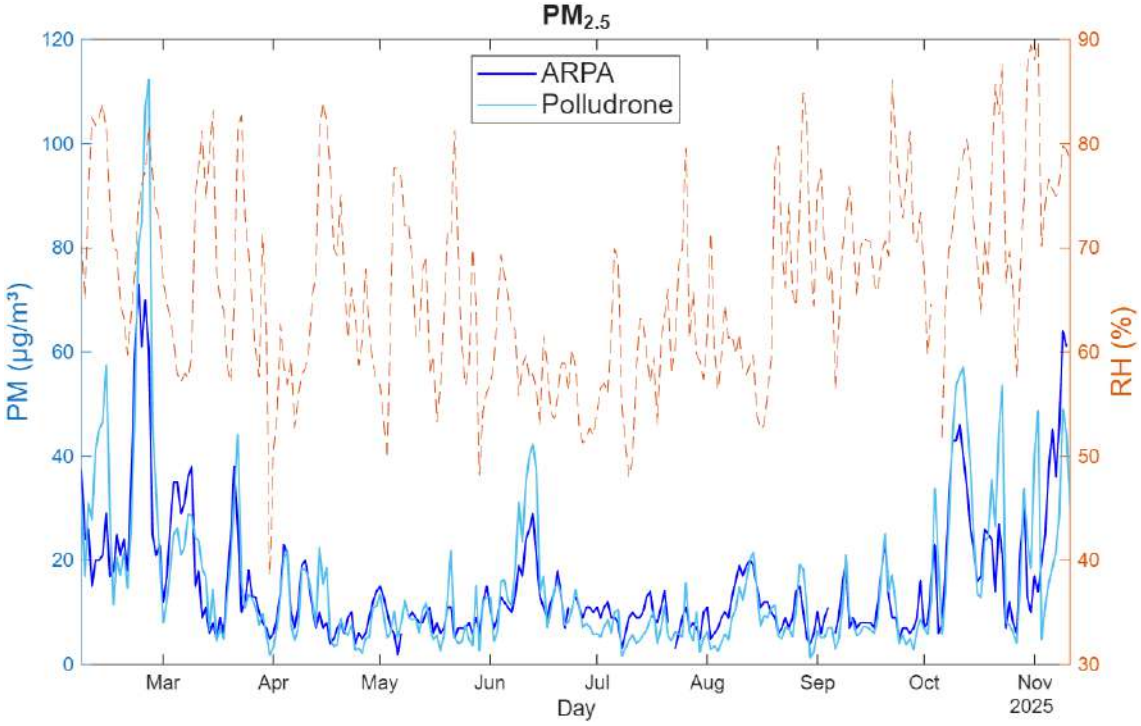

Figure 3.24. $PM_{2.5}$ concentration trend over time as daily averages for the Polludrone and reference ARPA data. The orange dashed line represents relative humidity levels measured by the Polludrone in the square.

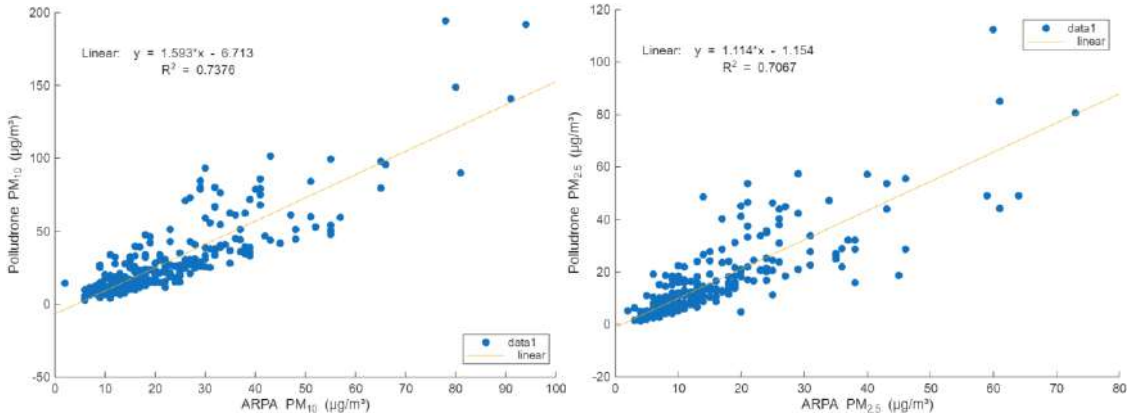

Figure 3.25. Linear correlation fit for PM_{10} (left) and $PM_{2.5}$ (right) data, between reference ARPA and Polludrone concentrations.

Ozone concentrations reported by the Polludrone unit followed closely the overall trend in concentrations reported by the reference ARPA Pascal monitoring station (figure 3.26). Moreover, the Polludrone showed strong correlation with reference data. While a linear fit showed strong correlation with reference data

(R^2 = 0.90), a quadratic relationship proved to be the best fit (figure 3.27) with an improved determination coefficient of R^2 = 0.92.

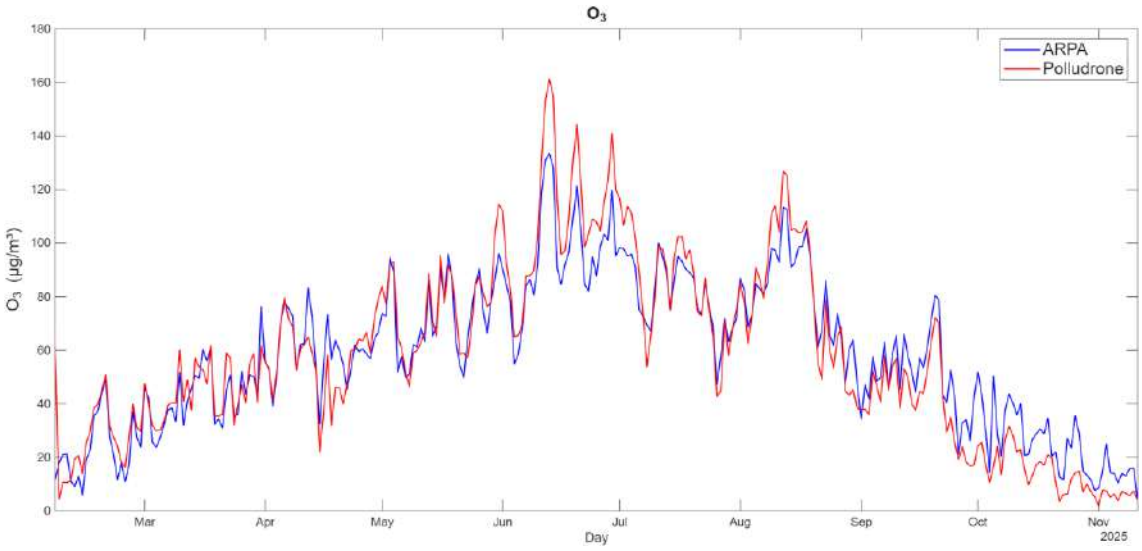

Figure 3.26. Ozone concentration trend over time as daily averages for the Polludrone and reference ARPA data.

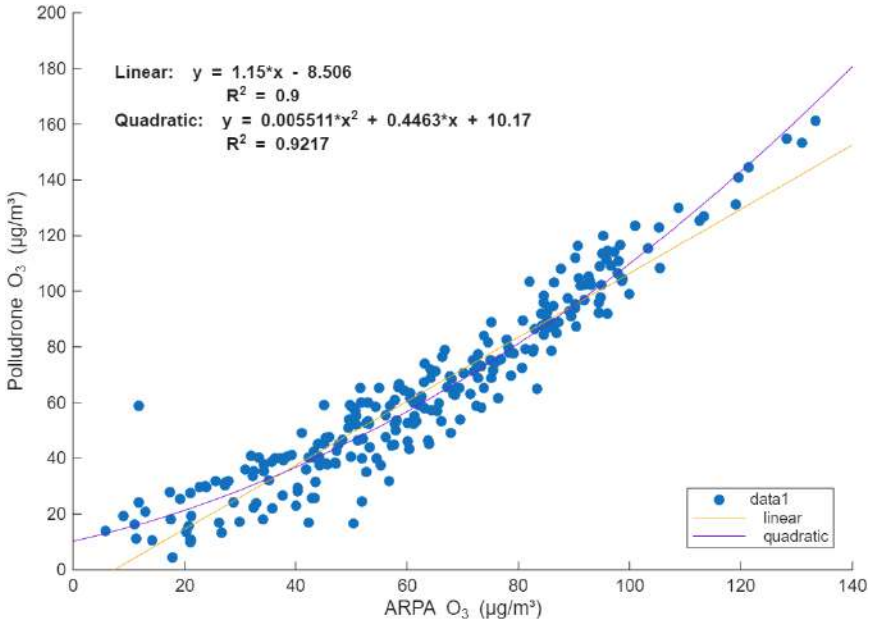

Figure 3.27. Linear correlation fit for ozone data, between reference ARPA and Polludrone concentrations.

Nitrogen dioxide (NO_2) concentrations for the Polludrone device followed the overall trend in concentrations reported by ARPA for most of the evaluated time

frame. However, the device showed a marked overestimation of reference NO_2 concentrations during the summer months, from May to the end of September. As shown in figure 3.28, this overestimation is more prominent in relation to ambient temperature levels, with a larger deviation at temperatures above 15°C, typical of the warmer months. While ARPA reference data show a typical trend for NO_2 in urban environments, with higher values in the colder months linked to increased emissions from motor vehicle traffic, domestic heating and a shallower planetary boundary layer, the data obtained from the Polludrone monitoring station show a constant trend over the months, seemingly unaffected by seasonality. Furthermore, *Piazza della Scienza* is located in an area of Milan characterised by concentrations of pollutants typical of an urban background, comparable to the ARPA Milano Pascal reference station, and not in the immediate vicinity of areas with high traffic density that could be linked to a significant increase in NO_2 values as observed. This trend translates into poor correlation between the device and reference data, with a R_2 value for linear fit of $R^2 = 0.2$ (figure 3.29). These first results suggest a possible limitation of the correction algorithm employed by Oizom, unable to correctly compensate for variations in temperature and actual environmental conditions for NO_2 measurements.

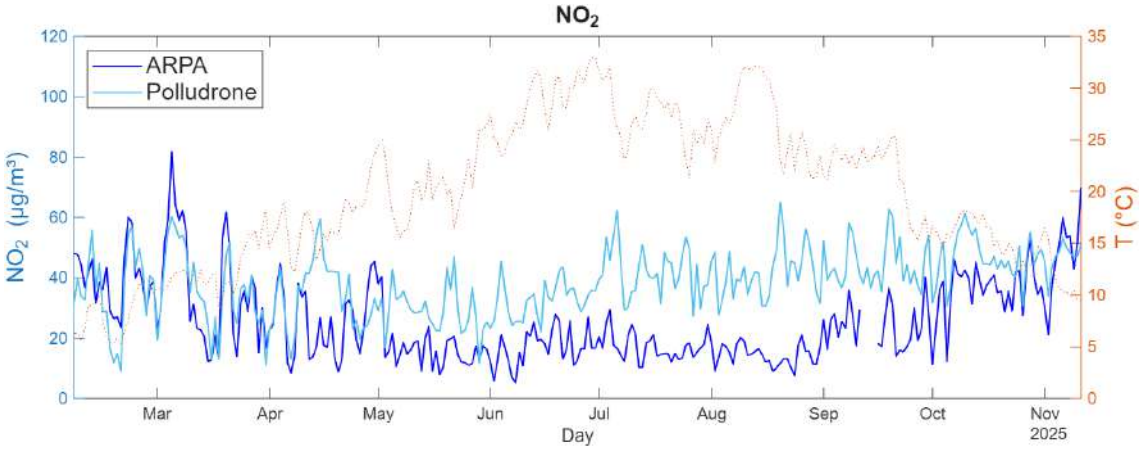

Figure 3.28. Nitrogen dioxide (NO_2) concentration trend over time as daily averages for the Polludrone and reference ARPA data. The orange dashed line represents relative humidity levels measured by the Polludrone in the square.

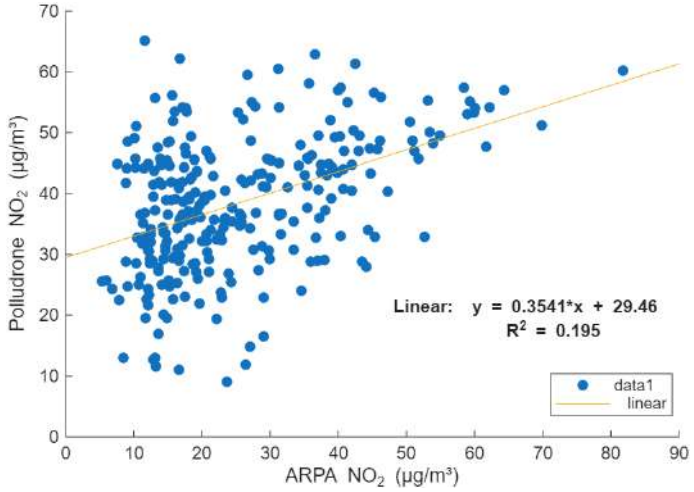

Figure 3.29. Linear correlation fit for nitrogen dioxide data, between reference ARPA and Polludrone concentrations.

The Polludrone proved to be unable to accurately estimate nitrogen monoxide (NO) concentrations, showing a consistent discrepancy with reference NO data. While NO concentrations obtained from the reference ARPA monitoring stations exhibit typical seasonality found in urban areas, with peak concentrations during the colder seasons and lower values during the hotter months, nitrogen monoxide trend outputted by the Polludrone follows an almost opposite trend, with an increase during the summer months (figure 3.30). Moreover, NO concentrations reported by the Polludrone appear to consistently follow the temperature trend over time reported by the device. This could suggest how the output of NO data is more dependent on the temperature value measured by the instrument itself than on the actual signal detected by the sensor in the proprietary algorithm employed by Oizom. Given these limitations, the Polludrone NO concentration during this first monitoring period shows no correlation with reference ARPA data, as reported in figure 3.31. These initial data obtained for the Polludrone air quality monitoring unit have highlighted some technical limitations of the device and the machine learning algorithm employed for continuous in-site calibration. While the device has performed reasonably well in monitoring PM and ozone, there are clear limitations in accurate detection of nitrogen oxides (NO_X) concentrations. Currently, given the results obtained, the Polludrone stands out as a valuable tool for monitoring pollutants as well as environmental and

meteorological conditions, although it still demonstrates the need for continuous control and calibration interventions on a seasonal or monthly basis.

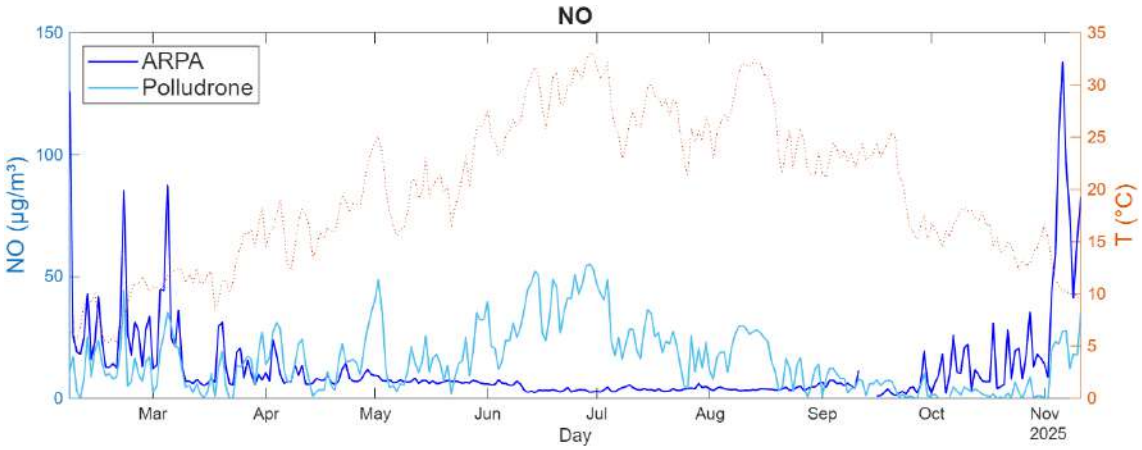

Figure 3.30. Nitrogen monoxide (NO) concentration trend over time as daily averages for the Polludrone and reference ARPA data. The orange dashed line represents relative humidity levels measured by the Polludrone in the square.

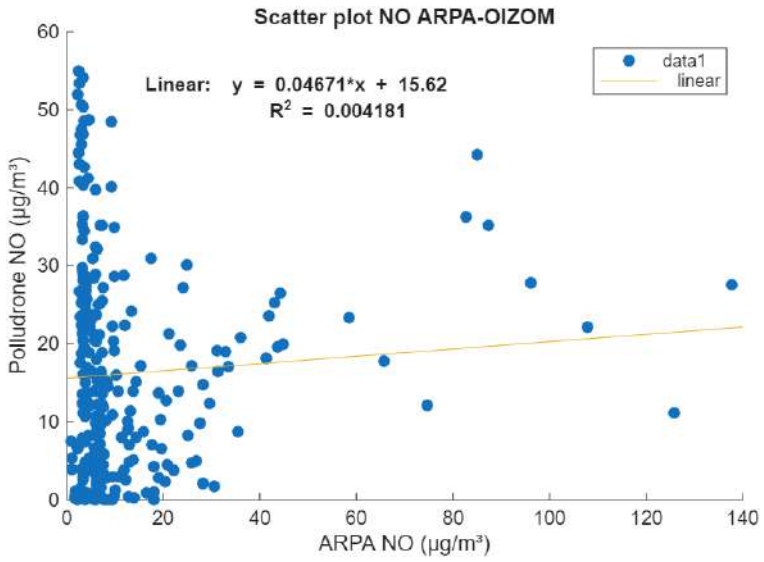

Figure 3.31. Linear correlation fit for nitrogen monoxide data, between reference ARPA and Polludrone concentrations.

The installation of four Purple Air Flex devices in the four corners of Piazza della Scienza (referred to as U1, U2, U3 and U4) following the completion of urban regeneration activities has enabled real-time, continuous and evenly distributed sampling of atmospheric particulate matter across the square. This configuration

allows for more accurate evaluation of PM concentrations and detection of any emissions events in specific locations. As each Purple Air Flex device is equipped with two separate PMS low-cost sensors for better data accuracy, in the following evaluation data from each of the deployed PA devices is reported a single value obtained as average of the two composed sensors.

An intercomparison between the four deployed Purple Air conducted over a period of seven months showed excellent agreement and repeatability of measurement between the devices for all three PM fraction (PM_1, $PM_{2.5}$ and PM_{10}), as observed in figure 3.32. The only differences are represented by very high concentration peaks, detected by a single instrument located in the square. Given the short duration of these increases, these peaks can be linked to individual sources or processes occurring in the respective corners. The square is in fact a place frequented by university students and workers, as well as by a wide variety of activities. Furthermore, the sensors are positioned in places where students frequently meet and gather, thus exposing them to emissions such as cigarette smoke, and relatively near the underground parking exits and entrances, thus exposing them to potential vehicle emissions.

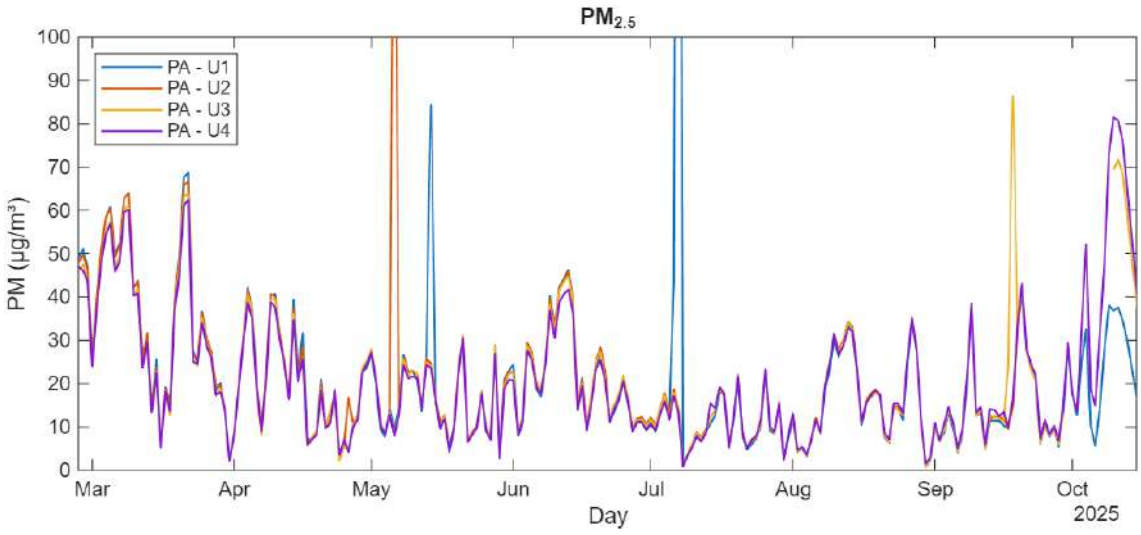

Figure 3.32. Particulate matter (as PM2.5 fraction) concentration trend over time as daily averages for the four Purple Air Flex devices installed on the square. Each devices is named after the relative corner of the square where it was installed.

Purple Air PM concentrations were then evaluated against reference data from the reference ARPA monitoring station of Milano Pascal. Given the high precision in PM measurement observed between the four deployed PA devices, the following evaluation will be conducted considering the average of the four sensors as a single value representing the square. PM concentrations obtained from the PA devices in the square followed closely the overall trend in concentration reported by ARPA reference data, for both $PM_{2.5}$ and PM_{10} fractions, as shown in figure 3.33 and 3.34. However, PA data clearly overestimates PM concentrations in both fractions, as highlighted by the slope of linear fit equal to s = 1.78 for $PM_{2.5}$ and s = 1.42 for PM_{10} (figure 3.35). Observing the trend over time in relation to the relative humidity levels measured in the square, it appears how the overestimation reported by the PA sensors is more pronounced during days with high relative humidity. Overall, the PA sensors correlate well with reference ARPA data, with coefficients of determination equal to $R^2 = 0.66$ for PM_{10} and $R^2 = 0.66$ for $PM_{2.5}$.

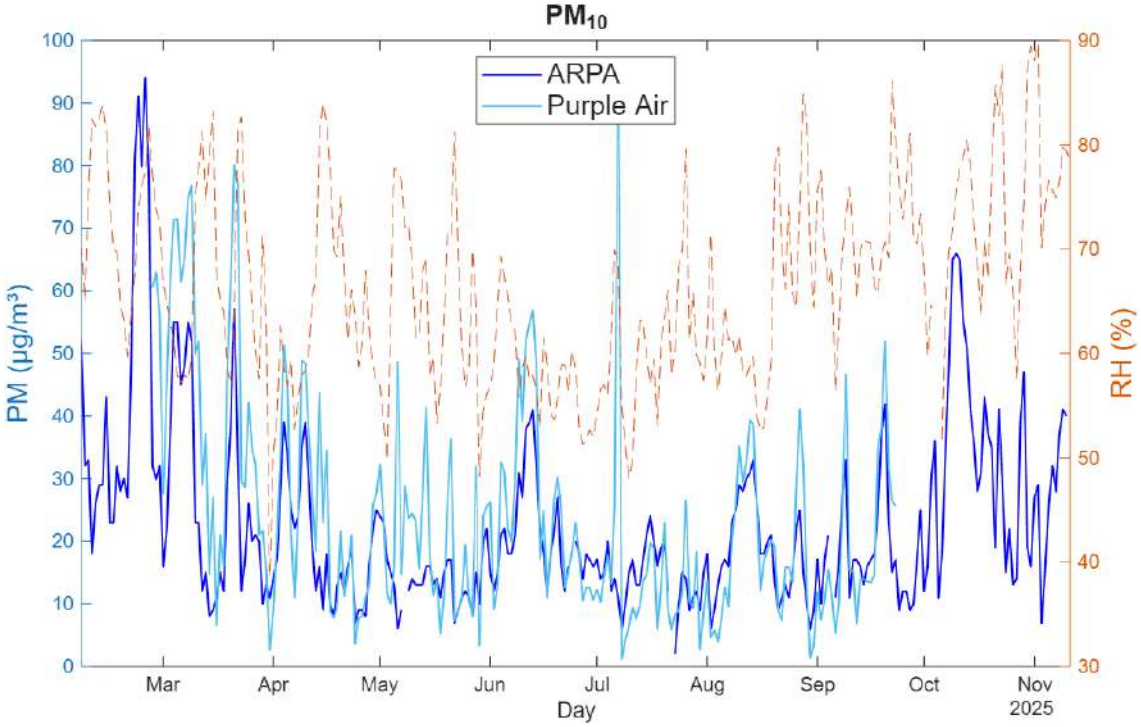

Figure 3.33. PM_{10} concentration trend over time as daily averages for the Purple Air (as average of four devices) and reference ARPA data. The orange dashed line represents relative humidity levels measured by the Polludrone in the square.

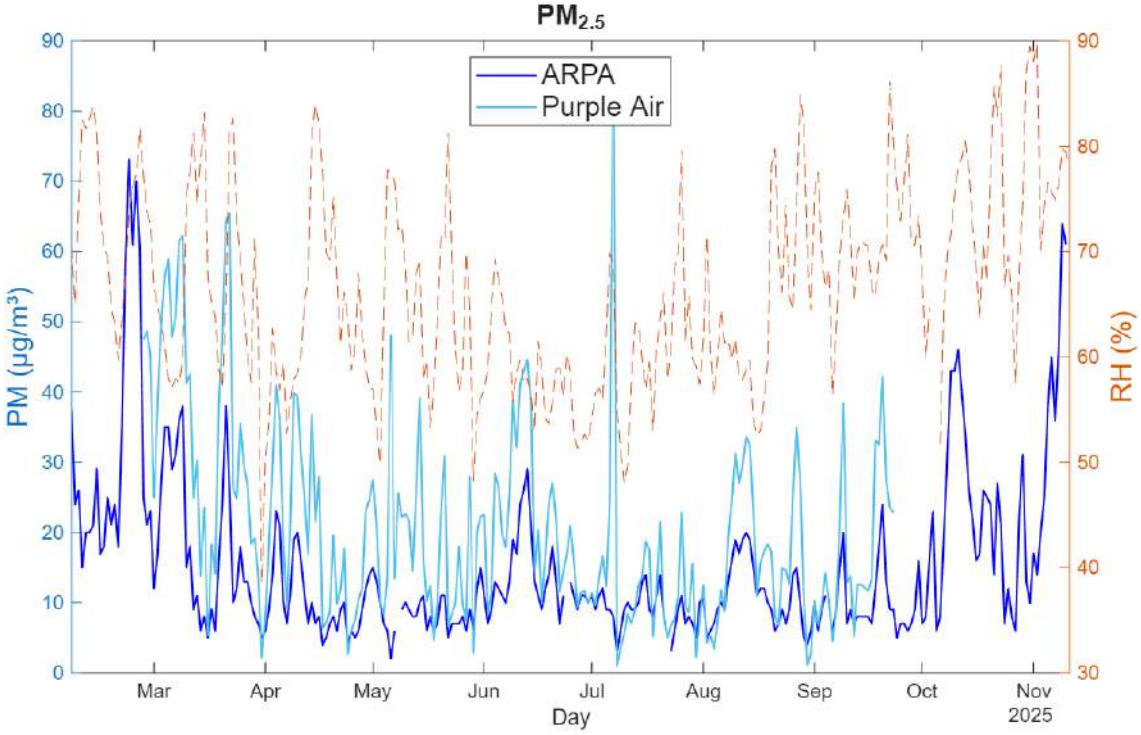

Figure 3.34. $PM_{2.5}$ concentration trend over time as daily averages for the Purple Air (as average of four devices) and reference ARPA data. The orange dashed line represents relative humidity levels measured by the Polludrone in the square.

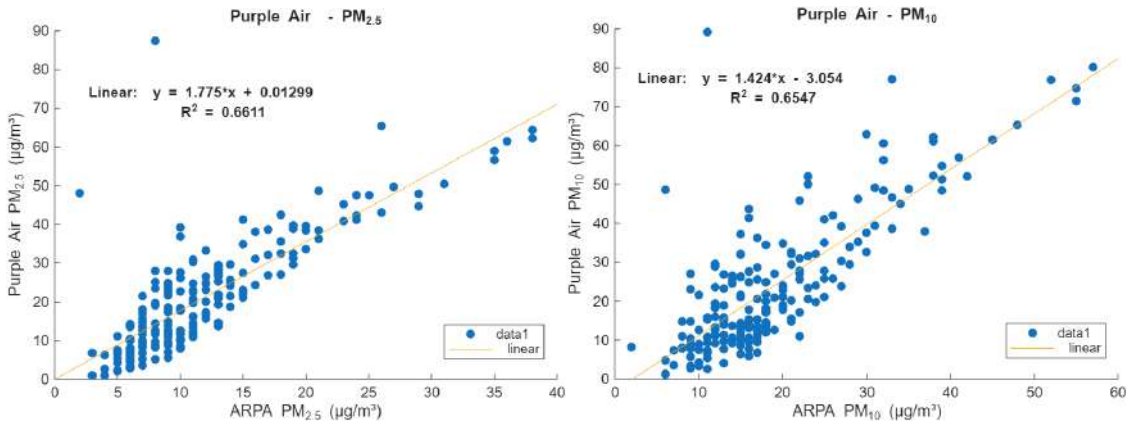

Figure 3.35. Linear correlation fit for $PM_{2.5}$ (left) and PM_{10} (right) data, between reference ARPA and Purple Air (as average of four devices) concentrations

For an initial correction of PM data, the corrective algorithm C.F. = 3.4 proposed by Wallace et al. (2022) and implemented directly in the online interface of the Purple Air sensors was applied to the raw PM data. The correction factor

significantly improved the overall correlation with reference ARPA data for both $PM_{2.5}$ and PM_{10}, with a R^2 coefficient for linear fit equal to $R^2 = 0.93$ and $R^2 = 0.82$ respectively. For the $PM_{2.5}$ fraction the applied correction only slightly improved the overestimation, with a slope of linear fit of s = 1.72. For the PM_{10} fraction, while the linear regression fit for corrected PM concentrations showed improved data correlation, a quadratic correlation appeared to be the best fit, with a R^2 coefficient of $R^2 = 0.87$. Moreover, for PM_{10} the correction actually significantly increased the overestimation, with a slope of linear fit of s = 5.2. This behaviour observed for the coarser fraction reflects what has been reported by the manufacturer itself and by previous laboratory and field comparisons (as reported by the AQMD), whereby these instruments are unable to accurately detect PM_{10} concentrations. The manufacturer Purple Air itself defines the PA Flex sensor as a particle monitor suitable for monitoring $PM_{2.5}$, defining PM_{10} measurements as unreliable. Nevertheless, this initial analysis shows that the Purple Air sensors perform comparably to reference data for both $PM_{2.5}$ and PM_{10} fractions, despite a moderate correlation. After implementing the proposed correction factor C.F. = 3.4, the corrected $PM_{2.5}$ data showed excellent correlation with reference PM concentrations, proving to be a useful tool to improve data accuracy in field monitoring. However, given the moderate overestimation still present after data correction, a site-specific correction factor could further improve PA data.

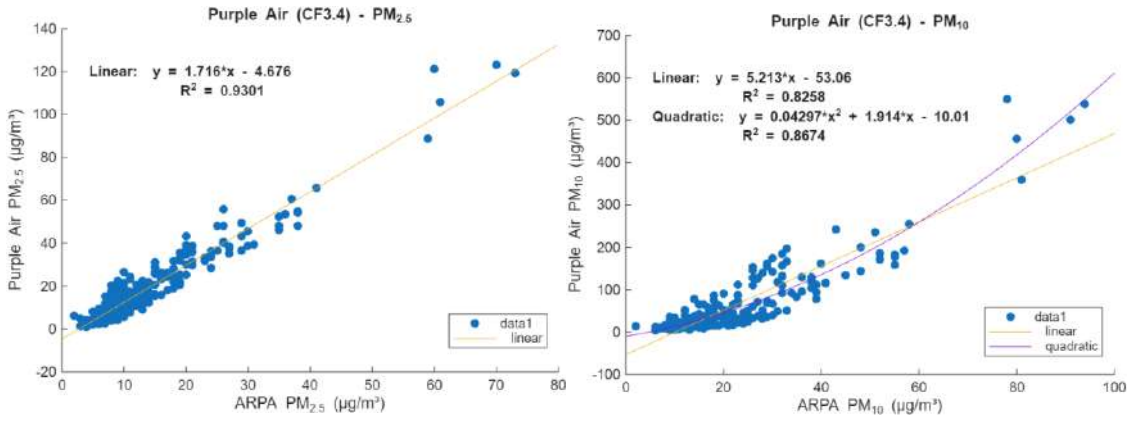

Figure 3.36. Linear correlation fit for $PM_{2.5}$ (left) and PM_{10} (right) data, between reference ARPA and Purple Air (as average of four devices) concentrations after the application of the CF = 3.4 correction factor.

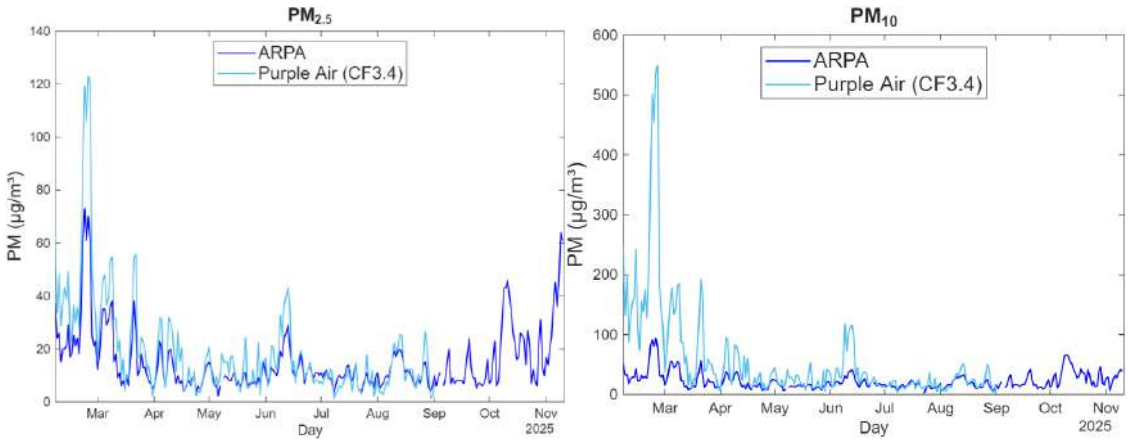

Figure 3.37. $PM_{2.5}$ (left) and PM_{10} (right) concentration trend over time as daily averages for the Purple Air (as average of four devices) and reference ARPA data.

3.4. Discussion

As urban regeneration becomes one of the main drivers of growth in modern cities, there is an ever-increasing need for a constant flow of data to facilitate decision-making, steer towards sustainability in all its forms, while protecting citizens' health and well-being. As low-cost sensors are proving to be a valuable tool for complementing environmental monitoring, it is even more necessary to carry out precise assessment, calibration and deployment activities in an increasing number of environments and conditions. In the urban area of Milan, the MUSA ecosystem has pioneered this kind of initiative through the urban regeneration project of *Piazza della Scienza*, combining scientific research with the needs of the city and its citizens. Air quality monitoring during the redevelopment project on the square carried out two main activities involving the application of low-cost sensors: assessing the impact of the project activities on the air quality in the square, monitoring particle emissions and quantifying the overall impact of the construction phase as well as for the entire regeneration project; the installation and analysis of sensors for continuous, real-time monitoring of atmospheric pollutants on the square, with the aim of guiding scientific research and fostering interest and awareness of environmental issues among students and citizens.

The application, against reference instrumentation, of the low-cost and portable sensors (OPC-N3, Alphasense; Partector-2, Naneos) in monitoring the progress of the square's regeneration work in its three main phases (pre-construction, construction and post-construction) highlighted the strengths and limitation of this new type of instrumentation, which is becoming an increasingly important focal point in the field of air quality. The Partector-2 device showed great correlation and comparability with the reference monitor (Nanoscan SMPS, TSI) employed, proving to be a great asset for monitoring nanoparticles concentrations with high time resolution. The low-cost OPC-N3 showed excellent correlation with the reference optical particle counter (Environmental Dust Monitor, Grimm), although a severe underestimation of PM concentrations has been reported. Obtaining site-specific correction factors from the comparison with the reference data from the OPC Grimm, based on the computation of new apparent densities to replace the constant value used by the low-cost instrument, led to a significant improvement in the data returned by the sensor during all three construction phases of the urban regeneration plan in *Piazza della Scienza*. After calibration, the low-cost sensor dataset was employed in the assessment of the urban regeneration project impact on air quality. Firstly, the impact of the construction works required to renew the university's spaces was assessed. This work mainly involved removing the old flooring and laying new materials, moving soil to plant new green areas, and de-sealing the soil to improve rainwater drainage. The calculated impact for the entire construction phase for PM mass concentrations was 11.1 ± 23.8 $\mu g/m^3$ for PM_1, 33.6 ± 53.0 $\mu g/m^3$ for $PM_{2.5}$ and 82.1 ± 79.4 $\mu g/m^3$ for PM_{10}. For PNC in the nanometric fraction, the calculated impact was -3318.3 ± 3825.6 cm^{-3}. While PM concentrations showed an increase in all three fractions, only for PM10 the increase was statistically significant. Nanometric PNC showed a general decrease during this phase, although a net zero impact cannot be excluded given the high uncertainty (CI at 95% confidence level) in the calculation. For indoor environments, the calculated impact for the entire construction phase for PM mass concentrations was 0.3 ± 6.9 $\mu g/m^3$ for PM_1, 3.9 ± 12.6 $\mu g/m^3$ for $PM_{2.5}$ and 2.3 ± 29.2 $\mu g/m^3$ for PM_{10}. For PNC in the nanometric fraction, the calculated impact was -8056.3 ± 2418.4 cm^{-3}. Similar to the outdoor case, the increase observed for PM is not statistically significant. For

PNC, on the other hand, there is a significant decrease in concentrations, mainly attributable to the air circulation and air conditioning system present in the university campus environments, effectively capable of removing finer particles. The second impact assessment was conducted during the post-construction phase, after all renovation work on the square had been completed and following its reopening to the public. This allowed for an assessment of the urban regeneration project and the innovations proposed by the MUSA ecosystem within the square as a whole. During the post-construction phase the derived impact on PM mass concentrations was -5.2 ± 5.5 μg/m^3 for PM_1, -5.6 ± 6.4 μg/m^3 for $PM_{2.5}$ and -5.9 ± 8.6 μg/m^3 for PM_{10}. For PNC in the nanometric fraction, the calculated impact was 5640.1 ± 4588.5 cm^{-3}. All three PM fractions showed a decrease in concentration after work completion; however, the uncertainty in the calculation precludes the ability to assert with statistical significance that the decrease is not zero. This result is predictable, as the measures taken to renovate the square are unlikely to have a significant impact on air quality and particle emissions, usually dominated by the local urban background concentrations. For PNC in the nanometric fraction, however, a statistically significant increase in concentration was observed. While this trend is detrimental to the overall air quality of the square, the result is consistent with some of the modification of the square environment: in fact, this positive impact could be explained by increased emissions of biogenic volatile organic compounds (VOCs) following the higher vegetation cover of the square, resulting in the formation of secondary organic aerosols (SOA) from nucleation and condensation processes in the atmosphere. For indoor environments, the calculated impact in the post-construction phase for PM mass concentrations was -1.3 ± 1.4 μg/m^3 for PM_1, -0.8 ± 2.0 μg/m^3 for $PM_{2.5}$ and -2.5 ± 8.7 μg/m^3 for PM_{10}. For PNC in the nanometric fraction, the calculated impact was -286.9 ± 1227.3 cm^{-3}. Overall, the calculated impact on indoor environments showed a decreasing trend for all fractions monitored, albeit not being statistically significant. This result was expected, as the work mainly involved outdoor environments. To summarize, the construction work conducted on the square mainly resulted in an increase of PM concentrations in the coarse fraction, as expected given the nature of the type of work conducted. The overall assessment of the impact of the entire urban regeneration project in

Piazza della Scienza planned by the MUSA ecosystem showed a general downward trend in PM concentrations, suggesting that the measures taken have had a positive effect, although in general this decrease was not statistically significant enough to quantify this result with certainty. The positive impact observed in the increase in nanoparticles linked to the presence of greater green coverage in the square is, however, significant.

The second part of the project involved the installation of low-cost sensors (Purple Air Flex; Polludrone, Oizom) in fixed locations to facilitate continuous monitoring of pollutants. This initiative has the dual objective of promoting scientific research with a continuous flow of data on pollutant concentrations in the square, as well as promoting the dissemination of environmental issues related to pollution and involving students and citizens. The initial data analysed showed good agreement with particulate matter data from the ARPA Pascal reference station for both devices. For the Purple Air devices, the application of the correction factor (C.F. = 3.4) proposed in the scientific literature for outdoor monitoring greatly improved the sensors' correlation for the $PM_{2.5}$ fraction. Throughout the entire months of monitoring considered, both devices showed a general overestimation of PM concentrations. This result suggests the need to derive specific corrective factors for the environments of Piazza della Scienza and will be the main focus of future activities and studies conducted in the square. Regarding gaseous pollutants concentrations, the Oizom Polludrone proved to be effective in detecting O_3 concentrations throughout all the considered months; the device, however, showed some technical limitations in correctly assessing NO_X concentrations, mainly linked to the inability of the proprietary machine learning algorithm in managing changes in seasonality and environmental conditions. However, the future of Piazza della Scienza presents itself as an excellent field for air quality research, where the continuous supply of pollutant data will enable ongoing evaluation of the instruments and improvement of performance, as well as providing a space dedicated to dissemination.

4. Evaluation of the low-cost aethalometer bcMeter at an urban background site

Aiming to transform the city into a laboratory for sustainable urban innovation, the MUSA ecosystem envisioned the application of innovative technology for environmental monitoring. In this context the bcMeter, a low-cost device for environmental monitoring of black carbon, has become increasingly popular in recent years. As part of this work was conducted one of the first environmental monitoring campaigns employing the bcMeter, assessing its performance and accuracy in detecting black carbon (BC) concentrations against a reference aethalometer. The data obtained from this campaign and reported below are extensively detailed in the scientific paper by Doldi et al. (2025).

4.1. Introduction

As already detailed in chapter 1, Black Carbon (BC) is a major component of fine particulate. BC is usually directly emitted in the atmosphere as a result of incomplete combustion processes involving fossil fuels, biofuels, and biomass (Elomaa et al., 2024). The scientific literature extensively reports the detrimental effect of black carbon exposure on human health, climate and anthropogenic materials. Given its nature and size, BC can easily enter the respiratory tract, diffuse into the bloodstream, thus leading to negative health effects (Janssen et al., 2011; Segersson et al., 2017), increasing the risk of cardiovascular and pulmonary diseases, damaging vital organs, as well as an increase in cancer incidence (Caubel et al., 2018; Lequy et al., 2021). BC is also well known to alter the atmospheric radiative balance, by absorbing radiation in a broad spectral range, from ultraviolet (UV) to infrared (IR) wavelengths, and by functioning as cloud condensation nuclei, thereby modifying the properties and longevity of clouds (Chung et al., 2002; Zhang et al., 2011). Additionally, BC may also cause changes to the radiation balance on snow and ice-covered surfaces, leading to a positive feedback effect (Zhang et al., 2011; Rypdal et al., 2009). However, currently no specific regulation is in place to address the measurement and monitoring of atmospheric black carbon. Nevertheless, it has assumed an increasingly prominent role in the World Health Organization's guidelines

(Elomaa et al., 2024). While recently the revised EU Air Quality Directive (EU, 2024) has addressed BC measurements, specific thresholds for atmospheric BC concentrations must still be issued. Within the European Union, the environmental monitoring of BC concentrations is governed by the EN 16909:2017 standard (CEN, 2017), which establishes reference methods for the measurement of Elemental Carbon (EC) and Organic Carbon (OC) on filters, while the Aerosol, Clouds and Trace Gases Research Infrastructure (ACTRIS, 2024) recommends standard procedures and instrument specifications for BC monitoring in aerosol observatories.

Usually, black carbon is measured by means of offline filter-based instruments, or by employing optical detectors (Hagler et al., 2011), measuring the attenuation of a laser source at a specific infrared wavelength of 880nm though a filter (Hansen et al., 1984). Although these devices are able to measure BC concentration with high accuracy, the high cost and complexity of field deployment often limit spatial and temporal availability of black carbon measurements. This often restricts BC data availability to a restricted number of reference monitoring sites across the territory. In light of the recent WHO guidelines, which explicitly advocate for systematic measurements in urban areas to mitigate the ambiguity surrounding spatial and temporal variability of BC (WHO, 2021), the integration of low-cost sensors with conventional research-grade instruments holds considerable promise. This approach is poised to establish more intricate BC measurement networks, thereby substantially enhancing the spatial and temporal resolution of data acquisition. In this context fits the bcMeter, an innovative and small BC monitoring device, recently released open source and aimed at environmental and industrial monitoring and community use. The device functions on the same physical principle as a traditional aethalometer, namely the measurement of the attenuation of infrared light (IR, 880 mm) after absorption of BC on a filter. Thanks to its affordability (< 300€ for total bill of materials) and ease of assembly and use, the bcMeter is designed to enhance spatial coverage of BC measurements, whilst also fostering community engagement through citizen science initiatives. The present study evaluated the performance of two bcMeter sensors over a five-month period at an urban background site against a research-grade aethalometer. The employment

of the new low-cost sensor in this context enabled the highlighting of both its merits and shortcomings, whilst evaluating its accuracy in comparison to a research-grade aethalometer.

4.2. Materials and methods

In Chapter 2 re extensively detailed the technical characteristics and measuring principle of the bcMeter. This chapter will define the experimental methodology applied to conduct the monitoring campaign for the evaluation and calibration of the bcMeter.

This work saw the employment of two identical bcMeter (revision 3.3). It should be noted that the bcMeter is regularly updated with new software and hardware revisions by the developer, thus the revision employed in this study may not correspond to the most recent version of the device. Two bcMeter were installed from 17/05/2024 to 30/09/2024 in a monitoring container operated by the Institut für Umwelt & Energie, Technik & Analytik e. V. (IUTA) located at an urban background site in Mülheim-Styrum, Germany, (51.453459° N, 6.86505° E) (Asbach et al., 2024, Asbach et al., 2020). BC concentrations were compared to reference data (as hourly averages) obtained from an AE33 aethalometer (Magee Scientific) from a co-located container (hereinafter referred to as STYR) operated by LANUK (State Office for Nature, Environment and Climate North Rhine-Westphalia). As the bcMeter operates employing single wavelength, in this work reference aethalometer data was taken into account considering only absorption at 880 nm. Relative humidity (RH) values were obtained from a LANUK reference station LANUK located in Essen, Germany (name LAB1, coordinates 51.406846°N 6.965589°E), as the STYR monitoring station does not provide data relating to environmental and meteorological parameters. Both bcMeter devices were equipped with the standard filter employed in the AE33 aethalometer (M8060, filter scattering factor 1.39), and were set to sample at a flow rate of 0.25 l/min and a 5-minute time resolution, which was averaged to 1 hour resolution after data collection in order to allow direct comparison with data obtained from the LANUK station.

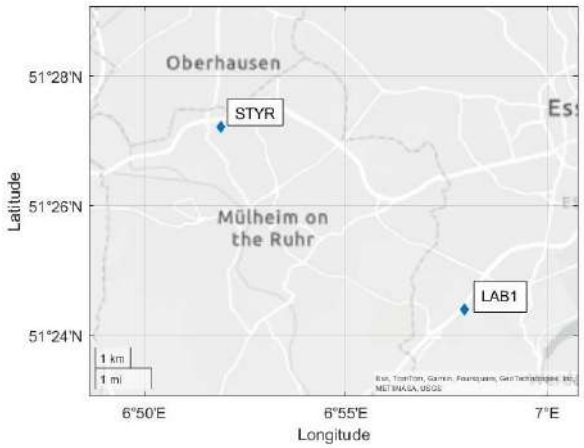

Figure 4.1. Location of the LANUV containers in Mülheim-Styrum and Essen (Doldi et al., 2025).

4.3. Results

During the campaign, data coverage was approximately 75% for both bcMeters. Both devices experienced a substantial loss of data, primarily attributable to software and firmware issues, which consequently resulted in disruptions to the sampling process. Furthermore, the inlet tube of bcMeter1 detached on two occasions during the course of the entire campaign, resulting in the sampling of air inside the container rather than that of the outdoors for a brief period. As these data are not indicative of the comparison, they were disregarded for both sensors as, during this period, the sampling line was open, and sampling involved mixed indoor/outdoor aerosol. Additionally, data exhibiting a negative ATN value, usually observed directly after each filter change, was discarded before data analysis as it can be a direct consequence of an instrumental bias. The percentage of negative ATN values observed relative to the total data collected was 8.3% for bcMeter1 and 11% for bcMeter2. From 19/09/2024 to 30/09/2024, bcMeter1 exhibited an abnormally high ATN value (ATN > 400) following a forced shutdown. While this value indicated a fully loaded filter, the actual filter was found to be only partially loaded with BC. Consequently, this data sample was identified as an outlier and was subsequently excluded from the analysis. Following the process of data cleansing, the percentage of valid data analysed was found to be 48.5% for bcMeter1 and 55.8% for bcMeter2. Table 4.1 summarizes the slope and coefficient of determination (R^2) values of linear correlation fit

obtained for both bcMeters against the AE33 aethalometer at different time averages. As shown in Figure 4.2, hourly averages of BC concentrations obtained for both bcMeters exhibit significant variability and cannot directly be employed in evaluating the sensor's performance. This is primarily attributable to the high instrumental noise of the implemented sensor, which has resulted in a substantial number of negative spikes in BC concentration. The linear correlation fit for both bcMeter and the reference LANUK AE33 aethalometer (figure 4.3) highlights how there is practically no correlation between the devices (R^2 = 0.22-0.28).

Averaging	bcMeter1		bcMeter2	
period	slope	R^2	slope	R^2
1 h	0.53	0.22	0.51	0.28
12 h	0.47	0.49	0.53	0.69
24 h	0.40	0.49	0.53	0.79

Table 4.1. Slope value and coefficient of determination (R^2) for each bcMeter vs. the reference AE33 for different data averages (Doldi et al., 2025).

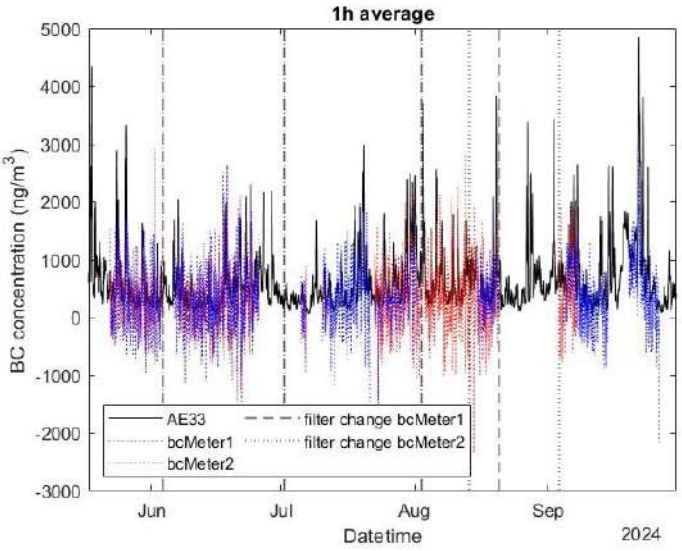

Figure 4.2. BC concentration over time as 1-hour averages for AE33 (black), bcMeter1 (red) and bcMeter2 (blue). Dashed and dotted lines indicate manual filter change procedures (Doldi et al., 2025).

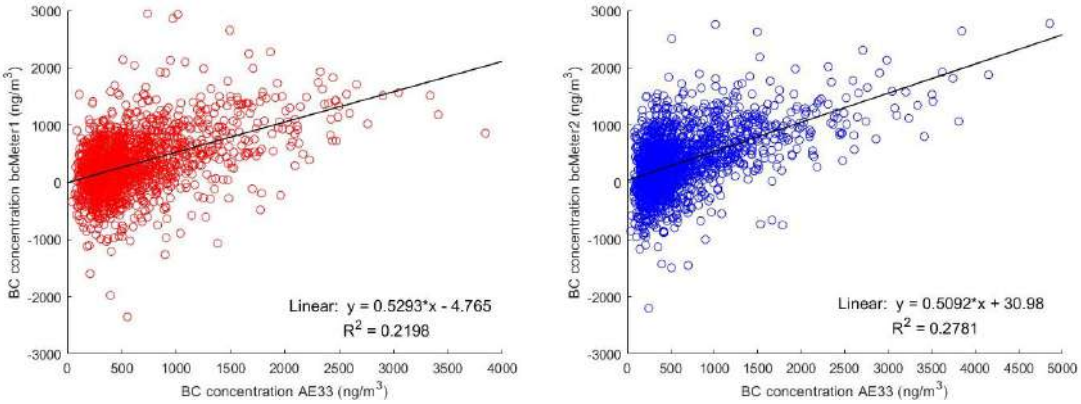

Figure 4.3. Linear fit for BC concentration (1-hour averages) for bcMeter1 (left) and bcMeter2 (right) vs. AE33 from LANUV with linear correlation fit (Doldi et al., 2025).

A reduction in the time resolution to 12-hour averages resulted in an overall improvement in data correlation for both bcMeter sensors when compared with the reference AE33. It was observed how both sensors demonstrated a comparable trend in BC concentration to that of the reference aethalometer. The reduction of instrumental noise in the BC concentration has brought to light a significant issue for the bcMeter: despite both sensors being identical, they have been found to perform rather differently. Specifically, bcMeter1 displayed increased data scattering, leading to a lower correlation (R^2 = 0.49) with the LANUK data compared to bcMeter 2 (R^2 = 0.69). Given that the two sensors were operated under identical setup and environmental conditions, the observed difference may be attributable to issues experienced throughout the campaign. Such issues included interruptions due to filter overloading and both software and firmware issues, as well as airflow fluctuations resulting from leakages in the 3D-printed case. The available data was insufficient to provide a comprehensive understanding of the precise factors contributing to the observed discrepancy between the two sensors. Daily (24-hour) averages revealed how both bcMeters displayed the same BC concentration trend as the reference AE33 aethalometer over time (see figure 4.4). Although the data from bcMeter1 is more scattered (R^2 = 0.49), the data from bcMeter2 correlated reasonably well with the reference sensor (R^2 = 0.79). A robust regression was conducted on daily averages for bcMeter1 to improve data dispersion. We removed the outliers identified by the model from the dataset, which resulted in an improved linear correlation fit (R^2

= 0.77) between the sensor and the reference AE33 (Figure 4.5). This provided comparable values as bcMeter2. It's important to note that while the outlier removal improved the data quality for bcMeter1, it also resulted in further data loss.

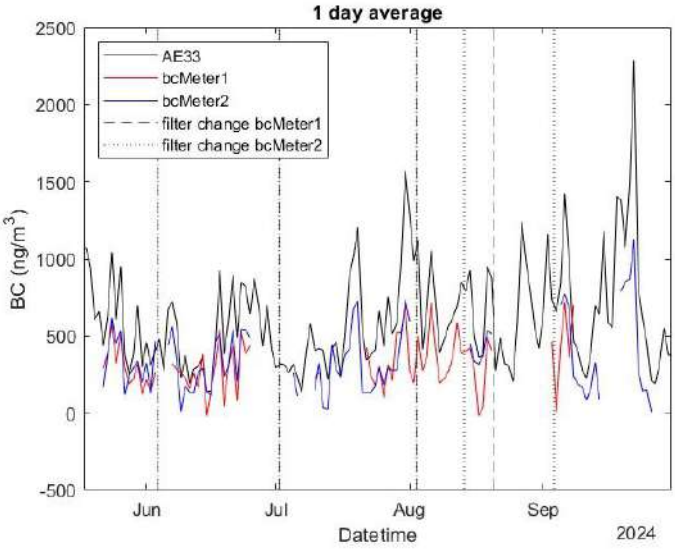

Figure 4.4. BC concentration over time as 24-hour averages for AE33 (black), bcMeter1 (red) and bcMeter2 (blue). Dashed and dotted lines indicate manual filter change procedures (Doldi et al., 2025).

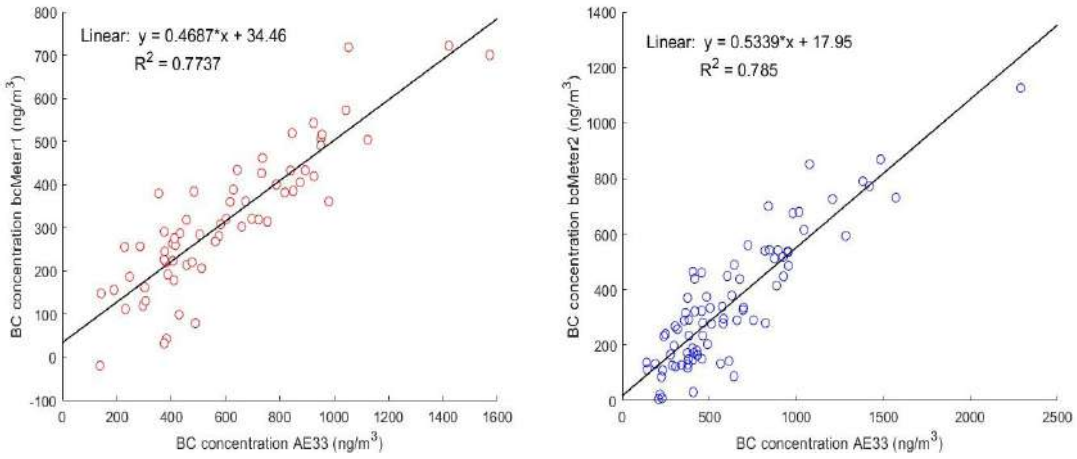

Figure 4.5. Scatter plot of BC concentration (daily averages) for bcMeter1 with outliers removed via robust regression (left) and bcMeter2 (right) vs. AE33 from LANUV with linear correlation fit (Doldi et al., 2025).

A consistent underestimation was observed for both bcMeters the entire monitoring campaign conducted. A possible reason for this underestimation could be explained by an inadequate airflow during sampling. In fact, even

though the air flow for both bcMeter was set to 0.25 L/min and the internal measurement reported an average of 0.2498 ± 0.0034 L/min (bcMeter1) and 0.2413 ± 0.0262 L/min (bcMeter2) (Figure 4.6), at the start of the monitoring period the effective flow measured at the inlet using an external flow meter was around half the reported value (0.12 L/min) for both sensors. As BC concentration and total airflow exhibit a linear relationship in the BC calculation algorithm employed by the bcMeter, the discrepancy highlighted between actual and reported airflow could account for the observed underestimation. There are two main contributing factors to the reported difference in airflow: first, the presence of air leaks in the 3D-printed case could lead to a loss in total airflow; moreover, an incorrectly calibrated flow controller could affect the airflow measure. For each sensor, a correction factor was calculated as the ratio of the average reported airflow (as measured during the entire monitoring campaign) to the externally measured flow (monitored with an externa flow meter and approximated to a fixed value of 0.125 L/min). Integrating the derived correction factors (1.9982 and 1.9301 for bcMeter1 and bcMeter2, respectively) in the BC calculation algorithm effectively corrected the underestimation reported for bcMeter2(slope of linear fit of s = 1.02), as shown in figure 4.8. Before outlier removal, the airflow correction applied to bcMeter1 could not account for all observed underestimation (slope of linear fit of s = 0.8). However, after data cleaning, the correction factor was effective in correcting most of the underestimation (slope of linear fit of s = 0.94). Results from this work suggest the bcMeter performance is heavily affected by fluctuations in BC concentrations that, as of now, cannot be linked to a specific cause. In order to account for the observed variability in the BC data, BC concentration obtained from the bcMeter was correlated to relative humidity (RH) readings recorded at the reference LANUK monitoring station located in Essen (LAB1). No significant correlation was identified, indicating that the observed variations in RH do not appear to have a substantial impact on the BC measurements acquired in this study. Furthermore, in order to investigate the potential effect of filter loading on black carbon concentrations, the measured BC was plotted against the attenuation (ATN) value reported by the sensor. The analysis revealed no significant

correlation between the data, thereby excluding filter loading as a potential cause of the substantial variations observed.

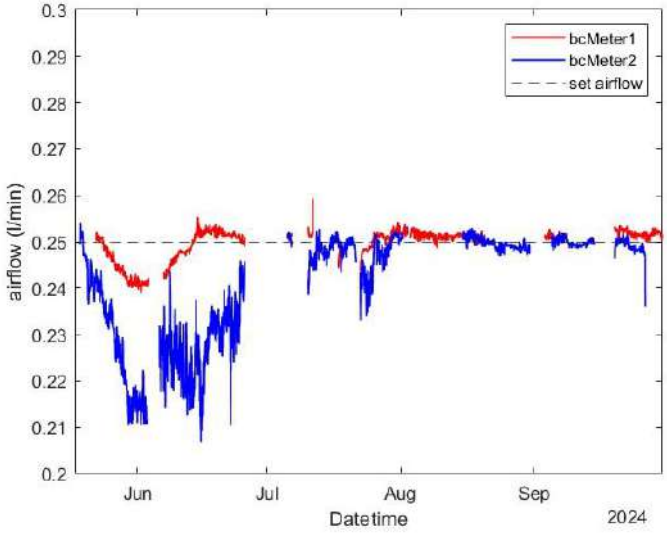

Figure 4.6. Reported airflow (1-hour averages) by bcMeter1 (red) and bcMeter2 (blue). Dashed line indicates the airflow value set at the instrument interface (Doldi et al., 2025).

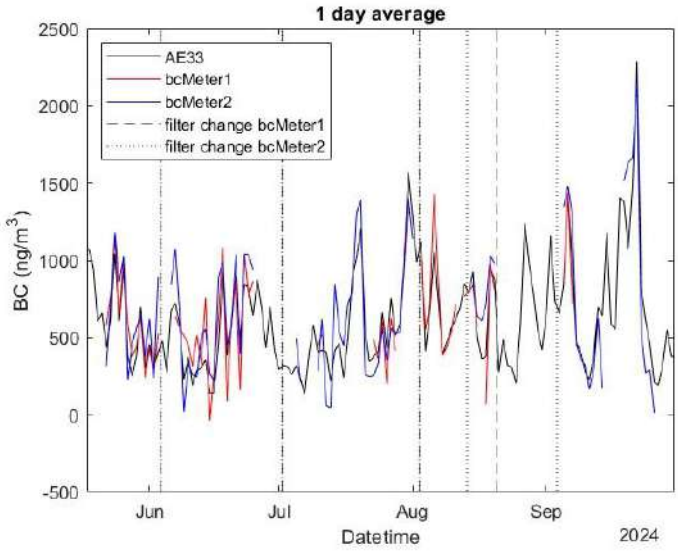

Figure 4.7. BC concentration corrected for the airflow as 24-hour averages for bcMeter1 (red) and bcMeter2 (blue), and BC concentration for the AE33 (black) obtained from the LANUV station in Mülheim-Styrum (STYR). Dashed and dotted lines indicate manual filter change procedures (Doldi et al., 2025).

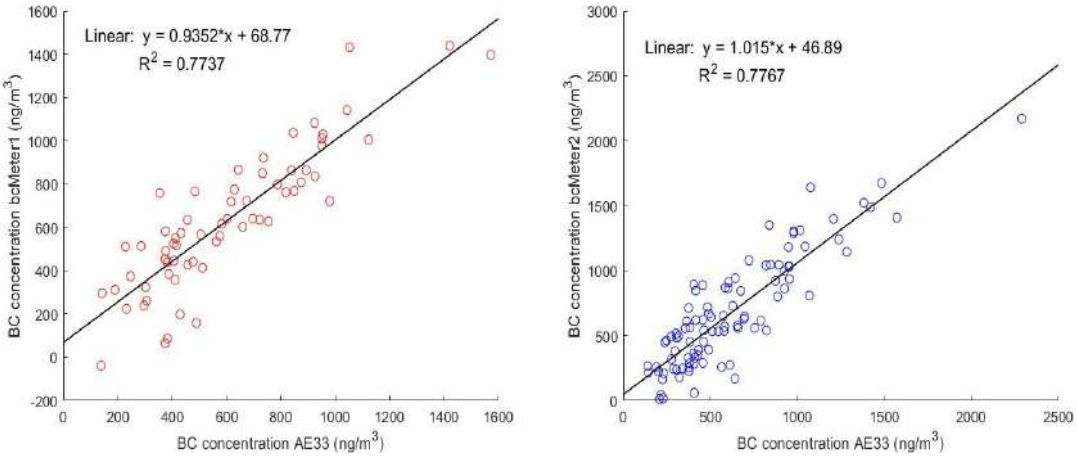

Figure 4.8. Scatter plot of BC concentration (daily averages) for bcMeter1 (left) and bcMeter2 (right) corrected for the airflow bias vs. AE33 from LANUV with linear correlation fit (Doldi et al., 2025).

4.4. Discussion

This study constituted on of the first application of the low-cost BC monitoring device bcMeter, assessing its performance in environmental monitoring in comparison with a standard reference aethalometer (AE33, Magee Scientific). In light of the growing focus of air quality monitoring in recent years, this device aims to provide an affordable solution for the measurement of black carbon in both environmental and industrial application. Thanks to its affordability, ease of assembly and user-friendly design, the bcMeter could foster significant community engagement and serve as a complementary resource for air quality research. During the five-month BC monitoring campaign conducted at an urban background location in Mülheim-Styrum, Germany, the effectiveness of the BC meter in assessing environmental BC concentrations was demonstrated. In summary, the two sensors exhibited a congruent trend in BC concentration over time, aligning with the reference AE33 aethalometer operated by the LANUV station in 24-hours averages. The two sensors employed in this study exhibited different performance levels. The bcMeter2 sensor demonstrated a strong correlation (R^2 = 0.78 for 24-hours averages) with the reference data, while the bcMeter1 sensor exhibited significant data dispersion, albeit being operated under identical conditions. Employing a robust regression for outlier removal led

to the reduction of data dispersion for bcMeter1, ensuring comparable correlation (R^2 = 0.77 for 24-hour averages) with the reference AE33 as obtained for bcMeter2. Additionally, it was found that an increase in temporal resolution (to 12-hour and 1-hour averages) resulted in a significant amplification of the impact of instrumental noise, leading to highly scattered BC concentrations that could not be meaningfully analysed. This study revealed a consistent underestimation of BC concentrations by both sensors. This discrepancy was attributed to a disparity between the actual airflow measured at the inlet though an external flowmeter and the value reported by the internal flow controller. The observed discrepancy could be attributed to a number of factors. Firstly, the airflow controller mounted on the device may have been improperly calibrated, requiring a specific correction. Moreover, leakage resulting from the 3D-printed outer case likely led to a reduction in the total airflow at the inlet. Furthermore, the manufacturer recently reported an issue with the design of the outer case of the bcMeter, as some devices were released with a softer air seal, which could result in a loss in airtightness over time. To address the underestimation found in this work, a correction factor was obtained as the ratio of the average reported flow to the externally measured value. The proposed correction was effective in correcting data for one of the sensors (bcMeter2), successfully addressing the underestimation (with a slope of linear fit of s = 1.02 for 24-hour averages, after correction). For bcMeter1, the proposed correction factor successfully compensated the found underestimation (resulting slope of 0.94 for 24-hour averages) after outlier removal. Overall, the bcMeter achieved comparable results to a reference aethalometer (AE33, Magee Scientific) for daily averages. Nevertheless, the sensor exhibited several technical limitations that affected the whole campaign, resulting in frequent interruptions to the measurements. Some of the outages experienced could be explained as results of software and firmware issues, while defects in the structure of the outer 3D-printed case may have resulted in air leakages. These leakages, along with pump malfunctions and an inaccurate calibration of the internal flow sensor. Furthermore, the manufacturer reports that the sensor is highly sensitive to changes in temperature and light, which can cause signal distortion and data fluctuations. It should be noted that the version of the bcMeter (revision 3.3) employed in this study is currently an

outdated version, as the bcMeter is regularly improved and updated by the manufacturer at both software and hardware levels. Recent revisions have already addressed some of the hardware and software issues reported in this work, per the manufacturer. Considering the substantial data dispersion at higher time resolutions, the bcMeter version (revision 3.3) evaluated in this study proved to be inadequate for short-term environmental monitoring of BC. Nevertheless, the sensor emerges as a promising option for future monitoring networks daily 824-hours) data resolution is sufficient. To summarize, the results of this study suggest how the bcMeter is a promising tool for monitoring atmospheric BC concentrations with a wide spatial resolution and at low cost. In consideration of the sensor's capabilities, the bcMeter has the potential to facilitate applications in a range of indoor and outdoor settings where the accessibility of BC concentration data remains limited. Still, there are several shortcomings in the design and components of the sensor, especially with regard to airflow control, air leakage from the 3D-printed housing, and inter-sensor variability. Overcoming these issues is essential for the bcMeter to become a more reliable BC monitoring tool with adequate data coverage.

5. Low-cost sensors for Cultural Heritage Preservation: The Case of the "Grande Brera" Museum Complex in Milan

5.1. Introduction

As described in detail in Chapter 1 of this work, atmospheric pollutants can negatively impact, among many others, materials of anthropogenic origin. Of particular note are materials concerning our cultural heritage, encompassing historic buildings, sculptures, paintings and frescoes, as well as works that have exerted any artistic or cultural influence on the annals of world history. Preserving this heritage is therefore essential to avert incalculable losses. This preservation process primarily involves protecting heritage assets from atmospheric agents and pollutants, always present in the atmosphere and consequently incessantly in contact with the works. However, in the field of cultural heritage conservation, predicting the impact of air pollution on materials is a complex task due to the high variability of atmospheric contaminants, which behave differently depending on the materials involved. As an example, wood and bricks, commonly used as building materials, react differently than marble statues or canvas paintings (Morabito et al., 2012). Most cultural heritage sites and artworks are usually located in urban or heavily anthropized areas, thus directly affected by high concentrations of atmospheric agents and pollutants (Sablier & Garrigues, 2014). In addition, most cultural heritage artifacts are located within indoor environments, such as museums, libraries, or historic buildings. This further influences the variability of atmospheric contaminants, as each indoor environment has specific characteristics and is highly subject to a number of environmental and architectural factors. While outdoor environments are extensively studied and regulated by specific legislation on atmospheric pollutants, scientific research on indoor environments is still limited and has only gained prominence in recent years. Recently, the UNI 11976:2025 standard defined specific guidelines for assessing indoor air quality (IAQ). This legislation defined key parameters to be monitored in sensitive environments, including atmospheric particulate matter ($PM_{2.5}$, PM_{10}), CO_2 and volatile organic compounds (VOCs), defined standardised monitoring protocols, i.e. the need for

seasonal monitoring to assess differences between summer and winter periods, and promoted the integration of and continuously monitored ventilation systems regulated according to actual environmental conditions. However, the purpose of this legislation is aimed at human health protection and increasing energy efficiency in buildings, with no specific recommendations for the preservation of cultural heritage. The protection of these environments is therefore still subject to decisions based on the specific conditions and needs of each environment.

Indoor monitoring within cultural heritage environments is often limited by certain features of traditional instruments employed for pollutant monitoring, which are often difficult to operate, bulky and loud. Furthermore, the need to monitor multiple, vastly different environments makes monitoring through traditional research-grade devices time-consuming and cost-intensive. This often results in a limited spatial and temporal resolution in the measurements, frequently failing to correctly detect fluctuation in pollutants concentrations over time and short-lived emission peaks (He et al., 2004). For this reason, the implementation of low-cost sensors for monitoring atmospheric pollutants is becoming increasingly popular in indoor environments. This type of sensor provides much greater spatial and temporal coverage than traditional instruments, at the expense of lower accuracy and precision in the measurements. Nevertheless, with proper testing and calibration targeted at specific environments, these devices could prove highly effective in complementing air quality measures alongside traditional instruments and methodologies.

This project involved monitoring of atmospheric pollutants in various cultural heritage indoor environments, combining traditional research-grade instruments with low-cost devices, ensuring greater coverage of data as well as a technical evaluation of the low-cost sensors implemented. During this project, exploratory monitoring campaigns were carried out within the "*Grande Brera*" museum complex in the city of Milan (Italy), which includes the Brera Art Gallery (*Pinacoteca di Brera*), *Palazzo Citterio*. In particular, the Pinacoteca di Brera and Palazzo Citterio environments have not been subjected to any type of environmental monitoring of atmospheric pollutants or ambient parameters to this date. This project therefore aims first and foremost to provide an initial assessment of the environments in which works of cultural significance are

displayed, monitoring particle concentrations, both as a mass fraction of atmospheric particulate matter (PM) and as a numerical concentration, with particular attention to the nanometric fraction. In addition, black carbon (BC) concentrations were monitored employing the low-cost bcMeter sensor, already described in Chapter 4. BC, which is highly relevant in the field of cultural heritage preservation, is mainly emitted by incomplete combustion processes and is therefore an excellent tracer of outdoor emissions and a good indicator of any infiltration of pollutants from outdoor air. Through these preliminary exploratory campaigns, it was possible to identify the most critical areas, as well as possible sources of emissions, and assess the influence of visitors within the selected environments. In addition, the initial data will allow for precise tuning of the ventilation and air conditioning systems present within the environments, in order to ensure the best preservation of displayed works.

5.2. Materials and methods

The monitoring campaigns carried out at the *Pinacoteca di Brera* and *Palazzo Citterio* followed the same experimental design. During April and May 2025, a total of six exploratory campaigns were carried out for each of the selected environments. Each sampling was carried out in three repetitions, to ensure statistical variability, for each selecting one day open to visitors and one day when the museums were closed, with only staff and workers allowed inside. The distinction in the monitoring process enabled the quantification of the impact of visitors on the designated environments. The selected museum environments were monitored in terms of atmospheric particles, measuring the mass concentration as PM fraction (PM_{10}, $PM_{2.5}$ and PM_1) and the particle number concentration (PNC) in the nanometric fraction, as well as the respective size distributions. Sampling was conducted following two separate methodologies: a mobile sampling, employing portable research-grade sensors, and fixed monitoring deploying low-cost devices in selected environments of interest. Mobile monitoring was carried out with portable reference sensors following the standard museum visiting itinerary, sampling in each room for a total time ranging from 5 to 15 minutes. PM concentrations and relative size distribution in

the range 0.25-32 μm were monitored by means of the optical particle counter Environmental Dust Monitor model 1.107 (GRIMM Aerosol Technik GmbH), hereinafter referred to as OPC Grimm. PNC in the nanometric fraction and relative size distribution in the range 10-420 nm were monitored employing a Nanoscan SMPS model 3910 (TSI); this sensor was coupled with the portable and smart sensor Partector-2 (Naneos) to monitor nanometric PNC with high temporal resolution (1 sec). Technical specifications for these sensors are detailed in Chapter 2 of this paper. All sensors were mounted on a moving platform to allow easy movement between sampling locations (figure 5.1).

Figure 5.1. Employed sensors for the Pinacoteca di Brera and Palazzo Citterio campaigns, mounted on a moving platform to allow fast switching between sampling locations.

Mobile sampling in the *Pinacoteca di Brera*'s environments was conducted over 28 sampling locations, selected between exhibition rooms containing paintings and sculptures, areas undergoing renovation or art restoration, the museum bar and a location on the outdoor terrace of the art gallery, to provide an outdoor reference point. The selected points and the itinerary followed during each sampling are highlighted on the art gallery map in Figure 5.2. For *Palazzo Citterio*'s environments, a total of 19 sampling locations were selected. The chosen locations include exhibition rooms, the ticket office on the ground floor and an outside area as an outdoor reference point. Selected points and the

followed itinerary are highlighted on the art gallery map in Figure 5.3. Mobile sampling of selected environments was then coupled with monitoring of pollutants at fixed locations selected in specific areas of interest within the respective museums, employing low-cost devices. PM concentrations and relative size distributions in the range 0.35-40 μm were monitored by means of four low-cost optical particle counters OPC-N3 (Alphasense). Additionally, BC concentrations were measured with two low-cost aethalometers bcMeter. The technical specifications for these sensors are outlined in Chapter 2 of this work. As regards the Brera Art Gallery, the four points of interest selected were: the museum cafeteria (*Caffè Fernanda*), a place characterised by a large number of visitors on opening days, typical catering activities, an opening to the outside leading to a direct exchange of air, and the presence of works of artistic interest in the environment itself; room 7, where Andrea Mantegna's famous painting "Cristo Morto" is displayed; room 24, where three of the gallery's most famous works are on display ("*Sposalizio della Vergine*" by Raffaello Sanzio, "*Pala Montefeltro*" by Piero della Francesca and "*Cristo alla colonna*" by Donato Bramante); , where Francesco Hayez's famous painting "*Il bacio*" is displayed. The selected exhibition rooms are among those with the greatest artistic and cultural interest and, as a result, are subject to a higher average flow of visitors. OPC-N3 sensors were installed in each of the selected rooms, while the two bcMeters were installed in the cafeteria and in room 24. Concerning Palazzo Citterio, the four sampling points of interest selected were: the ticket office near the entrance, a point with a high influx of visitors, a direct opening to the outside and the presence of carpeted flooring; room 40, one of the museum's main exhibition rooms, which houses Pellizza da Volpedo's painting "*Fiumana*"; areas A and C2, sections of the museum located on the second floor and dedicated to more modern exhibitions. The fixed sampling locations were chosen both for monitoring purposes and due to technical necessities agreed upon with the museum management. OPC-N3 sensors were installed in each of the selected environments, while the two bcMeters were installed in room 40 and area C2.

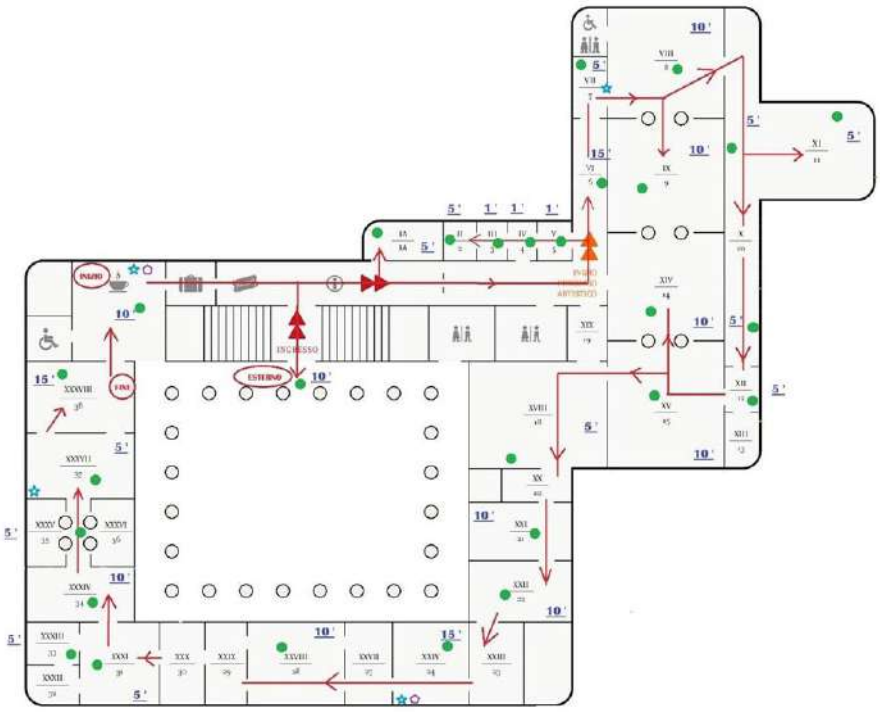

Figure 5.2. Detailed map of the Pinacoteca di Brera art gallery. The red arrows show the followed monitoring itinerary. Green dots indicate sampling position for mobile monitoring in each selected environment, while azure stars indicate the selected positions of installed low-cost devices.

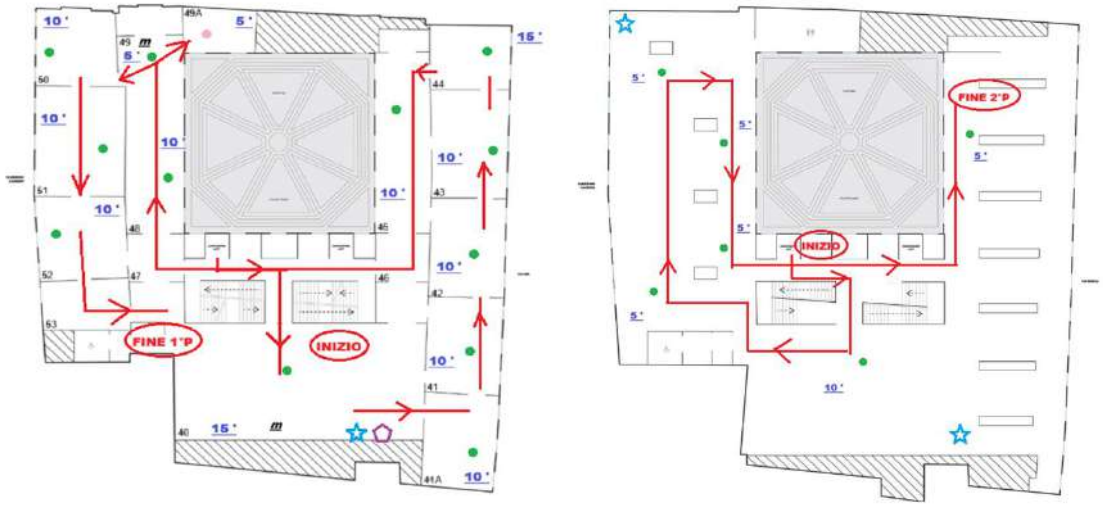

Figure 5.3. Detailed map of the Palazzo Citterio art gallery, for the first (left) and second floor (right). The red arrows show the followed monitoring itinerary. Green dots indicate sampling position for mobile monitoring in each

selected environment, while azure stars indicate the selected positions of installed low-cost devices.

5.3. Results

5.3.1. Air quality assessment of the selected museum's environments

The mobile monitoring carried out in the museum indoor environments at the *Pinacoteca di Brera* and *Palazzo Citterio* provided an initial assessment of the environments in terms of air quality, highlighting the spaces more exposed to atmospheric pollutants, while identifying the main sources of emissions within the monitored environments. Figures 5.4 and 5.5 report average PM and nanoparticle concentrations over all monitoring activities conducted in the gallery. Average PM concentrations were generally lower than the outdoor reference location for most of the monitored exhibition rooms. For Room 1A, located directly after the entrance and ticket office and before the actual exhibition halls, an average PM_{10} concentration of 176.9 ± 9.6 $\mu g/m^3$ was reported. The measured value was linked to maintenance and construction work carried out during the same period in the area directly opposite the room, which led to a marked emission of particles, especially in the coarse phase. The emission of particles resulting from these activities also affected adjacent rooms (rooms 2, 3, 4, and 5), although to a lesser extent due to the glass door that effectively isolates the gallery entrance from the exhibition spaces. As expected, the museum cafeteria (Caffè Fernanda) showed comparable values to outdoor concentrations, as this environment is subjected to significant air exchange with the outside due to the presence of automatic doors opening onto outdoor areas. The same conclusions can be drawn for PNCs in the nanometric range, with a significant impact observed due to maintenance work in front of room 1A. Regarding PNCs in the nanometric faction (figure 5.5), similar considerations can be drawn, with a strong particle emission observed due to maintenance work in the area facing room 1A and an average concentration comparable to the values outdoor values detected in the museum cafeteria, while concentrations measured in most exhibition rooms were significantly lower than reported outdoor concentrations. By decoupling the measurements taken on opening and closing days, an average

increase in concentrations was observed in the gallery's exhibition rooms when the museum was open to the public. The observed increase is mainly attributable to sources closely linked to the presence of visitors, such as dust resuspension and transport of pollutants from outside.

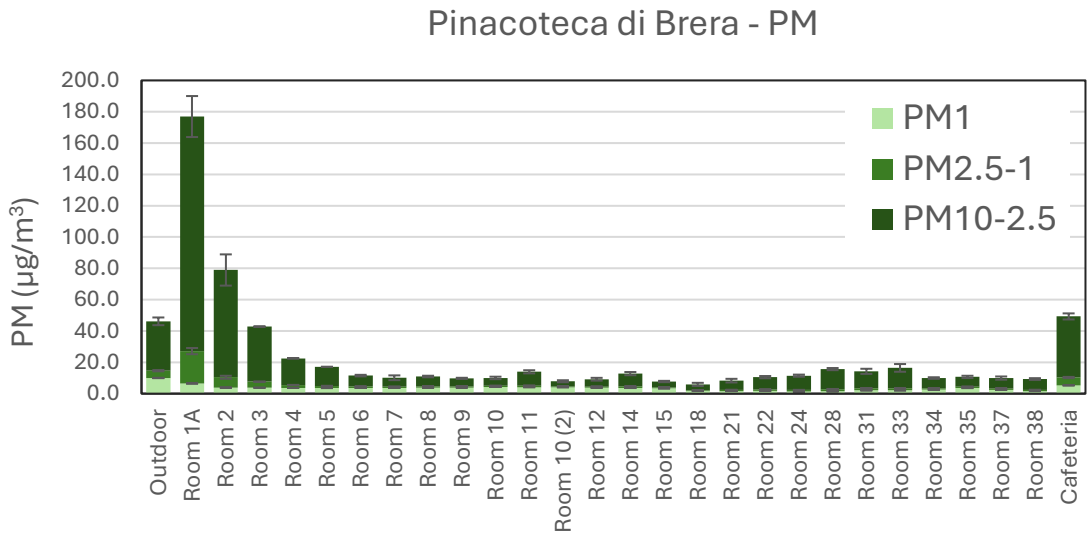

Figure 5.4. PM concentrations for each monitored environment at the Pinacoteca di Brera, as average of both opening and closing days. PM concentrations are reported as PM_{1}, $PM_{2.5-1}$ and $PM_{10-2.5}$ to better represent size fractions.

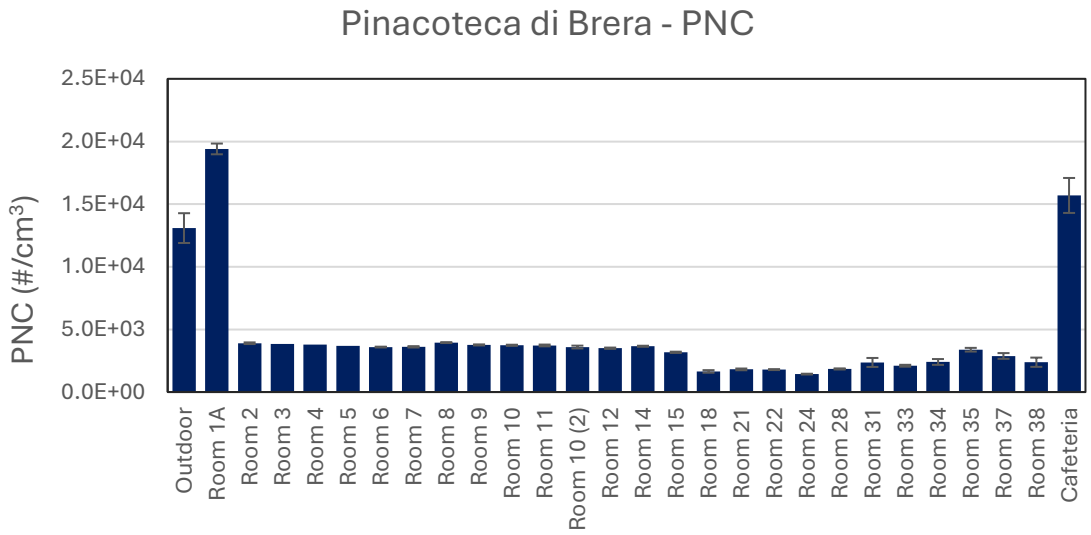

Figure 5.5. Particle number concentration (PNC) in the nanometric fraction measured by the Partector-2 (naneos) device for each monitored environment at the Pinacoteca di Brera, as average of both opening and closing days.

Figures 5.6 and 5.7 report average PM and nanoparticle concentrations over all monitoring activities conducted at *Palazzo Citterio*. The assessment of the environments of Palazzo Citterio highlighted the museum ticket office, located on the ground floor, as one of the most critical environments in terms of particle concentrations. An average PM_{10} concentration of 54.2 ± 11.5 µg/m³ was reported for all measurements conducted in the museum. This environment is characterised by a significant air exchange with the outdoors and the presence of carpeted flooring, which facilitates the resuspension of deposited coarse particulate matter. In addition, during public opening days, the ticket office sees a constant flow of visitors, which exacerbates the existing effects and introduces additional sources of particles. Other noteworthy environments are represented by rooms 40 and 49, both characterised by carpeted floors, again contributing to the resuspension of deposited particulate matter. In general, however, with the exception of the ticket office, the PM concentrations detected in the exhibition rooms were not deemed critical, as average values were consistently below the threshold limit concentration for PM_{10} of 30 µg/m³, selected by the museum management as an alert threshold for the preservation of the cultural heritage housed in the museum. Reported PNC in the nanometric fractions for all the environments monitored were significantly lower than the outdoor reported

value, with the exception of room 1A, where due to maintenance and restoration works conducted resulted in an average PNC of $1.9 \times 10^4 \pm 428.7$ particles/cm^3.

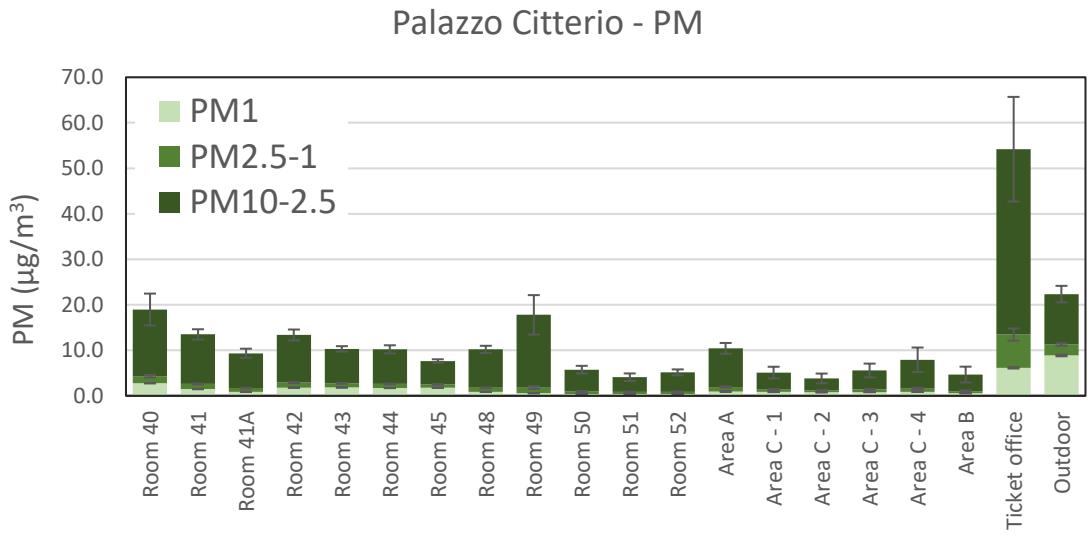

Figure 5.6. PM concentrations for each monitored environment at Palazzo Citterio, as average of both opening and closing days. PM concentrations are reported as PM_1, $PM_{2.5-1}$ and $PM_{10-2.5}$ to better represent size fractions.

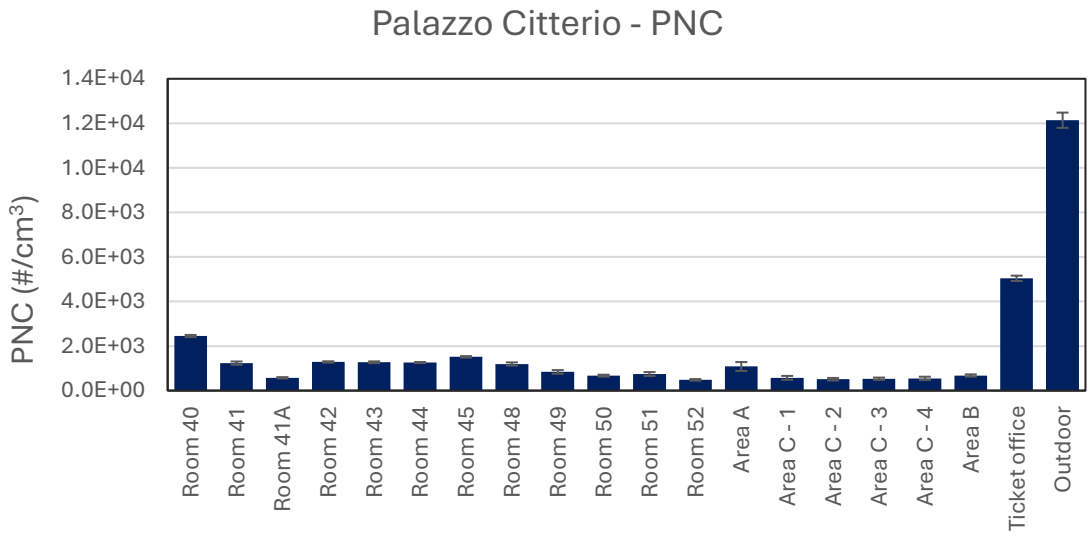

Figure 5.7. Particle number concentration (PNC) in the nanometric fraction measured by the Partector-2 (naneos) device for each monitored environment at Palazzo Citterio, as average of both opening and closing days.

5.3.2. Application of low-cost sensors for air quality control

The installation of low-cost sensors at fixed positions in selected environments throughout the studied museums has resulted in two major advantages during monitoring: primarily, thanks to their compact size, minimal noise impact and ease of installation, the sensors employed had a minimal impact on visitors, allowing for continuous operation even during public opening hours without any repercussions; secondly, continuous monitoring provided a complete picture of PM concentration trends over time in the rooms assessed, covering the period from closing days to public opening, while also allowing concentrations during the night to be assessed, which can act as a background value for the entire measurement. Figure 5.8 reports PM concentrations (as 1-hour averages) measured by one of the employed OPC-N3 (Alphasense), installed in Room 24 of the *Pinacoteca di Brera*. As mentioned above, this room is one of the most crowded during opening hours due to the valuable artworks it houses ("*Sposalizio della Vergine*" by Raffaello Sanzio, "*Pala Montefeltro*" by Piero della Francesca and "*Cristo alla colonna*" by Donato Bramante). During the closing day, represented by the leftmost portion of the plot, extremely low concentrations were recorded, up to approximately 2 µg/m^3 for PM_{10}, and comparable to the reported night-time concentrations, which reached a constant value throughout the entire period of approximately 0.2 µg/m^3.

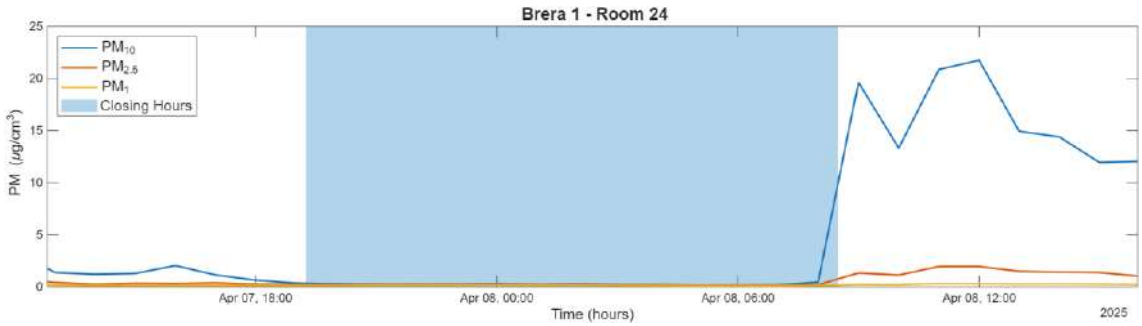

Figure 5.8. PM (PM_1, $PM_{2.5}$ and PM_{10}) concentration trend over time reported by the low-cost OPC-N3 installed in Room 24 at the Pinacoteca di Brera. The blue highlighted section refers to closing hours, as per the museum's schedule.

The deployment of OPC-N3 sensors also enabled the evaluation of the dimensional distribution of particulate matter in the examined rooms. Figure 5.9 reports numeric and volumetric size distributions, divided according to the

museum's opening hours (closed to the public, open to visitors and overnight closure). Size distributions reported for Room 24 (in figure 5.9 as average size distributions over all conducted monitoring days) highlight a clear trend: for the finer fraction (< 1 μm), the size channels showed comparable concentrations; in the coarse phase (< 10 μm), however, a greater discrepancy was observed between the three phases analysed, with a distribution for night-time closures generally lower than during visitor opening hours, while the size distributions for days without visitors was intermediate between the two limit cases. The same overall trend can be observed for both numeric and volumetric size distributions.

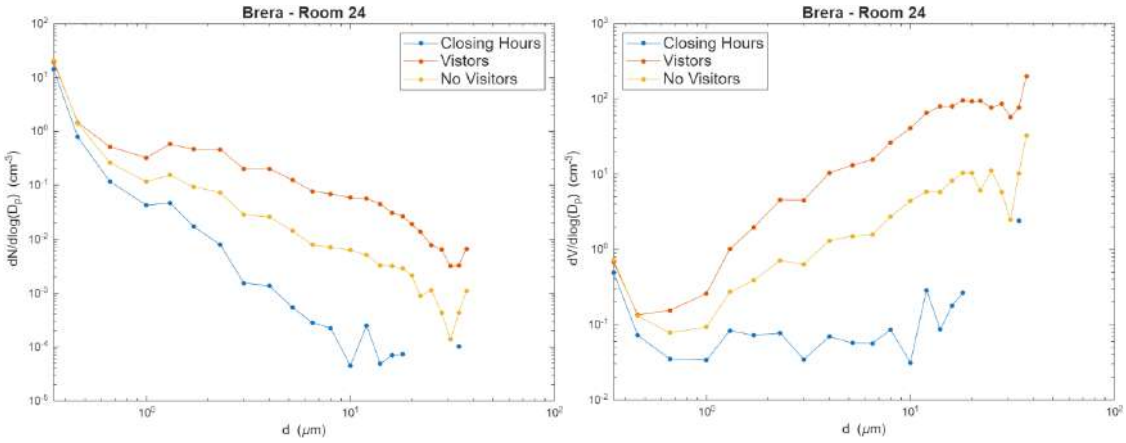

Figure 5.9. Reported number (left) and volume (right) size distributions for the OPC-N3 sensor installed in Room 24 at the Pinacoteca di Brera.

Figure 5.10 reports PM concentrations (as 1-hour averages) trend over time measured by one of the employed OPC-N3 (Alphasense), installed in the ticket office of *Palazzo Citterio*. This particular case highlights two significant emission events (> 250 μg/m^3 for PM_{10}; > 50 μg/m^3 for $PM_{2.5}$) that occurred within the environment under examination. This particular case highlights two significant emission events that occurred within the environment under examination during closing hours, mainly related to maintenance and cleaning activities. This observation is confirmed by the numerical and volumetric size distributions reported for the ticket office (figure 5.11) which, despite being reported as an average of all measurements taken, are influenced by these emission events. In fact, in contrast to the case study reported above for the Pinacoteca di Brera, a distribution with generally higher concentrations up to approximately 15 μm is observed for the closing day compared to visiting hours. The results reported in

this analysis are representative of individual case studies obtained from sampling, but the low-cost OPC-N3 devices installed in specific environments allowed to obtain comparable information on PM concentrations and size distributions throughout all measurement campaigns carried out at the *Pinacoteca di Brera* and *Palazzo Citterio*. Thanks to the deployment of these sensors, it was possible to identify long- and short-term emission events which, in some cases, could not be detected by standard mobile sampling, often limited by technical and organisational constraints. This highlights the importance of continuous monitoring with high temporal resolution in cultural heritage environments, where, despite low average concentrations, individual marked emission events can lead to an increased degradation and damage risk; therefore, low-cost sensors can also be useful to implement best practices to adopt, during closing hours, to mitigate the impact of each activity other than the one related to the visitors.

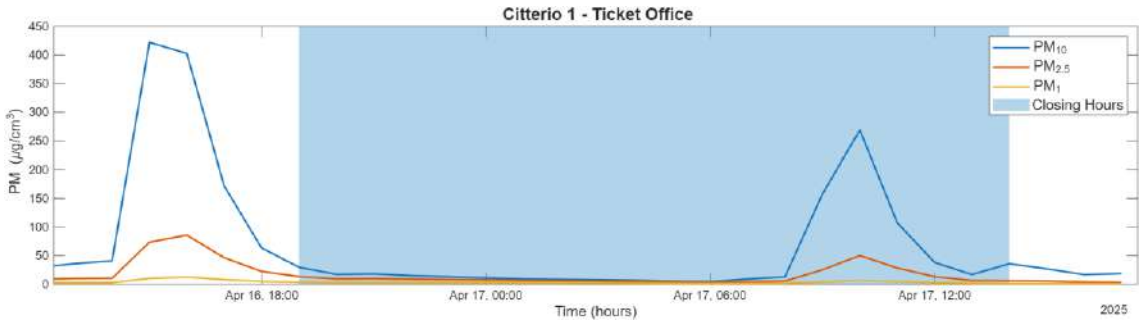

Figure 5.10. PM (PM_1, $PM_{2.5}$ and PM_{10}) concentration trend over time reported by the low-cost OPC-N3 installed in the ticket office at Palazzzo Citterio. The blue highlighted section refers to closing hours, as per the museum's schedule.

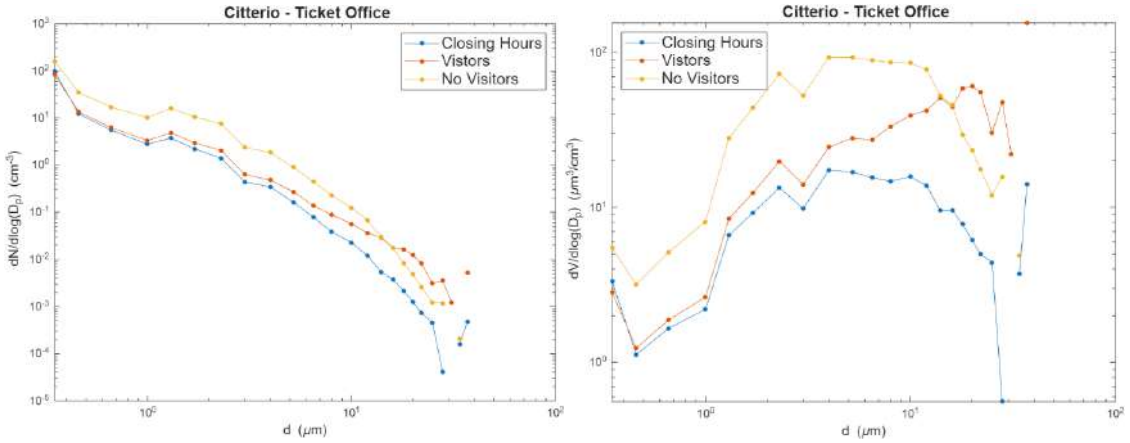

Figure 5.11. Reported number (left) and volume (right) size distributions for the OPC-N3 sensor installed in the ticket office at Palazzo Citterio.

5.3.3. OPC-N3 evaluation

To properly assess the overall performance of the low-cost OPC-N3 sensors deployed, each device was evaluated against reference data derived from the OPC Grimm employed in the mobile sampling. To ensure a valid comparison, given the different methodology applied for the two instruments, OPC-N3 data was considered for the comparison only during timeframes when the OPC Grimm, employed in the mobile monitoring, was sampling in the same rooms as each specific low-cost sensor. Figures 5.12 and 5.13 report average PM_{10} concentrations for the selected environments in each museum. It is clear how, for most of the analysed environments, OPC-N3 sensors appear to underestimate particulate concentrations, especially in the coarse fraction, compared to the reference values from the OPC Grimm. This trend is even more pronounced in environments with high PM concentrations.

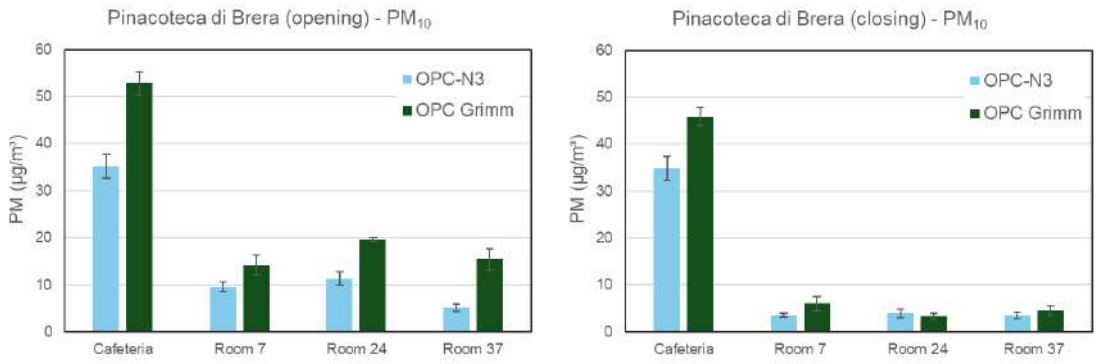

Figure 5.12. Average PM_{10} concentrations for the monitored environments at Pinacoteca di Brera during opening (left) and closing (right) days. OPC-N3 data was averaged considering only the timeframes when the OPC Grimm was sampling in the same room.

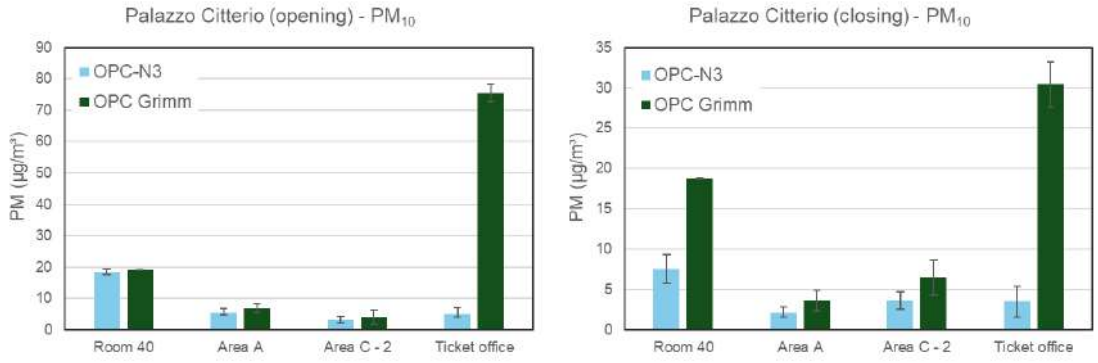

Figure 5.13. Average PM_{10} concentrations for the monitored environments at Palazzo Citterio during opening (left) and closing (right) days. OPC-N3 data was averaged considering only the timeframes when the OPC Grimm was sampling in the same room.

Analysing the numeric and volumetric size distribution (figures 5.14 and 5.15) derived for both the OPC-N3 and the OPC Grimm, two key factors have been identified as the underlying causes of the observed underestimation, consistent with the findings reported in Chapter 3 in the analysis of the OPC-N3 sensor. The cut-off at a minimum diameter of 0.35 µm in the OPC-N3 can affect the number concentration in the accumulation mode, although resulting in a minor loss when converted to mass concentrations. Similar to what was observed in the OPC-N3 analysis reported in Chapter 3, a discrepancy is observed in the size distributions between the OPC-N3 and OPC Grimm, particularly marked in the volumetric

distribution (up to a factor of 10), that could explain the observed underestimation in terms PM mass concentration. While figures 5.14 and 5.15 illustrate the numeric and volumetric distributions for two specific case studies (Room 40 during closing days for *Palazzo Citterio*; Room 24 during visiting hours for *Pinacoteca di Brera*), selected to highlight the aforementioned observations, the same behaviour was consistently reported for the other environments analysed. This confirms what was previously concluded about the performance of the low-cost OPC-N3 sensor, highlighting its technical limitations in accurately detecting PM concentrations.

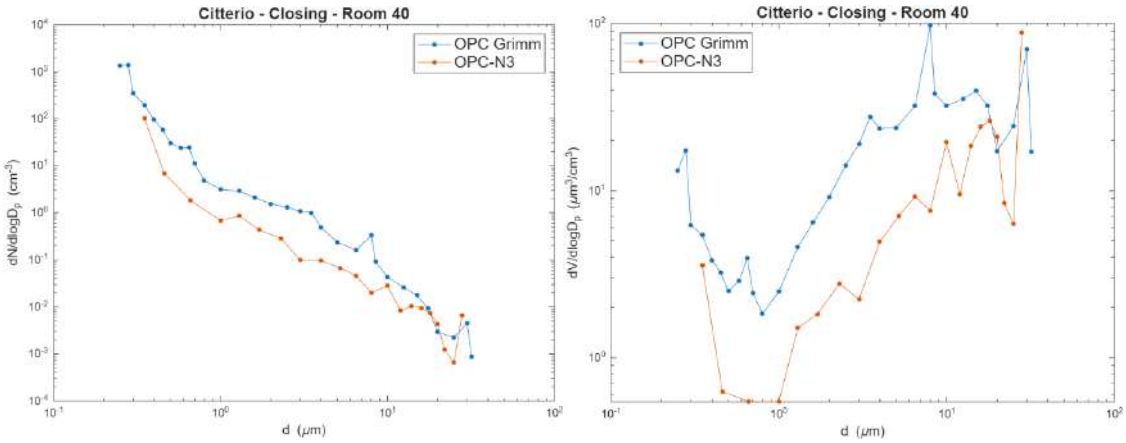

Figure 5.14. Numeric (left) and volumetric (right) size distribution reported by the OPC Grimm and the OPC-N3 for Room 40 (during closing hours) at Palazzo Citterio.

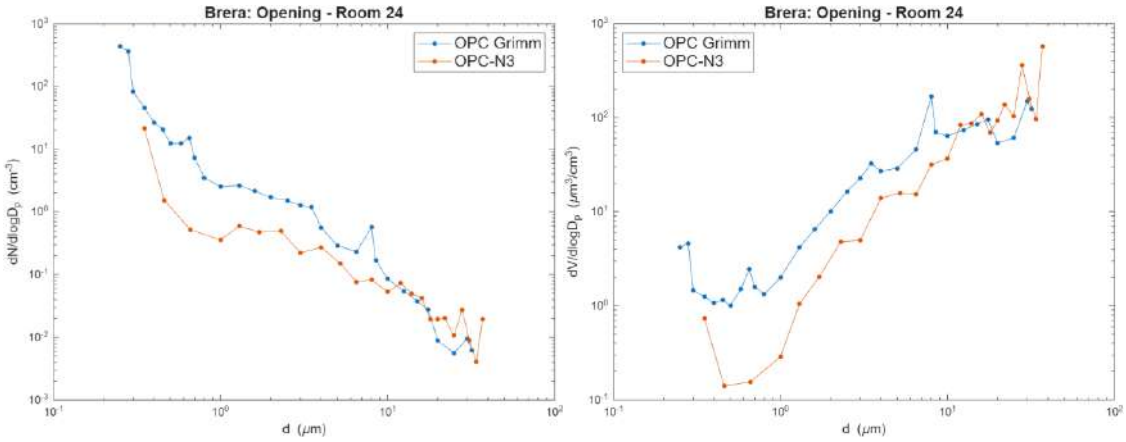

Figure 5.15. Numeric (left) and volumetric (right) size distribution reported by the OPC Grimm and the OPC-N3 for Room 24 (during visiting hours) at Pinacoteca di Brera.

To correct for the underestimation observed in the measurements, apparent density factors were calculated by means of a linear fit between the OPC-N3 and OPC Grimm data (as PM_1, $PM_{2.5-1}$ and $PM_{10-2.5}$) collected in each environment, analogous to the approach adopted in the OPC-N3 application conducted in Piazza della Scienza, as described in Chapter 3. However, given the high variability between indoor environments, the different sources of particles, and the conditions of each sampling carried out, apparent densities with widely diverging values were derived, as reported in tables 5.1 and 5.2. In addition, given the comparison method employed in the analysis, with the OPC Grimm dedicated to mobile sampling, the comparison with the OPC-N3 installed in the indoor spaces was limited to restricted time intervals, not allowing sufficient data collection for an accurate calculation of the correction factors. This result suggests the need to derive specific corrective factors for each type of environment evaluated, highlighting the difficulty of defining a single parameter given the significant variability of conditions of indoor environments.

		Pinacoteca di brera					
		Opening			Closing		
		PM_1	$PM_{2.5-1}$	$PM_{10-2.5}$	PM_1	$PM_{2.5-1}$	$PM_{10-2.5}$
Cafeteria	*Campaign 1*	42.50	43.09	46.98	14.46	43.76	48.73
	Campaign 2	6.15	1.91	2.16	6.16	1.79	1.78
	Campaign 3	5.84	1.76	2.00	7.25	1.98	2.33
Room 7	*Campaign 1*	0.90	1.08	1.15	\	\	\
	Campaign 2	2.20	4.65	3.97	1.24	1.89	1.51
	Campaign 3	5.51	2.31	1.52	5.71	1.45	0.72
Room 24	*Campaign 1*	7.78	2.19	1.50	7.27	1.78	0.08
	Campaign 2	7.27	1.78	1.67	5.91	0.39	0.26
	Campaign 3	5.96	1.86	1.75	9.33	2.01	0.87
Room 37	*Campaign 1*	9.46	2.01	1.77	3.54	1.26	0.62
	Campaign 2	6.86	1.61	1.74	8.35	3.29	0.36
	Campaign 3	6.92	1.59	0.89	8.35	1.82	0.64

Table 5.1. Derived apparent density factor for the OPC-N3 for the monitored environments at the Pinacoteca di Brera.

		Palazzo Citterio					
		Opening			Closing		
		PM_1	$PM_{2.5-1}$	$PM_{10-2.5}$	PM_1	$PM_{2.5-1}$	$PM_{10-2.5}$
Room 40	*Campaign 1*	4.80	1.81	1.35	6.57	2.68	2.52
	Campaign 2	6.22	1.64	1.38	7.28	1.88	1.66
	Campaign 3	6.08	2.09	1.74	5.23	2.70	4.92
Area A	*Campaign 1*	37.41	9.93	3.98	5.28	2.02	4.00
	Campaign 2	4.92	3.58	1.60	3.96	2.24	0.86
	Campaign 3	3.31	1.63	0.87	3.83	1.44	3.67
Area C - 2	*Campaign 1*	4.91	10.15	27.96	6.62	2.25	2.04
	Campaign 2	12.62	2.13	1.23	9.76	3.30	2.10
	Campaign 3	3.92	1.83	1.32	13.79	1.70	0.29
Ticket office	*Campaign 1*	4.86	2.22	2.65	3.73	1.43	2.06
	Campaign 2	3.43	1.63	2.39	\	\	\
	Campaign 3	4.53	1.70	1.35	5.42	1.61	2.91

Table 5.2. Derived apparent density factor for the OPC-N3 for the monitored environments at Palazzo Citterio.

5.3.4. Black carbon assessment through the low-cost bcMeter

Alongside PM monitoring conducted by employing the low-cost OPC-N3, the low-cost aethalometer bcMeter was installed in two selected environments in both museums. Black carbon, despite being mainly emitted by combustion processes and often a marker of motor vehicle traffic, is of great importance when assessing indoor air quality as, being a pollutant produced by predominantly outdoor sources, it allows the assessment of the infiltration of outdoor air into the environments examined. The deployment of the bcMeter devices in the environments examined allowed two outcomes: first, it was possible to obtain a qualitative measurement of BC concentrations inside the selected museums, comparing them with concentrations reported by outdoor reference stations; secondly, this campaign served as a testing ground for the first application of bcMeter devices in indoor monitoring, allowing an evaluation of the overall performance and accuracy in monitoring BC and their main technical limitations to be identified. To allow a first comparison of BC, reference concentrations were obtained from the reference monitoring stations of ARPA Lombardia, specifically

for Milano Senato and Milano Marche stations. However, some limitations encountered during this initial analysis should be addressed: the selected ARPA reference station is located in an area of Milan characterized by heavy traffic flows, while the museums analysed in this study are located within the restricted traffic zone in the city center of Milan ("Area C"); for this reason, the comparison conducted with the bcMeters cannot be used for a precise evaluation and calibration of the devices. However, the choice of this reference station was constrained by the reference data availability for the period selected for monitoring. Thus, the comparison was only carried out for three of the six samples taken (including both the closing and opening day), specifically for the first monitoring conducted at the *Pinacoteca di Brera* and for the first and third monitoring conducted at *Palazzo Citterio*. Figures 5.16 to 5.18 report average BC concentrations (as 1-hour averages) for both bcMeter installed at both the *Pinacoteca di Brera* and *Palazzo Citterio,* and the reference concentrations from the ARPA Marche monitoring station. Overall, BC concentration trends over time reported by the two bcMeter show significant fluctuations in the data, with consequent negative values that often influence the measurement. BC data outputted by both bcMeter does not follow the overall trend reported by the reference ARPA data in any way and appears highly scattered, showing no correlation with the reference concentrations (R^2 of linear fit < 0.2). However, the observed results reflect expected outcomes, due to some key limitations: first of all, the monitoring activity was limited in time and not continuous, which greatly reduced the number of valid data obtained. As reported in Chapter 4 of this work and extensively detailed by Doldi et al., (2025), the bcMeter has proven to be effective in monitoring BC in ambient air at 24-hours' time resolutions. By increasing the time resolution of the measurement, the data obtained from the bcMeter tend to be highly dispersed, analogously to what was observed during this analysis. In addition, the lack of reference instruments employed directly alongside the bcMeters, and comparison with reference data from the ARPA reference station located in a profoundly different urban area, heavily influenced the evaluation of the low-cost sensors. Due to significant instrumental limitations, the bcMeter proved inadequate for accurate BC monitoring of the museum environments under examination, requiring prolonged sampling over

time and a direct comparison with collocated scientific-grade instrumentation for a more accurate evaluation and calibration.

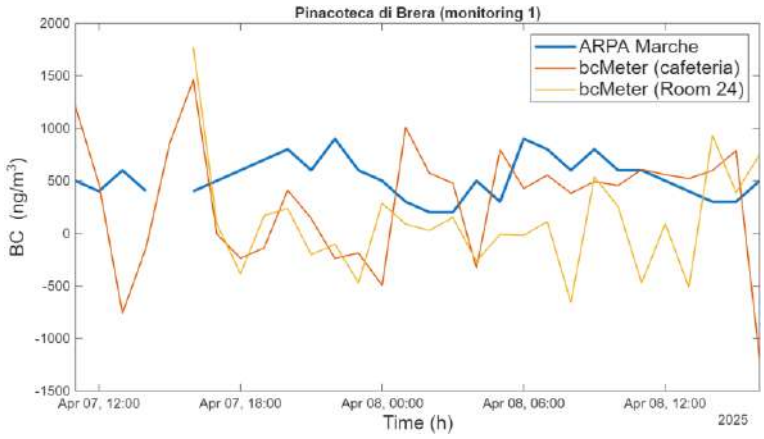

Figure 5.16. Black Carbon (BC) concentrations (as 1-hour averages) for the referenca station of ARPA Marche, and the bcMeter installed at the Pinacoteca di Brera, relative to the first leg of monitoring conducted.

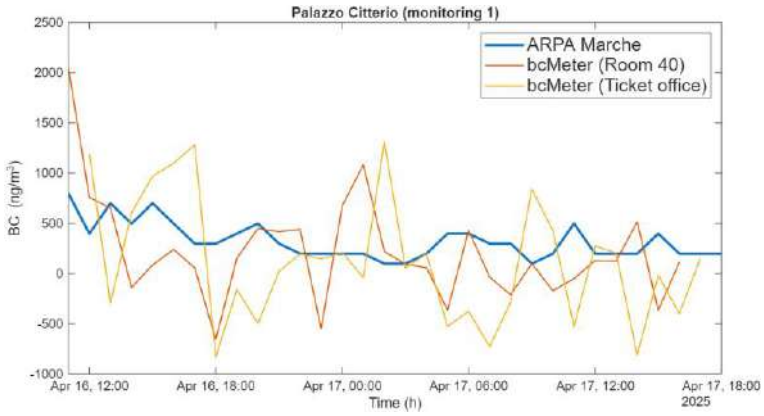

Figure 5.17. Black Carbon (BC) concentrations (as 1-hour averages) for the referenca station of ARPA Marche, and the bcMeter installed at Palazzo Citterio, relative to the first leg of monitoring conducted.

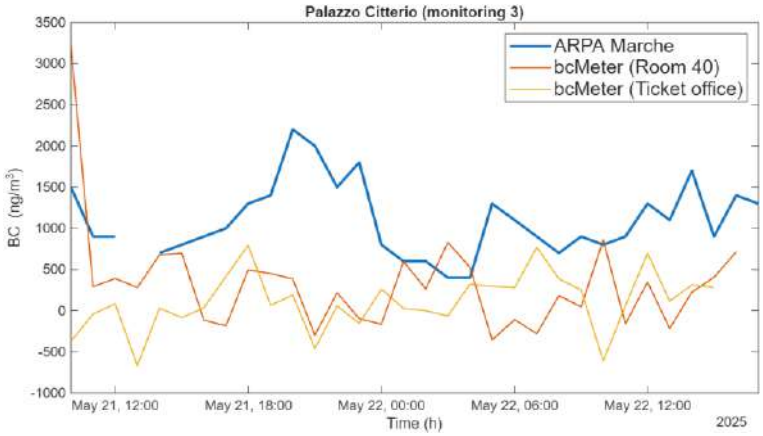

Figure 5.18. Black Carbon (BC) concentrations (as 1-hour averages) for the referenca station of ARPA Marche, and the bcMeter installed at Palazzo Citterio, relative to the third leg of monitoring conducted.

5.4. Discussion

Air pollution is one of the main risk factors for the deterioration and damage of cultural heritage. The interaction of surfaces with specific pollutants can lead to physical deterioration of surfaces, corrosion processes, and soiling, which can cause permanent damage. For this reason, preventive conservation plays a fundamental role in safeguarding cultural heritage. Monitoring pollutants becomes a crucial step in environments designed to house works of cultural significance, especially indoors, allowing pollution levels to be quantified, possible sources to be identified, and decisions to be made regarding the proper preservation of artworks. In this work, two explorative monitoring campaigns were conducted in two cultural heritage indoors sites comprised by the museum complex of “Grande Brera” in the city of Milan (Italy), specifically targeted at the *Pinacoteca di Brera*, one of one of the most important art galleries of the city, and *Palazzo Citterio*, an historic building now functioning as art exhibition. Through a mobile monitoring setup, employing research-grade portable devices, the museum environments under examination were assessed in terms of particle emissions (as both PM mass concentrations and PNC in the nanometric fraction), identifying the environments most at risk and potential sources of emissions. For both monitored environments, the spaces most subjected to high particle concentrations were those with direct air exchange with the outside, such as the

ticket office (*Palazzo Citterio*) and the cafeteria (*Pinacoteca di Brera*). In the exhibition rooms, the concentrations detected during the sampling were low, consistently below the limit of 30 μg/m^3 for PM_{10} defined as the alarm threshold by the museum management. Rooms with carpeted flooring, which facilitate the resuspension of deposited particulate matter, showed the highest average PM concentration especially on days when the museum was open to the public and therefore characterized by a greater influx of visitors. Additionally, maintenance and restoration works conducted in the monitored environments proved to be the most critical processes linked to particle emission, significantly affecting both PM mass concentration (average PM_{10} concentration of 176.9 ± 9.6 μg/m^3 measured for room 1A at the *Pinacoteca di Brera*) and PNC in the nanometric fraction (average PNC of 1.9×10^4 ± 428.7 particles/cm^3, room 1A at the *Pinacoteca di Brera*), thus posing the highest risk of exposure for the artworks housed in the museums.

In parallel, this project proved to be an excellent testing ground for implementing low-cost sensors for monitoring of pollutants in indoor cultural heritage environments. Four OPC-N3 optical particle counters (Alphasense) and two bcMeter were deployed in specific selected environments. The low-cost OPC-N3 device proved to be an effective tool for monitoring PM, ensuring real-time and continuous measurement of PM concentrations and relative size distributions in selected environments, compensating for some disadvantages of the applied mobile sampling such as low temporal and spatial resolution of measurements. The deployment of these type sensors, allowed to identify long- and short-term emission events not detected by standard mobile sampling, while also enabling a comprehensive evaluation of changes in particle size distribution during different opening hours and overnight. When compared with the data obtained through mobile monitoring for the Grimm OPC, an overall underestimation in PM concentrations was observed for OPC-N3. Consistent with the findings reported in Chapter 3 following the application of the same instrument in the MUSA project, this underestimation is attributable to a technical limitation of the sensor, unable to precisely detect particles in all its dimensional channels, showing a significant discrepancy in volumetric distributions compared to the reference, as well as truncation in the lower size

bins. The proposed corrective approach, which involves recalculating the PM following the application of apparent densities obtained on the basis of experimental comparison with reference data, was not practical, given the significant variability between the indoor environments monitored and the specific conditions present during the various sampling operations carried out, which led to widely differing apparent density values for each individual rooms assessed. This result highlights the need for site-specific correction factors to be derived for each indoor environment evaluated, taking into account the high variability of conditions in each specific setting. Moreover, the limited reference data pool resulted from the employment of the OPC Grimm in a mobile sampling, further limiting the validity of the data collected and the feasibility of the density-based correction approach. The application of the low-cost BC monitoring device bcMeter showed great limitations, as the device proved inadequate for indoor monitoring. The sensor evaluations, however, presented some limitations that will be addressed in future applications: first, the presented comparison was limited employed reference data from a non-collocated ARPA monitoring station, located in an area approximately 2.5 km away from the evaluated museum environments and with profoundly different characteristics in terms of atmospheric pollutants. In addition, the monitoring conducted in this study was carried out over a limited time frame, which did not allow for the collection of a sufficiently representative amount of data to evaluate the bcMeter device. In fact, in agreement with previous studies, this instrument showed too high data at time resolutions higher than 24 hours, limiting its usage to case studies where a daily average estimate is required. Nevertheless, the employed low-cost sensors proved to be useful tools in indoor air quality assessment, complementing standard instrumentation, granting higher temporal and spatial resolution of data. Given their compact size, negligible noise impact, and cost-effectiveness, these sensors proved to be a viable solution for monitoring indoor environments where application of traditional sensing equipment is often limited, as demonstrated in the present study aimed at cultural heritage preservation.

6. Low-cost sensors application in citizen-science initiatives

Given the advantages low-cost sensors exhibit overall, as extensively detailed in this dissertation, mainly their cost-effectiveness and ease of use, a recent shift in the paradigm of air quality research has been observed towards the involvement of the general public in air quality monitoring activities through citizen-science initiatives. This approach to air pollution research not only allows for better data dissemination, fostering greater public awareness on environmental issues, but can become a helpful tool for significantly increasing data collection and coverage. This chapter will focus on the testing and designing of new low-cost and homemade devices for air quality monitoring and their first applications in citizen-science activities.

6.1. Evaluation of a low-cost homemade integrated monitoring unit

In the context of the F.AIR (Fragile AIR - Unfair Health. Assessing Access to Healthy Environments from Schools to Communities) project, aimed at ensuring healthy environments in terms of air quality for citizens, with a particular focus on school environments and safeguarding the health of children and young adults, initial testing and calibration were conducted employing the Milano Smart Park (from now on referred to as MSP) integrated homemade multi-sensor monitoring unit against reference instrumentation. As detailed in Chapter 2 of this dissertation, this device was developed by the citizen-based initiative "Associazione Parco Segantini" in the urban area of Milan (Italy), in an effort to spread awareness on air quality and air pollution control in the city. Three low-cost devices, monitoring both PM concentrations as well as gaseous pollutants, particularly nitrogen oxides (NO_X), were deployed at the monitoring site of the atmospheric chemistry research group of the university of Milano-Bicocca (U9 building, University of Milano-Bicocca) alongside a reference gravimetric sampler (HYDRA Dual Sampler) and a reference NO_X analyzer (AC32M,

Chemiluminescent Nitrogen Oxides Analyzer). Data was collected over a period of approximately one month, between April and May 2025.

PM data highlighted how the MSP devices (as 24-hours averages, to allow direct comparison with the gravimetric sampler) were able to moderately follow the overall PM concentration trend reported by the gravimetric measurements. As reported in figure 6.1, MSP $PM_{2.5}$ concentrations showed a marked overestimation in the data (slope of linear fit of s = 1.38), while PM_{10} concentrations showed a fluctuating trend, overestimating reference concentration in some specific days, while reporting an overall underestimation of data (slope of linear fit of s = 0.83). Data correlation was evaluated for the average of the three MSP devices employed through a linear fit, highlighting moderate correlation between the two datasets, with a reported coefficient of determination (R^2) value of $R^2 = 0.45$ for $PM_{2.5}$ and $R^2 = 0.35$ for PM_{10}.

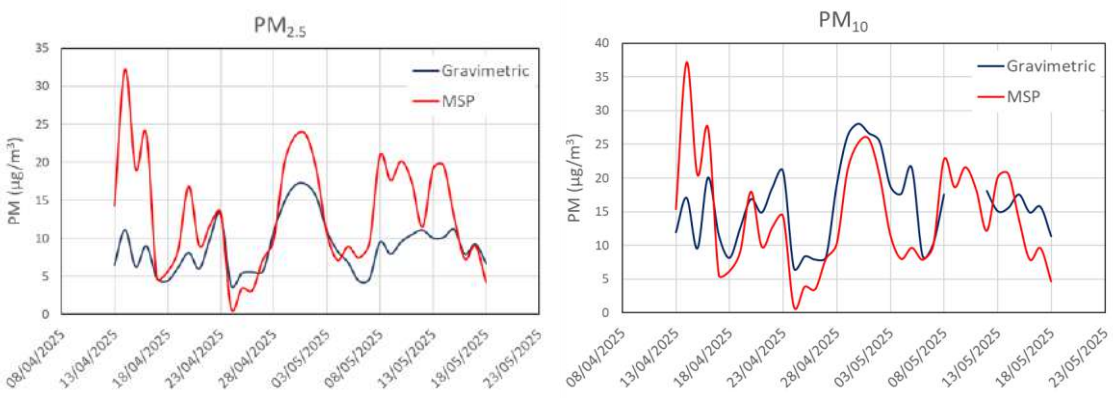

Figure 6.1. $PM_{2.5}$ (left) and PM_{10} (right) concentration trend over time for the MSP devices (as average of the three devices employed over a 24-hours' time period) and the reference gravimetric measurements.

To account for the observed overestimation, which can be traced to an effect of high relative humidity (RH) episodes affecting the optical measurement, a correction factor already employed by the Associazione Parco Segantini was applied to the raw PM data. This correction factor employs RH readings and two experimentally derived constant parameters, in order to minimize the influence of high relative humidity on the PM measure. The following equation reports the employed correction equation:

$$PM_{Corrected} = PM_{raw} \cdot \left(1 + \left(\frac{RH}{K_2}\right)^{-\frac{RH}{K_1}}\right)$$

Where PM_{raw} represents PM data directly outputted from the MSP devices; RH is the ambient relative humidity; K_1 and K_2 are the experimentally derived constant factor, which in this specific study were equivalent to $K_1 = 20$ e $K_2 = 200$, based on previous testing already carried out by *Associazione Parco Segantini*. Corrected PM data showed overall improvement for the $PM_{2.5}$ fraction showing strong correlation with reference gravimetric data, with a R^2 of linear fit equal to 0.87. The correction proved effective in correcting the overall overestimation, although corrected PM concentrations reported a slight overestimation of reference PM concentrations, with a slope of linear fit of s = 0.80, after correction. For the PM_{10} fraction the correction equation applied proved to be mostly ineffective in correcting MSP concentration, with only a minor improvement in data correlation ($R^2 = 0.37$). However, this result was mostly expected, as the low-cost sensors integrated in the device (PMS5003, Plantower Technology) is capable of effectively monitoring concentrations for the $PM_{2.5}$ fraction but has significant limitations in measuring the coarser fraction, as extensively detailed in the scientific literature regarding this type of sensor (Kaur & Kelly, 2023; Caseiro et al., 2024). A comparable result was detailed in Chapter 3 regarding the employment of the Purple Air devices, mounting a similar Plantower sensor (PMS6003), where the correction factor applied actually worsened the overestimation observed.

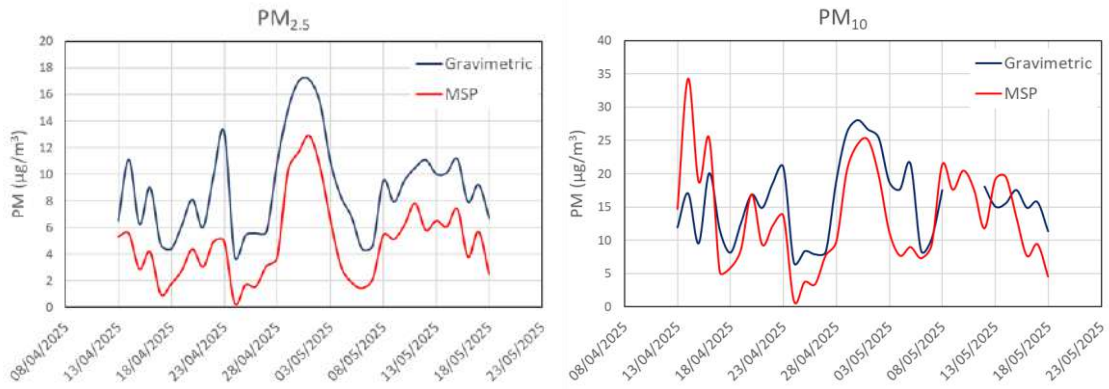

Figure 6.2. $PM_{2.5}$ (left) and PM_{10} (right) concentration trend over time for the MSP devices (as average of the three devices employed over a 24-hours' time period) after data correction, and the reference gravimetric measurements.

Nitrogen oxides (NO_X) concentrations reported by the MSP devices were evaluated during the same time frame against a reference NO_X analyser (AC32M). Figure 6.3 reports average (24-hours) NO_X concentrations for the three MSP devices and the reference NO_X analyzer. To ensure a further comparison, NO_X data from the reference ARPA monitoring station of Milano Pascal are reported. All three MSP devices reported different trends in NO_X concentrations and show an almost opposite trend compared to the reference analyser and the concentrations obtained by the ARPA monitoring station. This resulted in no correlation between the deployed devices ($R^2 < 0.1$, for two of the deployed MSP devices, referred to as MSP2 and MSP3 in figure 6.3). The best correlation was reported by the MSP1 device ($R^2 = 0.43$); however, this specific device showed a strong offset in NO_X concentrations, reporting values in the range 400-1200 $\mu g/m^3$.

Overall, the MSP devices showed good performance in detecting $PM_{2.5}$ concentrations, reporting strong correlation after correcting for relative humidity. PM_{10} concentrations reported worse overall results, with moderate correlation, and could not be effectively corrected with the proposed algorithm. Nevertheless, given the overall cost and technical specifications, the MSP integrated homemade multi-sensor monitoring unit proved to be an effective tool for PM environmental monitoring. Regarding NO_X concentrations however, the device highlighted the technical limitations of the mounted gas sensor (MiCS-6814, SGX Sensortech) in accurately assess ambient concentration, reporting low replicability between identical devices, marked offsets in reported concentrations, and no overall correlation with reference data. To further evaluate the NO_X sensor employed in the MSP devices, laboratory calibration in an exposure chamber at controlled gas concentrations and conditions will be employed.

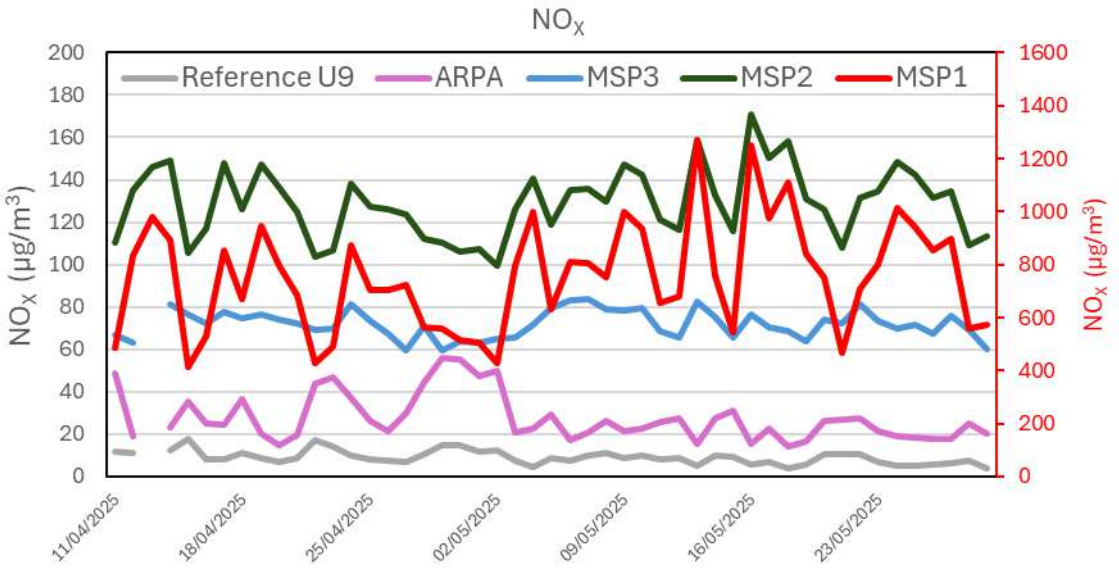

Figure 6.3. NOX concentrations (as 24-hours averages) reported for the three MSP devices, the reference AC32M analyzer and the reference monitoring station of ARPA Pascal. MSP1 data (in red) in scaled in the secondary y axis for better data visualization.

6.2. 6.2. RESPIRO – low-cost portable device for citizen-science and personal exposure assessment

As part of the MUSA ecosystem, with the participation of the Rome Advanced District (ROAD) and XearPro srl, a low-cost portable sensor has been recently developed by the POLARIS (Centro di ricerca Salute e Sontenibilità Ambientale) research group of the University of Milano-Bicocca, aimed at real-time air quality monitoring and personal exposure assessment. The developed sensor (officially named RESPIRO - *Real Time Environmental Sensing for Personal Intelligent Risk Optimization*) was designed as a tool for citizen science, enabling the direct involvement of citizens in the data collection process. The device was equipped with a low-cost PMS9103m (Plantower) sensor, allowing monitoring of atmospheric particulate matter (PM_1, $PM_{2.5}$, PM_{10}). Additionally, the device was equipped with two sensors to monitor CO and CO_2 concentrations, as well as environmental parameters (T, RH and pressure). In order to facilitate use,

simplify the user interface and obtain continuous GPS positioning, the device can be coupled with a downloadable smartphone application.

Figure 6.4. Overview of the low-cost RESPIRO device developed.

This device has multiple objectives: to involve the public in the measurement process, providing information on issues related to air quality and their effect on human health, and to provide a significant amount of data on personal exposure to atmospheric pollutants in different indoor and outdoor environments. To carry out an initial assessment of the performance of the developed device and highlight the initial critical issues from a hardware and software perspective, a pilot monitoring campaign was carried out, in which over forty devices were assigned to students and university staff of the university of Milano-Bicocca, on a voluntary basis, tasked with carrying out indoor/outdoor routes within the Bicocca district through pre-determined routes (figure 6.5). Figures 6.5 and 6.6 reports averaged concentrations measured by the RESPIRO devices employed during the pilot campaign. Figure 6.5 reports data obtained during colder days of the winter season, while figure 6.6 show average concentrations detected during days with atmospheric instability, highlighting how the RESPIRO devices were able to detect PM_x concentration variations related to different atmospheric conditions. This preliminary campaign was instrumental in highlighting the main hardware and software issues of the RESPIRO device, pointing towards an improvement of overall sensor performance and response. In the future, the device accuracy in monitoring PM_x concentration will be evaluated against reference instrumentation in both laboratory and environmental conditions, to ensure the best quality in the collected data. Future applications will also see the deployment of the sensors in school projects, involving children and young adults

in the data collection process, fostering air pollution awareness. Furthermore, the RESPIRO device will undergo precise testing and calibration in both laboratory and field conditions.

Figure 6.4. Map of the selected routes for the pilot monitoring campaign employing the RESPIRO devices.

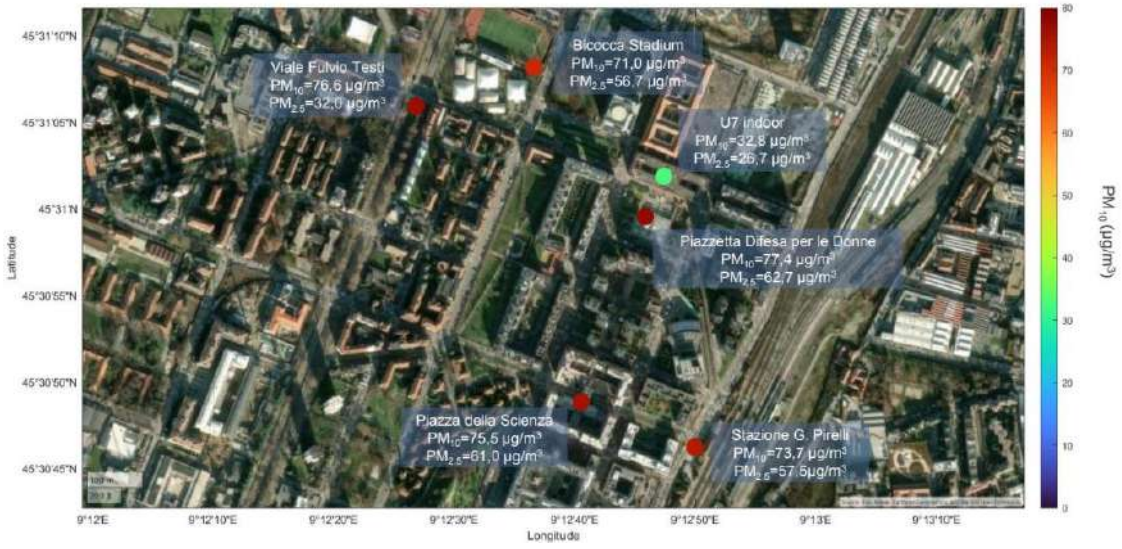

Figure 6.5. Map of the first route with average PM_{10} concentration for each sampling location obtained deploying the RESPIRO devices during the pilot campaign.

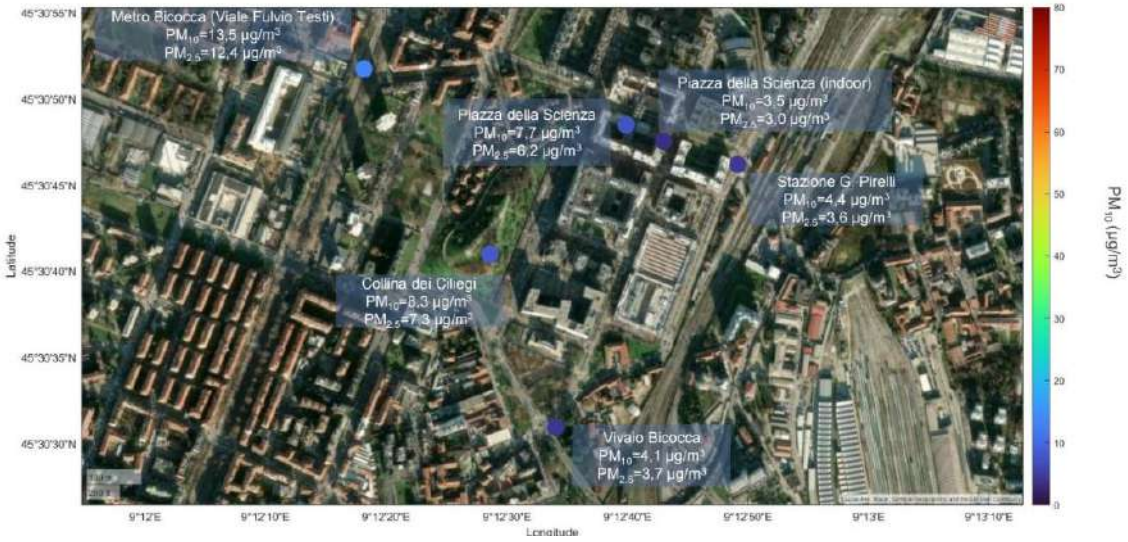

Figure 6.6. Map of the second route with average PM_{10} concentration for each sampling location obtained deploying the RESPIRO devices during the pilot campaign.

7. Conclusions

Air pollution has been recently linked to about 7 million deaths per year (WHO, 2024), and its negative effects encompassing our lives are now thoroughly detailed in scientific literature. For this reason, topics related to air quality are becoming increasingly prominent not only in the scientific community, but also at the legislative level and within public opinion. Air pollution's role in the role of pollution in the onset of respiratory, cardiovascular and neurological morbidity, damage to the reproductive system and cancer has now been extensively documented, especially considering the airborne particle fraction (Pope & Dockery, 2006; Bentayeb et al. 2013; Kyung & Jeong, 2020; Sahu et al., 2014). However, while the effect on health is among the most worrying given its implications, air pollution exerts constant pressure on our entire living environment. Depending on their chemical and physical properties, atmospheric pollutants can exert a forcing effect on the climate, altering the Earth's radiation budget (Bellouin et al., 2020; Mohnen et al., 1993; Feldman et al., 2015). In addition, air pollutants can interact across the entire ecosystem, with adverse effects on fauna, vegetation, and soil (Singh & Verma, 2023; Zuhara & Isaifan, 2018; Fuhrer et al., 2016). Atmospheric pollutants directly affect anthropogenic materials, from damage and soiling of civil structures (Rao et al., 2014) and cultural heritage sites (Vidović et al., 2022) to effects on electronic equipment and printed circuits (Gini et al., 2023; Ferrero et al., 2013), overall resulting in a tangible economic and cultural loss. To effectively manage air pollution and limit its impacts, general legislation and guidelines (EU Directive 2024/2881; WHO, 2021) were issued specifying threshold values for specific pollutants aimed at human health protection, and establishing unified monitoring methodologies. At the present time, environmental monitoring of atmospheric pollutants is achieved through certified reference monitoring stations, on a regional and international scale, and through the employment of scientific-grade reference instrumentation. However, given the excessive economic cost, difficulty of employment, and need for constant maintenance to ensure great accuracy, traditional air quality monitoring often offers inadequate spatial and temporal data coverage, unable to provide sufficient information on emission sources and hotspots (Kumar et al., 2015). For this reason, in recent years, both the market

and scientific research have seen the rise of low-cost technologies for monitoring of pollutants. This innovative type of sensor has emerged as a tool that can complement traditional monitoring through significantly reduced costs and ease of use, allowing for its widespread application and ensuring greater spatial and temporal coverage in the data. Nevertheless, this inevitably results in reduced accuracy and precision of measurements, requiring extensive testing and calibration in different environmental conditions and settings. In this context, this work focuses primarily on the application, testing and analysis of innovative low-cost, smart, and portable instrumentation for air quality monitoring, as powerful tools that can aid the scientific community, as well as the public, towards a more comprehensive understanding of the air we breathe. Multiple low-cost devices were employed in a wide array of environments, from environmental applications in urban and suburban settings, to indoor spaces, conducting specific testing and in-site calibration to properly evaluate these sensors in different conditions.

The first part of this work saw the employment of low-cost sensors as tools for air quality assessment during urban regeneration activities conducted in the science campus of the university of Milano-Bicocca as part of the MUSA (Multilayered Urban Sustainability Action) ecosystem, a project born in the urban area of Milan as a joint effort between universities, research institutions and public and private entities aimed at the establishment of a replicable model aimed at sustainability and citizen's well-being. Acting through one of its main branches (Spoke 1 – Urban), the ecosystem conducted a major urban regeneration effort at the University of Milano-Bicocca, renewing the architectural context of the university science campus of Piazza della Scienza. The application, against reference instrumentation, of the low-cost and portable sensors (OPC-N3, Alphasense; Partector-2, Naneos) in monitoring the progress of the square's regeneration work in its three main phases (pre-construction, construction and post-construction) highlighted the strengths and limitation of this new type of instrumentation, mainly the need for proper calibration. The Partector-2 device showed great correlation and comparability with the reference monitor (Nanoscan SMPS, TSI) employed, proving to be a great asset for monitoring nanoparticles concentrations with high time resolution. The low-cost

OPC-N3 showed excellent correlation with the reference optical particle counter (Environmental Dust Monitor, Grimm), although showing a severe underestimation of PM concentrations. Deriving site-specific correction factors from the comparison with the reference data from the OPC Grimm, based on the computation of new apparent densities (4.17-10.73 g/cm^3 for PM1; 1.44-5.47 g/cm^3 for $PM_{2.5-1}$; 1.67-5.79 g/cm^3 for $PM_{10-2.5}$) to replace the constant value used by the low-cost instrument, led to a significant improvement in the data returned by the sensor during all three construction phases of the urban regeneration plan in Piazza della Scienza. After calibration, the low-cost sensors data played a fundamental part in the assessment of the urban regeneration project impact on air quality. Through close monitoring in the three main phases of the urban regeneration project, it was assessed, in terms of particle emissions, the impact of both the construction activities (mainly aimed at depaving, installation of new flooring, and increasing green coverage), and the entire urban regeneration project carried out in Piazza della Scienza. The calculated impact for the entire construction phase for PM mass concentrations was 11.1 ± 23.8 µg/m3 for PM1, 33.6 ± 53.0 µg/m3 for PM2.5 and 82.1 ± 79.4 µg/m3 for PM10. For PNC in the nanometric fraction, the calculated impact was -3318.3 ± 3825.6 cm^{-3}. For indoor environments, the calculated impact for the entire construction phase for PM mass concentrations was 0.3 ± 6.9 µg/m^3 for PM1, 3.9 ± 12.6 µg/m^3 for PM2.5 and 2.3 ± 29.2 µg/m3 for PM10. For PNC in the nanometric fraction, the calculated impact was -8056.3 ± 2418.4 cm^{-3}. While PM concentrations showed an increase in all three fractions, only for PM10 the increase was statistically significant. As expected, given the nature of the type of activities conducted, construction work on the square mainly resulted in an increase of PM concentrations in the coarse fraction. During the post-construction phase the derived impact on PM mass concentrations was -5.2 ± 5.5 µg/m^3 for PM1, -5.6 ± 6.4 µg/m^3 for PM2.5 and -5.9 ± 8.6 µg/m3 for PM10. For PNC in the nanometric fraction, the calculated impact was 5640.1 ± 4588.5 cm^{-3}. For indoor environments, the calculated impact in the post-construction phase for PM mass concentrations was -1.3 ± 1.4 µg/m3 for PM1, -0.8 ± 2.0 µg/m^3 for $PM_{2.5}$ and -2.5 ± 8.7 µg/m^3 for PM_{10}. For PNC in the nanometric fraction, the calculated impact was -286.9 ± 1227.3 cm^{-3}. The overall assessment of the impact of the entire urban

regeneration project in Piazza della Scienza planned by the MUSA ecosystem showed a general decreasing trend in PM concentrations, suggesting how the measures envisioned by the MUSA ecosystem had a positive effect, although in general this decrease was not statistically significant enough to quantify this result with certainty. The positive impact observed in the increase in nanoparticles linked to the presence of greater green coverage in the square was, however, significant and was traced back to an increase in the vegetation cover, thus biogenic VOCs emission, with subsequent formation of secondary organic aerosols (SOA) via nucleation and coagulation processes. Upon completion of the urban regeneration effort, additional low-cost sensors (Purple Air Flex; Polludrone, Oizom) were installed in fixed locations throughout the square to facilitate continuous monitoring of pollutants. This step is aimed at fostering scientific research with a continuous flow of data on pollutant concentrations in the square, as well as promoting the dissemination of environmental issues related to pollution and involving students and citizens.

A second part of this work focused on of the first application of the recently developed low-cost BC monitoring device bcMeter, assessing its performance in environmental monitoring in comparison with a standard reference aethalometer (AE33, Magee Scientific) over a five-month period at an urban background location in Mülheim-Styrum, Germany. The bcMeter proved to be an effective tool for monitoring ambient BC concentrations in 24-hour averages, showing good correlation with the reference AE33 aethalometer ($R2 > 0.7$ for both devices, after outlier removal). However, at higher time resolution the reported BC data was highly scattered, with no meaningful interpretation. This study also revealed a consistent underestimation of BC concentrations by both sensors. This discrepancy was attributed to a disparity between the actual airflow measured at the inlet though an external flowmeter and the value reported by the internal flow controller. A correction factor was thus derived, effectively correcting and addressing the underestimation for both sensors (slope of linear fit of $s = 1.02$ and $s = 0.94$ for 24-hour averages, after correction). Overall, the bcMeter achieved comparable results to a reference aethalometer (AE33, Magee Scientific) for daily averages. Nevertheless, the sensor exhibited several technical limitations that affected the whole campaign, resulting in frequent interruptions

to the measurements. Some of the outages experienced could be explained as results of software and firmware issues, while defects in the structure of the outer 3D-printed case may have resulted in air leakages. Taking this into consideration, the bcMeter has the potential to facilitate applications in a range of indoor and outdoor settings where the accessibility of BC concentration data remains limited.

The same low-cost described were then employed in two explorative monitoring campaigns were conducted in two cultural heritage indoors sites comprised by the museum complex of "Grande Brera" in the city of Milan (Italy), specifically targeted at the Pinacoteca di Brera, one of one of the most important art galleries of the city, and Palazzo Citterio, an historic building now functioning as art exhibition. Through a mobile monitoring setup, employing research-grade portable devices, the museum environments under examination were assessed in terms of particle emissions (as both PM mass concentrations and PNC in the nanometric fraction), identifying the environments most at risk and potential sources of emissions. In parallel, four OPC-N3 optical particle counters (Alphasense) and two bcMeter were deployed in specific selected environments throughout the museums. The low-cost OPC-N3 device proved to be an effective tool for monitoring PM, ensuring real-time and continuous measurement of PM concentrations and relative size distributions in selected environments, compensating for some disadvantages of the applied mobile sampling such as low temporal and spatial resolution of measurements. The deployment of these type sensors, allowed to identify long- and short-term emission events not detected by standard mobile sampling, while also enabling a comprehensive evaluation of changes in particle size distribution during different opening hours and overnight. Consistently with the findings reported during the sensor testing under the MUSA project, the OPC-N3 underestimated PM concentrations when compared to reference OPC Grimm data. This finding was linked to a technical limitation of the sensor, showing a significant discrepancy in volumetric distributions compared to the reference, as well as truncation in the lower size bins. The proposed corrective approach, which involved PM recalculation following the application of apparent densities obtained on the basis of experimental comparison with reference data, was not practical, given the

significant variability between the indoor environments monitored and the specific conditions present during the various sampling operations carried out, which led to widely differing apparent density values for each individual rooms assessed. This result thus highlights the need for site-specific correction factors to be derived for each indoor environment evaluated, taking into account the high variability of conditions in each specific setting. The application of the low-cost BC monitoring device bcMeter showed great limitations, as the device proved inadequate for indoor monitoring, showing no correlation with reference data ($R2 < 0.2$). As the methodology applied for this evaluation however presented some limitations, further indoor testing should be conducted to properly evaluate the sensor accuracy in such environments. Overall, given their compact size, negligible noise impact, and cost-effectiveness, these sensors proved to be a viable solution for monitoring indoor environments where application of traditional sensing equipment is often limited, as demonstrated in the present study aimed at cultural heritage preservation.

In general, through the studies conducted, we explored a wide range of settings and applications for the employment of low-cost sensors in air quality research. A common thread among all low-cost sensors is the need for precise calibration of data in the field, in order to provide accuracy comparable to reference instruments. However, as detailed, in order to obtain the best results, the calibration process must be tailored to the specific environment and conditions of use, given the high variability of environments (both indoor and outdoor), emission sources, and potential interferences. As low-cost sensors become increasingly popular on the market and continuous technological innovations bring more innovation in air quality monitoring, these steps are increasingly essential in ensuring accurate results that can effectively protect our world.

8. References

Lou, B., Barbieri, D. M., Passavanti, M., Hui, C., Gupta, A., Hoff, I., Lessa, D. A., Sikka, G., Chang, K., Fang, K., Lam, L., Maharaj, B., Ghasemi, N., Qiao, Y., Adomako, S., Foroutan Mirhosseini, A., Naik, B., Banerjee, A., Wang, F., … Agarwal, N. (2021). Air pollution perception in ten countries during the COVID-19 pandemic. *Ambio 2021 51:3*, *51*(3), 531–545. https://doi.org/10.1007/S13280-021-01574-2

Sustainable Development Goal indicator 3.9.1: mortality attributed to air pollution. Geneva: World Health Organization; 2024. Licence: CC BY-NC-SA 3.0 IGO

Cohen, A. J., Brauer, M., Burnett, R., Anderson, H. R., Frostad, J., Estep, K., Balakrishnan, K., Brunekreef, B., Dandona, L., Dandona, R., Feigin, V., Freedman, G., Hubbell, B., Jobling, A., Kan, H., Knibbs, L., Liu, Y., Martin, R., Morawska, L., … Forouzanfar, M. H. (2017). Estimates and 25-year trends of the global burden of disease attributable to ambient air pollution: an analysis of data from the Global Burden of Diseases Study 2015. *The Lancet*, *389*(10082), 1907–1918. https://doi.org/10.1016/S0140-6736(17)30505-6

Burnett, R., Chen, H., Szyszkowicz, M., Fann, N., Hubbell, B., Pope, C. A., Apte, J. S., Brauer, M., Cohen, A., Weichenthal, S., Coggins, J., Di, Q., Brunekreef, B., Frostad, J., Lim, S. S., Kan, H., Walker, K. D., Thurston, G. D., Hayes, R. B., … Spadaro, J. v. (2018). Global estimates of mortality associated with longterm exposure to outdoor fine particulate matter. *Proceedings of the National Academy of Sciences of the United States of America*, *115*(38), 9592–9597. https://doi.org/10.1007/s13280-021-01574-2

Unger, N. (2012). Global climate forcing by criteria air pollutants. Annual Review of Environment and Resources, 37(Volume 37, 2012), 1–24. https://doi.org/10.1146/ANNUREV-ENVIRON-082310-100824/CITE/REFWORKS

Maione, M., Fowler, D., Monks, P. S., Reis, S., Rudich, Y., Williams, M. L., & Fuzzi, S. (2016). Air quality and climate change: Designing new win-win policies

for Europe. Environmental Science & Policy, 65, 48–57. https://doi.org/10.1016/J.ENVSCI.2016.03.011

Mohapatra, K., & Biswal, S. (2014). Effect of particulate matter (PM) on plants, climate, ecosystem and human health. Int. J. Adv. Technol. Eng. Sci, 2(02).

Manisalidis, I., Stavropoulou, E., Stavropoulos, A., & Bezirtzoglou, E. (2020). Environmental and Health Impacts of Air Pollution: A Review. Frontiers in Public Health, 8, 505570. https://doi.org/10.3389/FPUBH.2020.00014/BIBTEX

Özkara, A., & Akyıl, D. (2018). Environmental Pollution and the Effects of the Pollutants on the Ecosystem. *Turkish Journal of Scientific Reviews*, *11*(2), 11–17. https://dergipark.org.tr/en/pub/derleme/issue/41716/451356

Ferrero, L., D'Angelo, L., Rovelli, G., Sangiorgi, G., Perrone, M. G., Moscatelli, M., Casati, M., Rozzoni, V., & Bolzacchini, E. (2015). Determination of aerosol deliquescence and crystallization relative humidity for energy saving in free-cooled data centers. International Journal of Environmental Science and Technology, 12(9), 2777–2790. https://doi.org/10.1007/s13762-014-0680-2

Matrali, A., Kodros, J. K., Papathanasiou, M., & Pandis, S. N. (2023). Quantification of the degradation of paintings due to the deposition of atmospheric aerosols. *Journal of Cultural Heritage*, *62*, 322–328. https://doi.org/10.1016/J.CULHER.2023.06.008

Vidović, K., Hočevar, S., Menart, E., Drventić, I., Grgić, I., & Kroflič, A. (2022). Impact of air pollution on outdoor cultural heritage objects and decoding the role of particulate matter: a critical review. Environmental Science and Pollution Research 2022 29:31, 29(31), 46405–46437. https://doi.org/10.1007/S11356-022-20309-8

Directive 2008/50/EC of the European Parliament and of the Council of 21 May 2008 on ambient air quality and cleaner air for Europe.

Directive (EU) 2024/2881 of the European Parliament and of the Council of 23 October 2024 on ambient air quality and cleaner air for Europe.

WHO. (2021). WHO global air quality guidelines. Particulate matter (PM2.5 and PM10), ozone, nitrogen dioxide, sulfur dioxide and carbon monoxide.

Kumar, P., Morawska, L., Martani, C., Biskos, G., Neophytou, M., di Sabatino, S., Bell, M., Norford, L., & Britter, R. (2015). The rise of low-cost sensing for managing air pollution in cities. Environment International, 75, 199–205. https://doi.org/10.1016/J.ENVINT.2014.11.019

Snyder, E. G., Watkins, T. H., Solomon, P. A., Thoma, E. D., Williams, R. W., Hagler, G. S. W., Shelow, D., Hindin, D. A., Kilaru, V. J., & Preuss, P. W. (2013). The Changing Paradigm of Air Pollution Monitoring. Environmental Science and Technology, 47(20), 11369–11377. https://doi.org/10.1021/ES4022602

Jovašević-Stojanović, M., Bartonova, A., Topalović, D., Lazović, I., Pokrić, B., & Ristovski, Z. (2015). On the use of small and cheaper sensors and devices for indicative citizen-based monitoring of respirable particulate matter. In Environmental Pollution (Vol. 206). https://doi.org/10.1016/j.envpol.2015.08.035

Morawska, L., Thai, P. K., Liu, X., Asumadu-Sakyi, A., Ayoko, G., Bartonova, A., Bedini, A., Chai, F., Christensen, B., Dunbabin, M., Gao, J., Hagler, G. S. W., Jayaratne, R., Kumar, P., Lau, A. K. H., Louie, P. K. K., Mazaheri, M., Ning, Z., Motta, N., … Williams, R. (2018). Applications of low-cost sensing technologies for air quality monitoring and exposure assessment: How far have they gone? Environment International, 116, 286–299. https://doi.org/10.1016/J.ENVINT.2018.04.018

Ruiter, S., Bard, D., Jeddi, H. ben, Saunders, J., Snawder, J., Warren, N., Gorce, J. P., Cauda, E., Kuijpers, E., & Pronk, A. (2023). Exposure Monitoring Strategies for Applying Low-Cost PM Sensors to Assess Flour Dust in Industrial Bakeries. Annals of Work Exposures and Health, 67(3), 379–391. https://doi.org/10.1093/ANNWEH/WXAC088

Howard, J., Murashov, V., Cauda, E., & Snawder, J. (2022). Advanced sensor technologies and the future of work. American Journal of Industrial Medicine, 65(1), 3–11. https://doi.org/10.1002/AJIM.23300;WGROUP:STRING:PUBLICATION

Siddique, A., Al-Shamlan, M. Y. M., Al-Romaihi, H. E., & Khwaja, H. A. (2025). Beyond the outdoors: indoor air quality guidelines and standards - challenges, inequalities, and the path forward. Reviews on Environmental Health, 40(1), 21–35. https://doi.org/10.1515/REVEH-2023-0150/XML

Bousiotis, D., Alconcel, L. N. S., Beddows, D. C. S., Harrison, R. M., & Pope, F. D. (2023). Monitoring and apportioning sources of indoor air quality using low-cost particulate matter sensors. Environment International, 174, 107907. https://doi.org/10.1016/J.ENVINT.2023.107907

Hoskins, J. A. (2003). Health Effects due to Indoor Air Pollution. Indoor and Built Environment, 12(6), 427–433. https://doi.org/10.1177/1420326X03037109

U.S. EPA. Integrated Science Assessment (ISA) for Particulate Matter (Final Report, Dec 2019). U.S. Environmental Protection Agency, Washington, DC, EPA/600/R-19/188, 2019

Raes, F., van Dingenen, R., Vignati, E., Wilson, J., Putaud, J. P., Seinfeld, J. H., & Adams, P. (2000). Formation and cycling of aerosols in the global troposphere. *Atmospheric Environment*, *34*(25), 4215–4240. https://doi.org/10.1016/S1352-2310(00)00239-9

Seinfeld, J. H. and Pandis, S. N., 2006. Atmospheric Chemistry and Physics: From Air Pollution To Climate Change, 2nd ed., John Wiley & Sons, New York.

U.S. EPA. Air Quality Criteria for Particulate Matter (Final Report, 2004). U.S. Environmental Protection Agency, Washington, DC, EPA 600/P-99/002aF-bF, 2004

Ferrero, L., Sangiorgi, G., Ferrini, B. S., Perrone, M. G., Moscatelli, M., D'Angelo, L., Rovelli, G., Ariatta, A., Truccolo, R., & Bolzacchini, E. (2013). Aerosol Corrosion Prevention and Energy-Saving Strategies in the Design of Green Data Centers. *Environmental Science and Technology*, *47*(8), 3856–3864. https://doi.org/10.1021/ES304790F

Savadkoohi, M., Pandolfi, M., Favez, O., Putaud, J. P., Eleftheriadis, K., Fiebig, M., Hopke, P. K., Laj, P., Wiedensohler, A., Alados-Arboledas, L., Bastian, S.,

Chazeau, B., María, Á. C., Colombi, C., Costabile, F., Green, D. C., Hueglin, C., Liakakou, E., Luoma, K., … Querol, X. (2024). Recommendations for reporting equivalent black carbon (eBC) mass concentrations based on long-term pan-European in-situ observations. Environment International, 185, 108553. https://doi.org/10.1016/J.ENVINT.2024.108553

Zhang, G., Ding, C., Jiang, X., Pan, G., Wei, X., & Sun, Y. (2020). Chemical Compositions and Sources Contribution of Atmospheric Particles at a Typical Steel Industrial Urban Site. *Scientific Reports*, *10*(1), 7654-. https://doi.org/10.1038/S41598-020-64519-X

Shi, J., Hong, J., Ma, N., Luo, Q., He, Y., Xu, H., Tan, H., Wang, Q., Tao, J., Zhou, Y., Han, S., Peng, L., Xie, L., Zhou, G., Xu, W., Sun, Y., Cheng, Y., & Su, H. (2022). Measurement report: On the difference in aerosol hygroscopicity between high and low relative humidity conditions in the North China Plain. *Atmospheric Chemistry and Physics*, *22*(7), 4599–4613. https://doi.org/10.5194/ACP-22-4599-2022

Nurowska, K., & Markowicz, K. M. (2023). Determination of Hygroscopic Aerosol Growth Based on the OPC-N3 Counter. *Atmosphere 2024, Vol. 15, Page 61*, *15*(1), 61. https://doi.org/10.3390/ATMOS15010061

Liu, Z., Gao, W., Yu, Y., Hu, B., Xin, J., Sun, Y., Wang, L., Wang, G., Bi, X., Zhang, G., Xu, H., Cong, Z., He, J., Xu, J., & Wang, Y. (2018). Characteristics of PM2.5 mass concentrations and chemical species in urban and background areas of China: Emerging results from the CARE-China network. Atmospheric Chemistry and Physics, 18(12), 8849–8871. https://doi.org/10.5194/ACP-18-8849-2018

Holland, R ;, Seifert, K ;, Saboya, E ;, Khan, M. A. H. ;, Derwent, R. G. ;, Shallcross, D E, Zhao, K., Gao, J., Wu, Y., Holland, Rayne, Seifert, Katya, Saboya, Eric, Anwar, M., Khan, H., Derwent, R. G., & Shallcross, Dudley E. (2024). Elucidating the Effects of COVID-19 Lockdowns in the UK on the O3-NOx-VOC Relationship. *Atmosphere 2024, Vol. 15, Page 607*, *15*(5), 607. https://doi.org/10.3390/ATMOS15050607

Lelieveld, J., & Dentener, F. J. (2000). What controls tropospheric ozone? *Journal of Geophysical Research Atmospheres*, *105*(D3), 3531–3551. https://doi.org/10.1029/1999JD901011

Fishman, J., Watson, C. E., Larsen, J. C., & Logan, J. A. (1990). Distribution of tropospheric ozone determined from satellite data. *Journal of Geophysical Research*, *95*(D4), 3599–3617. https://doi.org/10.1029/JD095ID04P03599;ISSUE:ISSUE:DOI

Guicherit, R., & Roemer, M. (2000). Tropospheric ozone trends. Chemosphere - Global Change Science, 2(2), 167–183. https://doi.org/10.1016/S1465-9972(00)00008-8

Lelieveld, J., & Dentener, F. J. (2000). What controls tropospheric ozone? *Journal of Geophysical Research: Atmospheres*, *105*(D3), 3531–3551. https://doi.org/10.1029/1999JD901011

Finlayson-Pitts, B. J., & Pitts, J. N. (1993). Atmospheric chemistry of tropospheric ozone formation: Scientific and regulatory implications. Air and Waste, 43(8), 1091–1100. https://doi.org/10.1080/1073161X.1993.10467187

Jaffe, L. S. (1968). Ambient carbon monoxide and its fate in the atmosphere. *Journal of the Air Pollution Control Association*, *18*(8), 534–540. https://doi.org/10.1080/00022470.1968.10469168

Twigg, M. v. (2011). Catalytic control of emissions from cars. Catalysis Today, 163(1), 33–41. https://doi.org/10.1016/J.CATTOD.2010.12.044

Mott, J. A., Wolfe, M. I., Alverson, C. J., Macdonald, S. C., Bailey, C. R., Ball, L. B., Moorman, J. E., Somers, J. H., Mannino, D. M., & Redd, S. C. (2002). National Vehicle Emissions Policies and Practices and Declining US Carbon Monoxide–Related Mortality. *JAMA*, *288*(8), 988–995. https://doi.org/10.1001/JAMA.288.8.988

Bjork, B. J., Bui, T. Q., Heckl, O. H., Changala, P. B., Spaun, B., Heu, P., Follman, D., Deutsch, C., Cole, G. D., Aspelmeyer, M., Okumura, M., & Ye, J. (2016). Direct frequency comb measurement of OD + CO→DOCO kinetics. *Science*, *354*(6311), 444–448. https://doi.org/10.1126/SCIENCE.AAG1862

Daniel, J. S., & Solomon, S. (1998). On the climate forcing of carbon monoxide. Journal of Geophysical Research Atmospheres, 103(D11), 13249–13260. https://doi.org/10.1029/98JD00822

IPCC. Summary for Policymakers. In Climate Change 2013: The Physical Science Basis; Contribution of Working Group I to the Fifth Assessment Report of the Intergovernmental Panel on Climate Change; Stocker, T.F., Qin, D., Plattner, G.-K., Tignor, M., Allen, S.K., Boschung, J., Nauels, A., Xia, Y., Bex, V., Midgley, P.M., Eds.; Cambridge University Press: Cambridge, UK; New York, NY, USA, 2013; Volume 3, pp. 3–29.

Du, B., Tandoc, M. C., Mack, M. L., & Siegel, J. A. (2020). Indoor CO2 concentrations and cognitive function: A critical review. *Indoor Air*, *30*(6), 1067–1082. https://doi.org/10.1111/INA.12706

Orellano, P., Reynoso, J., Quaranta, N., Bardach, A., & Ciapponi, A. (2020). Short-term exposure to particulate matter (PM10 and PM2.5), nitrogen dioxide (NO2), and ozone (O3) and all-cause and cause-specific mortality: Systematic review and meta-analysis. Environment International, 142, 105876. https://doi.org/10.1016/J.ENVINT.2020.105876

Bellouin, N., Quaas, J., Gryspeerdt, E., Kinne, S., Stier, P., Watson-Parris, D., et al. (2020). Bounding global aerosol radiative forcing of climate change. *Reviews of Geophysics*, 58, e2019RG000660. https://doi.org/10.1029/2019RG000660

Charlson, R. J., Schwartz, S. E., Hales, J. M., Cess, R. D., Coakley, J. A., Hansen, J. E., & Hofmann, D. J. (1992). Climate Forcing by Anthropogenic Aerosols. *Science*, *255*(5043), 423–430. https://doi.org/10.1126/SCIENCE.255.5043.423

Levy, H., Horowitz, L. W., Schwarzkopf, M. D., Ming, Y., Golaz, J. C., Naik, V., & Ramaswamy, V. (2013). The roles of aerosol direct and indirect effects in past and future climate change. *Journal of Geophysical Research Atmospheres*, *118*(10), 4521–4532. https://doi.org/10.1002/JGRD.50192

Singh, D., Verma, S.K. (2023). Impacts of Particulate Matter Pollution on Plants. In: Aftab, T. (eds) New Frontiers in Plant-Environment Interactions. Environmental Science and Engineering. Springer, Cham. https://doi.org/10.1007/978-3-031-43729-8_17

Tan, Z., Lu, K., Dong, H., Hu, M., Li, X., Liu, Y., Lu, S., Shao, M., Su, R., Wang, H., Wu, Y., Wahner, A., & Zhang, Y. (2018). Explicit diagnosis of the local ozone production rate and the ozone-NOx-VOC sensitivities. *Science Bulletin*, *63*(16), 1067–1076. https://doi.org/10.1016/J.SCIB.2018.07.001

Forster, P., V. Ramaswamy, P. Artaxo, T. Berntsen, R. Betts, D.W. Fahey, J. Haywood, J. Lean, D.C. Lowe, G. Myhre, J. Nganga, R. Prinn, G. Raga, M. Schulz and R. Van Dorland, 2007: Changes in Atmospheric Constituents and in Radiative Forcing. In: Climate Change 2007: The Physical Science Basis. Contribution of Working Group I to the Fourth Assessment Report of the Intergovernmental Panel on Climate Change [Solomon, S., D. Qin, M. Manning, Z. Chen, M. Marquis, K.B. Averyt, M.Tignor and H.L. Miller (eds.)]. Cambridge University Press, Cambridge, United Kingdom and New York, NY, USA.

Mohnen, V. A., Goldstein, W., & Wang, W. C. (1993). Tropospheric Ozone and Climate Change. *Air & Waste*, *43*(10), 1332–1334. https://doi.org/10.1080/1073161X.1993.10467207

Sudo, K. (2023). Atmospheric Mixing Ratios of O3 and Radiative Forcing. Handbook of Air Quality and Climate Change, 1–33. https://doi.org/10.1007/978-981-15-2527-8_30-1

Fuhrer, J., Val Martin, M., Mills, G., Heald, C. L., Harmens, H., Hayes, F., Sharps, K., Bender, J., & Ashmore, M. R. (2016). Current and future ozone risks to global terrestrial biodiversity and ecosystem processes. Ecology and Evolution, 6(24), 8785–8799. https://doi.org/10.1002/ECE3.2568

Feldman, D. R., Collins, W. D., Gero, P. J., Torn, M. S., Mlawer, E. J., & Shippert, T. R. (2015). Observational determination of surface radiative forcing by CO2 from 2000 to 2010. *Nature 2015 519:7543*, *519*(7543), 339–343. https://doi.org/10.1038/nature14240

Daniel, J. S., & Solomon, S. (1998). On the climate forcing of carbon monoxide. Journal of Geophysical Research Atmospheres, 103(D11), 13249–13260. https://doi.org/10.1029/98JD00822

Zuhara, S., & Isaifan, R. (2018). The Impact of criteria air pollutants on soil and water: A review, J. Env. Sci. Pollut. Res. 4(2) 278–284. https://doi.org/10.30799/jespr.133.18040205

Grantz, D. A., Garner, J. H. B., & Johnson, D. W. (2003). Ecological effects of particulate matter. Environment International, 29(2–3), 213–239. https://doi.org/10.1016/S0160-4120(02)00181-2

Singh, A., & Agrawal, M. (2008). Acid rain and its ecological consequences. Journal of Environmental Biology.

Kampa, M., & Castanas, E. (2008). Human health effects of air pollution. Environmental Pollution, 151(2), 362–367. https://doi.org/10.1016/J.ENVPOL.2007.06.012

Oberdörster, G., Oberdörster, E., & Oberdörster, J. (2005). Nanotoxicology: an emerging discipline evolving from studies of ultrafine particles. *Environmental health perspectives*, *113*(7), 823.

Oberdörster, G., Sharp, Z., Atudorei, V., Elder, A., Gelein, R., Kreyling, W., & Cox, C. (2004). Translocation of Inhaled Ultrafine Particles to the Brain. *Inhalation Toxicology*, *16*(6–7), 437–445. https://doi.org/10.1080/08958370490439597

Sanità di Toppi, L., Sanità di Toppi, L., & Bellini, E. (2020). Novel Coronavirus: How Atmospheric Particulate Affects Our Environment and Health. *Challenges*, *11*(1), 6. https://doi.org/10.3390/challe11010006

Basith, S., Manavalan, B., Shin, T. H., Park, C. B., Lee, W. S., Kim, J., & Lee, G. (2022). The Impact of Fine Particulate Matter 2.5 on the Cardiovascular System: A Review of the Invisible Killer. *Nanomaterials*, *12*(15), 2656. https://doi.org/10.3390/NANO12152656

Krittanawong, C., Qadeer, Y. K., Hayes, R. B., Wang, Z., Thurston, G. D., Virani, S., & Lavie, C. J. (2023). PM2.5 and cardiovascular diseases: State-of-the-Art review. *International Journal of Cardiology Cardiovascular Risk and Prevention*, *19*, 200217. https://doi.org/10.1016/J.IJCRP.2023.200217

Bentayeb, M., Simoni, M., Norback, D., Baldacci, S., Maio, S., Viegi, G., & Annesi-Maesano, I. (2013). Indoor air pollution and respiratory health in the elderly.

Journal of Environmental Science and Health, Part A, 48(14), 1783–1789. https://doi.org/10.1080/10934529.2013.826052

Kyung, S. Y., & Jeong, S. H. (2020). Particulate-matter related respiratory diseases. *Tuberculosis and respiratory diseases*, *83*(2), 116.

Guillam, M. T., Pédrono, G., Le Bouquin, S., Huneau, A., Gaudon, J., Leborgne, R., ... & Ségala, C. (2013). Chronic respiratory symptoms of poultry farmers and model-based estimates of long-term dust exposure. *Annals of Agricultural and Environmental Medicine*, *20*(2).

Gao, Y., Chan, E. Y. Y., Li, L., Lau, P. W. C., & Wong, T. W. (2014). Chronic effects of ambient air pollution on respiratory morbidities among Chinese children: a cross-sectional study in Hong Kong. BMC Public Health 2014 14:1, 14(1), 105-. https://doi.org/10.1186/1471-2458-14-105

Sahu, D., Kannan, G. M., & Vijayaraghavan, R. (2014). Carbon Black Particle Exhibits Size Dependent Toxicity in Human Monocytes. *International Journal of Inflammation*, *2014*(1), 827019. https://doi.org/10.1155/2014/827019

Raaschou-Nielsen, O., Beelen, R., Wang, M., Hoek, G., Andersen, Z. J., Hoffmann, B., Stafoggia, M., Samoli, E., Weinmayr, G., Dimakopoulou, K., Nieuwenhuijsen, M., Xun, W. W., Fischer, P., Eriksen, K. T., Sørensen, M., Tjønneland, A., Ricceri, F., de Hoogh, K., Key, T., ... Vineis, P. (2016). Particulate matter air pollution components and risk for lung cancer. *Environment International*, *87*, 66–73. https://doi.org/10.1016/J.ENVINT.2015.11.007

Hamra, G. B., Guha, N., Cohen, A., Laden, F., Raaschou-Nielsen, O., Samet, J. M., Vineis, P., Forastiere, F., Saldiva, P., Yorifuji, T., & Loomis, D. (2014). Outdoor particulate matter exposure and lung cancer: A systematic review and meta-analysis. *Environmental Health Perspectives*, *122*(9), 906–911. https://doi.org/10.1289/EHP.1408092

Pope, C. A., & Dockery, D. W. (2006). Health effects of fine particulate air pollution: Lines that connect. *Journal of the Air and Waste Management Association*, *56*(6), 709–742. https://doi.org/10.1080/10473289.2006.10464485

Nuvolone, D., Petri, D., & Voller, F. (2017). The effects of ozone on human health. *Environmental Science and Pollution Research 2017 25:9*, *25*(9), 8074–8088. https://doi.org/10.1007/S11356-017-9239-3

Bell, M. L., McDermott, A., Zeger, S. L., Samet, J. M., & Dominici, F. (2004). Ozone and Short-term Mortality in 95 US Urban Communities, 1987-2000. *JAMA*, *292*(19), 2372–2378. https://doi.org/10.1001/JAMA.292.19.2372

Liu, H., Liu, S., Xue, B., Lv, Z., Meng, Z., Yang, X., Xue, T., Yu, Q., & He, K. (2018). Ground-level ozone pollution and its health impacts in China. *Atmospheric Environment*, *173*, 223–230. https://doi.org/10.1016/J.ATMOSENV.2017.11.014

Jerrett, M., Burnett, R. T., Pope, C. A., Ito, K., Thurston, G., Krewski, D., Shi, Y., Calle, E., & Thun, M. (2009). Long-Term Ozone Exposure and Mortality. *New England Journal of Medicine*, *360*(11), 1085–1095. https://doi.org/10.1056/NEJMOA0803894

Wang, Y., Wild, O., Chen, X., Wu, Q., Gao, M., Chen, H., Qi, Y., & Wang, Z. (2020). Health impacts of long-term ozone exposure in China over 2013–2017. *Environment International*, *144*, 106030. https://doi.org/10.1016/J.ENVINT.2020.106030

Theodorakidou, M., & Lambrou, G. I. (2017). Public health issues from the exposure to nitrogen oxides: a brief review. *ARC J Public Health Community Med*, *2*, 44-56. https://doi.org/10.20431/2456-0596.0204008

Tao, Y., Huang, W., Huang, X., Zhong, L., Lu, S. E., Li, Y., Dai, L., Zhang, Y., & Zhu, T. (2011). Estimated Acute Effects of Ambient Ozone and Nitrogen Dioxide on Mortality in the Pearl River Delta of Southern China. *Environmental Health Perspectives*, *120*(3), 393. https://doi.org/10.1289/EHP.1103715

Belanger, K., Gent, J. F., Triche, E. W., Bracken, M. B., & Leaderer, B. P. (2005). Association of indoor nitrogen dioxide exposure with respiratory symptoms in children with asthma. *American Journal of Respiratory and Critical Care Medicine*, *173*(3), 297–303. https://doi.org/10.1164/RCCM.200408-1123OC

Abelsohn, A., Sanborn, M. D., Jessiman, B. J., & Weir, E. (2002). Identifying and managing adverse environmental health effects: 6. Carbon monoxide poisoning. *Cmaj*, *166*(13), 1685-1690.

U.S. Environmental Protection Agency. (1984). *Revised evaluation of health effects associated with carbon monoxide exposure: An addendum to the 1979 EPA air quality criteria document for carbon monoxide* (Report No. EPA-600/8-83-033F). Office of Health and Environmental Assessment. https://nepis.epa.gov/Exe/ZyPURL.cgi?Dockey=30001C1L.TXT

Ernst, A., & Zibrak, J. D. (1998). Carbon Monoxide Poisoning. *New England Journal of Medicine*, *339*(22), 1603–1608. https://doi.org/10.1056/NEJM199811263392206

Chen, K., Breitner, S., Wolf, K., Stafoggia, M., Sera, F., Vicedo-Cabrera, A. M., Guo, Y., Tong, S., Lavigne, E., Matus, P., Valdés, N., Kan, H., Jaakkola, J. J. K., Ryti, N. R. I., Huber, V., Scortichini, M., Hashizume, M., Honda, Y., Nunes, B., … Schneider, A. (2021). Ambient carbon monoxide and daily mortality: a global time-series study in 337 cities. *The Lancet Planetary Health*, *5*(4), e191–e199. https://doi.org/10.1016/S2542-5196(21)00026-7

Dimitroulopoulou, S., Dudzińska, M. R., Gunnarsen, L., Hägerhed, L., Maula, H., Singh, R., Toyinbo, O., & Haverinen-Shaughnessy, U. (2023). Indoor air quality guidelines from across the world: An appraisal considering energy saving, health, productivity, and comfort. Environment International, 178, 108127. https://doi.org/10.1016/J.ENVINT.2023.108127

Samudro, H., Samudro, G., & Mangkoedihardjo, S. (2022). Prevention of indoor air pollution through design and construction certification: A review of the sick building syndrome conditions. Journal of Air Pollution and Health, 7(1), 81–94. https://doi.org/10.18502/JAPH.V7I1.8922

Brimblecombe, P., & Grossi, C. M. (2010). Potential damage to modern building materials from 21st century air pollution. *TheScientificWorldJournal*, *10*(1), 116–125. https://doi.org/10.1100/TSW.2010.17

Rao, N. V., Rajasekhar, M., & Rao, G. C. (2014). Detrimental effect of air pollution, corrosion on building materials and historical structures. *American Journal of Engineering Research*, *3*(3), 359-364.

Sharma, S., Dakshina Murthy, N. R., & Sumanth, C. (2023). Effect of air pollution on building materials. Materials Today: Proceedings. https://doi.org/10.1016/J.MATPR.2023.04.631

Ruffolo, S. A., la Russa, M. F., Rovella, N., & Ricca, M. (2023). The Impact of Air Pollution on Stone Materials. *Environments 2023, Vol. 10, Page 119*, *10*(7), 119. https://doi.org/10.3390/ENVIRONMENTS10070119

Cardell-Fernández, C., Vleugels, G., Torfs, K., & van Grieken, R. (2002). The processes dominating Ca dissolution of limestone when exposed to ambient atmospheric conditions as determined by comparing dissolution models. Environmental Geology, 43(1–2), 160–171. https://doi.org/10.1007/S00254-002-0640-X

Sablier, M., & Garrigues, P. (2014). Cultural heritage and its environment: An issue of interest for Environmental Science and Pollution Research. Environmental Science and Pollution Research, 21(9), 5769–5773. https://doi.org/10.1007/S11356-013-2458-3

Vidović, K., Hočevar, S., Menart, E., Drventić, I., Grgić, I., & Kroflič, A. (2022). Impact of air pollution on outdoor cultural heritage objects and decoding the role of particulate matter: a critical review. *Environmental Science and Pollution Research 2022 29:31*, *29*(31), 46405–46437. https://doi.org/10.1007/S11356-022-20309-8

Barca, D., Comite, V., Belfiore, C. M., Bonazza, A., la Russa, M. F., Ruffolo, S. A., Crisci, G. M., Pezzino, A., & Sabbioni, C. (2014). Impact of air pollution in deterioration of carbonate building materials in Italian urban environments. *Applied Geochemistry*, *48*, 122–131. https://doi.org/10.1016/J.APGEOCHEM.2014.07.002

Comite, V., & Fermo, P. (2018). *The effects of air pollution on cultural heritage: The case study of Santa Maria delle Grazie al Naviglio Grande (Milan)*. https://doi.org/10.1140/epjp/i2018-12365-6

Grau-Bové, J., & Strlič, M. (2013). Fine particulate matter in indoor cultural heritage: A literature review. Heritage Science, 1(1), 1–17. https://doi.org/10.1186/2050-7445-1-8

Motta, O., Pironti, C., Ricciardi, M., Rostagno, C., Bolzacchini, E., Ferrero, L., Cucciniello, R., & Proto, A. (2022). Leonardo da Vinci's "Last Supper": a case study to evaluate the influence of visitors on the Museum preservation systems. *Environmental Science and Pollution Research*, *29*(20), 29391–29398. https://doi.org/10.1007/S11356-021-13741-9

Gini, I., Balzarini, A., Pirovano, G., Toppetti, A. M., Fialdini, L., Omodeo, P., Pirovano, G., Marzinotto, M., Mancini, A., Losi, N., Cefalì, A. M., Doldi, A., Bolzacchini, E., & Ferrero, L. (2023). On the Chemical Composition and Hygroscopicity of Aerosols Deposited on the Insulators of Italian Power Lines. Applied Sciences Switzerland, 13(23). https://doi.org/10.3390/app132312788

Ferrero, L., Sangiorgi, G., Ferrini, B. S., Perrone, M. G., Moscatelli, M., D'Angelo, L., Rovelli, G., Ariatta, A., Truccolo, R., & Bolzacchini, E. (2013). Aerosol corrosion prevention and energy-saving strategies in the design of green data centers. *Environmental Science and Technology*, *47*(8), 3856–3864. https://doi.org/10.1021/es304790f

Ferrero, L., D'Angelo, L., Rovelli, G., Sangiorgi, G., Perrone, M. G., Moscatelli, M., Casati, M., Rozzoni, V., & Bolzacchini, E. (2015). Determination of aerosol deliquescence and crystallization relative humidity for energy saving in free-cooled data centers. *International Journal of Environmental Science and Technology*, *12*(9), 2777–2790. https://doi.org/10.1007/s13762-014-0680-2

Howell, S. G., Clarke, A. D., Shinozuka, Y., Kapustin, V., McNaughton, C. S., Huebert, B. J., Doherty, S. J., & Anderson, T. L. (2006). Influence of relative humidity upon pollution and dust during ACE-Asia: Size distributions and implications for optical properties. Journal of Geophysical Research Atmospheres, 111(6), 6205. https://doi.org/10.1029/2004JD005759

Decreto Ministeriale 2 aprile 2002, n. 60 (2002, 13 aprile). *Procedure operative ai fini della certificazione di equivalenza dei metodi e dei sistemi per il*

campionamento e la misura del PM10 da parte dei laboratori primari di riferimento.

European Committee for Standardization. (2023). *Ambient air - Standard gravimetric measurement method for the determination of the PM10 or PM2.5 mass concentration of suspended particulate matter* (EN 12341:2023).

Grimm, H., & Eatough, D. J. (2009). Aerosol Measurement: The Use of Optical Light Scattering for the Determination of Particulate Size Distribution, and Particulate Mass, Including the Semi-Volatile Fraction. *Journal of the Air & Waste Management Association*, *59*(1), 101–107. https://doi.org/10.3155/1047-3289.59.1.101

Sousan, S., Regmi, S., Park, Y. M., Piuzzi, E., & Palermo, E. (2021). *Laboratory Evaluation of Low-Cost Optical Particle Counters for Environmental and Occupational Exposures*. https://doi.org/10.3390/s21124146

Kaur, K., & Kelly, K. E. (2023). Laboratory evaluation of the Alphasense OPC-N3, and the Plantower PMS5003 and PMS6003 sensors. *Journal of Aerosol Science*, *171*, 106181. https://doi.org/10.1016/j.jaerosci.2023.106181

deSouza, P., Wang, A., Machida, Y., Duhl, T., Mora, S., Kumar, P., Kahn, R., Ratti, C., Durant, J. L., & Hudda, N. (2023). Evaluating the Performance of Low-Cost PM2.5 Sensors in Mobile Settings. *Environmental Science and Technology*, *57*(41), 15401–15411. https://doi.org/10.1021/ACS.EST.3C04843

Dupont, S., Lamaud, E., Irvine, M. R., Bonnefond, J. M., González-Romero, A., Alastuey, A., González-Flórez, C., Querol, X., Kandler, K., Klose, M., & Pérez García-Pando, C. (2025). Performance of a low-cost optical particle counter (Alphasense OPC-N3) in estimating size-resolved dust emission flux using eddy covariance. *Atmospheric Measurement Techniques*, *18*(9), 2183–2200. https://doi.org/10.5194/AMT-18-2183-2025

Nurowska, K., Mohammadi, M., Malinowski, S., & Markowicz, K. (2023). Applicability of the low-cost OPC-N3 optical particle counter for microphysical measurements of fog. *Atmospheric Measurement Techniques*, *16*(9), 2415–2430. https://doi.org/10.5194/AMT-16-2415-2023

Schneiders, K., Moormann, L., Dupont, S., Koenen, D., Rabe, J., Dagsson Waldhauserová, P., Schepanski, K., Panta, A., Klose, M., Meyer, H., González-Flórez, C., González-Romero, A., Querol, X., Alastuey, A., Yus-Díez, J., Pérez García-Pando, C., and Kandler, K. (2025). Long-term aerosol measurements of the Alphasense OPC-N3 in arctic regions: Sensor performance and corrections, EGU General Assembly 2025, Vienna, Austria, 27 Apr–2 May 2025, EGU25-19762, https://doi.org/10.5194/egusphere-egu25-19762

South Coast Air Quality Management District (AQMD). AQ-SPEC Sensor Summary Table. (n.d.). Retrieved January 9, 2026, from https://www.aqmd.gov/aq-spec/evaluations/summary-table#~:test:=PurpleAir

Tryner, J., L'Orange, C., Mehaffy, J., Miller-Lionberg, D., Hofstetter, J. C., Wilson, A., & Volckens, J. (2020). Laboratory evaluation of low-cost PurpleAir PM monitors and in-field correction using co-located portable filter samplers. *Atmospheric Environment*, *220*, 117067. https://doi.org/10.1016/J.ATMOSENV.2019.117067

Stavroulas, I., Grivas, G., Michalopoulos, P., Liakakou, E., Bougiatioti, A., Kalkavouras, P., Fameli, K. M., Hatzianastassiou, N., Mihalopoulos, N., & Gerasopoulos, E. (2020). Field Evaluation of Low-Cost PM Sensors (Purple Air PA-II) Under Variable Urban Air Quality Conditions, in Greece. Atmosphere 2020, Vol. 11, Page 926, 11(9), 926. https://doi.org/10.3390/ATMOS11090926

Johnson, K., A. Holder, S. Frederick, G. Hagler, AND A. Clements. PurpleAir PM2.5 performance across the U.S.#2. Meeting between ORD, OAR/AirNow, and USFS, Research Triangle Park, NC, February 03, 2020.

Heintzelman A, Filippelli GM, Moreno-Madriñan MJ, Wilson JS, Wang L, Druschel GK, Lulla VO. Efficacy of Low-Cost Sensor Networks at Detecting Fine-Scale Variations in Particulate Matter in Urban Environments. *International Journal of Environmental Research and Public Health*. 2023; 20(3):1934. https://doi.org/10.3390/ijerph20031934

Kaur, K., & Kelly, K. E. (2023). Laboratory evaluation of the Alphasense OPC-N3, and the Plantower PMS5003 and PMS6003 sensors. *Journal of Aerosol Science*, *171*, 106181. https://doi.org/10.1016/j.jaerosci.2023.106181

Ouimette, J. R., Malm, W. C., Schichtel, B. A., Sheridan, P. J., Andrews, E., Ogren, J. A., & Arnott, W. P. (2022). Evaluating the PurpleAir monitor as an aerosol light scattering instrument. *Atmos. Meas. Tech*, *15*, 655–676. https://doi.org/10.5194/amt-15-655-2022

Nilson, B., Jackson, P. L., Schiller, C. L., & Parsons, M. T. (2022). Development and evaluation of correction models for a low-cost fine particulate matter monitor. *Atmospheric Measurement Techniques*, *15*(11), 3315–3328. https://doi.org/10.5194/AMT-15-3315-2022

Barkjohn, K. K., Holder, A. L., Frederick, S. G., & Clements, A. L. (2022). Correction and Accuracy of PurpleAir PM2.5 Measurements for Extreme Wildfire Smoke. *Sensors*, *22*(24), 9669. https://doi.org/10.3390/S22249669/S1

Barkjohn, K. K., Gantt, B., & Clements, A. L. (2021). Development and application of a United States-wide correction for $PM_{2.5}$ data collected with the PurpleAir sensor. *Atmospheric Measurement Techniques*, *14*(6), 4617–4637. https://doi.org/10.5194/AMT-14-4617-2021

Wallace, L., Zhao, T., & Klepeis, N. E. (2022). Calibration of PurpleAir PA-I and PA-II Monitors Using Daily Mean PM2.5 Concentrations Measured in California, Washington, and Oregon from 2017 to 2021. *Sensors*, *22*(13), 4741. https://doi.org/10.3390/S22134741/S1

Subramaniam, S., Ganesan, A., Raju, N., & Prakash, C. (2023). Investigation of indoor air quality and pulmonary function status among power loom industry workers in Tamil Nadu, South India. *Air Quality, Atmosphere & Health 2023 17:1*, *17*(1), 215–230. https://doi.org/10.1007/S11869-023-01439-5

Shankar, S., Abbas, G., Nithyaprakash, R., Naveenkumar, R., Rakesh Mohanty, S., Sabarinathan, A., & Karthick, S. (2023). Study on the Impact of Firecrackers on Atmospheric Pollutants during Diwali Festival in Tamil Nadu, India. *E3S Web of Conferences*, *453*, 01004. https://doi.org/10.1051/E3SCONF/202345301004

Gulia, S., Prasad, P., Goyal, S. K., & Kumar, R. (2020). Sensor-based Wireless Air Quality Monitoring Network (SWAQMN) - A smart tool for urban air quality management. *Atmospheric Pollution Research*, *11*(9), 1588–1597. https://doi.org/10.1016/J.APR.2020.06.016

Kurtenbach, R., Ulianova, K., Gibilisco, R. G., Villena, G., & Wiesen, P. (2022). 2.8 Validation of low-cost sensors for gases and particulate matter in the city centre of Wuppertal, Germany. In *Transport and Air Pollution (TAP) Conference* (p. 75).

Doldi, A., Pagliarulo, L., Bolzacchini, E., Ferrero, L., Freitag, S., Schute, L. G., Junk, K., Todea, A. M., & Asbach, C. (2025). Evaluating the performance of the low-cost black carbon sensor bcMeter at an urban background site. *Gefahrstoffe Reinhaltung Der Luft*, *85*(1–2). https://doi.org/10.37544/0949-8036-2025-01-02-05

Ferrero, L., Losi, N., Rigler, M., Gregorič, A., Colombi, C., D'Angelo, L., Cuccia, E., Cefalì, A. M., Gini, I., Doldi, A., Cerri, S., Maroni, P., Cipriano, D., Markuszewski, P., & Bolzacchini, E. (2024). Determining the Aethalometer multiple scattering enhancement factor C from the filter loading parameter. *Science of the Total Environment*, *917*. https://doi.org/10.1016/j.scitotenv.2024.170221

Virkkula, A., Mäkelä, T., Hillamo, R., Yli-Tuomi, T., Hirsikko, A., Hämeri, K., & Koponen, I. K. (2007). A simple procedure for correcting loading effects of aethalometer data. Journal of the Air & Waste Management

Tritscher, T., Koched, A., Han, H.-S., -, al, Kim, H., Chul Yang, J., Kim -, T., Graber, V., Ronchi, M., Pardo-Araujo, C., Beeston, M., Zerrath, A. F., Elzey, S., Krinke, T. J., Filimundi, E., & Bischof, O. F. (2013). NanoScan SMPS – A Novel, Portable Nanoparticle Sizing and Counting Instrument. *Journal of Physics: Conference Series*, *429*(1), 012061. https://doi.org/10.1088/1742-6596/429/1/012061

Fierz, M., Meier, D., Steigmeier, P., & Burtscher, H. (2014). Aerosol measurement by induced currents. *Aerosol Science and Technology*, *48*(4), 350–357. https://doi.org/10.1080/02786826.2013.875981

Fierz, M., Meier, D., Steigmeier, P., & Burtscher, H. (2015). Miniature nanoparticle sensors for exposure measurement and TEM sampling. *Journal of Physics: Conference Series*, *617*(1), 012034. https://doi.org/10.1088/1742-6596/617/1/012034

Opoku, A., and Akotia, J. (2020). Special issue: urban regeneration for sustainable development. Construction Economics and Building, 20:2, 1-5. http://dx.doi.org/10.5130/AJCEB.v20i2.7191

Nazari, S. (2025). Explaining a sustainable urban regeneration model with an approach to improving the quality of urban space. *International Journal of Urban Management and Energy Sustainability*, *6*(2), 86–103. https://doi.org/10.22034/IJUMES.2025.2061781.1312

Asbach, C., Todea, A. M., & Kaminski, H. (2024). Evaluation of a Partector Pro for atmospheric particle number size distribution and number concentration measurements at an urban background site. *Aerosol Research*, *2*(1), 1–12. https://doi.org/10.5194/AR-2-1-2024

Todea, A. M., Beckmann, S., Kaminski, H., Bard, D., Bau, S., Clavaguera, S., Dahmann, D., Dozol, H., Dziurowitz, N., Elihn, K., Fierz, M., Lidén, G., Meyer-Plath, A., Monz, C., Neumann, V., Pelzer, J., Simonow, B. K., Thali, P., Tuinman, I., … Asbach, C. (2017). Inter-comparison of personal monitors for nanoparticles exposure at workplaces and in the environment. *Science of The Total Environment*, *605–606*, 929–945. https://doi.org/10.1016/J.SCITOTENV.2017.06.041

Bezantakos, S., Varnava, C. K., Papaconstantinou, R., & Biskos, G. (2024). Performance of the Naneos partector 2 multi-metric nanoparticle detector at reduced temperature and pressure conditions. *Aerosol Science and Technology*, *58*(5), 584–593. https://doi.org/10.1080/02786826.2024.2330471

Hänninen, O. O., Lebret, E., Ilacqua, V., Katsouyanni, K., Künzli, N., Srám, R. J., & Jantunen, M. (2004). Infiltration of ambient PM2.5 and levels of indoor generated non-ETS PM2.5 in residences of four European cities. *Atmospheric Environment*, *38*(37), 6411–6423. https://doi.org/10.1016/J.ATMOSENV.2004.07.015

Hoek, G., Kos, G., Harrison, R., de Hartog, J., Meliefste, K., ten Brink, H., Katsouyanni, K., Karakatsani, A., Lianou, M., Kotronarou, A., Kavouras, I., Pekkanen, J., Vallius, M., Kulmala, M., Puustinen, A., Thomas, S., Meddings, C., Ayres, J., van Wijnen, J., & Hameri, K. (2008). Indoor–outdoor relationships of

particle number and mass in four European cities. *Atmospheric Environment*, *42*(1), 156–169. https://doi.org/10.1016/J.ATMOSENV.2007.09.026

Sangiorgi, G., Ferrero, L., Ferrini, B. S., lo Porto, C., Perrone, M. G., Zangrando, R., Gambaro, A., Lazzati, Z., & Bolzacchini, E. (2013). Indoor airborne particle sources and semi-volatile partitioning effect of outdoor fine PM in offices. *Atmospheric Environment*, *65*, 205–214. https://doi.org/10.1016/J.ATMOSENV.2012.10.050

Guenther, A. (1995). A global model of natural volatile organic compound emissions. *Journal of Geophysical Research*, *100*(D5), 8873–8892. https://doi.org/10.1029/94JD02950

Joutsensaari, J., Loivamäki, M., Vuorinen, T., Miettinen, P., Nerg, A. M., Holopainen, J. K., & Laaksonen, A. (2005). Nanoparticle formation by ozonolysis of inducible plant volatiles. *Atmospheric Chemistry and Physics*, *5*(6), 1489–1495. https://doi.org/10.5194/ACP-5-1489-2005

Holopainen, J. K., Kivimäenpää, M., & Nizkorodov, S. A. (2017). Plant-derived Secondary Organic Material in the Air and Ecosystems. *Trends in Plant Science*, *22*(9), 744–753. https://doi.org/10.1016/j.tplants.2017.07.004

Wu, K., Yang, X., Chen, D., Gu, S., Lu, Y., Jiang, Q., Wang, K., Ou, Y., Qian, Y., Shao, P., & Lu, S. (2020). Estimation of biogenic VOC emissions and their corresponding impact on ozone and secondary organic aerosol formation in China. *Atmospheric Research*, *231*, 104656. https://doi.org/10.1016/J.ATMOSRES.2019.104656

Elomaa, T., Luoma, K., Harni, S., Virkkula, A., Timonen, H., & Petäjä, T. (2024). *Applicability of small-scale black carbon sensors to explore high resolution spatial variability of ambient black carbon*. https://doi.org/10.5194/ar-2024-12.

Janssen, N. A. H., Hoek, G., Simic-Lawson, M., Fischer, P., van Bree, L., Brink, H. ten, Keuken, M., Atkinson, R. W., Ross Anderson, H., Brunekreef, B., & Cassee, F. R. (2011). *Black carbon as an additional indicator of the adverse health effects of airborne particles compared with pm10 and pm2.5*. In Environmental Health

Perspectives (Vol. 119, Issue 12, pp. 1691–1699). Public Health Services, US Dept of Health and Human Services. https://doi.org/10.1289/ehp.1003369.

Segersson, D., Eneroth, K., Gidhagen, L., Johansson, C., Omstedt, G., Nylén, A. E., & Forsberg, B. (2017). *Health impact of PM10, PM2.5 and black carbon exposure due to different source sectors in Stockholm, Gothenburg and Umea, Sweden*. International Journal of Environmental Research and Public Health, 14(7). https://doi.org/10.3390/ijerph14070742.

Caubel, J. J., Cados, T. E., & Kirchstetter, T. W. (2018). *A new black carbon sensor for dense air quality monitoring networks*. Sensors (Switzerland), 18(3). https://doi.org/10.3390/s18030738.

Lequy, E., Siemiatycki, J., de Hoogh, K., Vienneau, D., Dupuy, J. F., Garès, V., Hertel, O., Christensen, J. H., Zhivin, S., Goldberg, M., Zins, M., & Jacquemin, B. (2021). *Contribution of long-term exposure to outdoor black carbon to the carcinogenicity of air pollution: Evidence regarding risk of cancer in the gazel cohort*. Environmental Health Perspectives, 129(3). https://doi.org/10.1289/EHP8719.

Chung, S. H., & Seinfeld, J. H. (2002). *Global distribution and climate forcing of carbonaceous aerosols*. *J*ournal of Geophysical Research Atmospheres, 107(19), AAC 14-1-AAC 14-33. https://doi.org/10.1029/2001JD001397.

Zhang, H., & Wang, Z. (2011). *Advances in the study of black carbon effects on climate*. In Advances in Climate Change Research (Vol. 2, Issue 1, pp. 23–30). Science Press. https://doi.org/10.3724/SP.J.1248.2011.00023.

Rypdal, K., Rive, N., Berntsen, T. K., Klimont, Z., Mideksa, T. K., Myhre, G., & Skeie, R. B. (2009). *Costs and global impacts of black carbon abatement strategies*. Tellus, Series B: Chemical and Physical Meteorology, 61(4), 625–641. https://doi.org/10.1111/j.1600-0889.2009.00430.x.

European Parliament (EU 2024), *Directive 2024/2881 of the European Parliament and of the Council of 23 October 2024 on ambient air quality and cleaner air for Europe*.

European Committee for Standardization (CEN, 2017). *Ambient air - Measurement of elemental carbon (EC) and organic carbon (OC) collected on filters* (EN 16909:2017).

ACTRIS (2024). *Standard Procedures for In-Situ Aerosol Sampling, Measurements, and Analyses at ACTRIS Observatories*. Center for Aerosol In-Situ Measurement European Center for Aerosol Calibration and Characterization (CAIS-ECAC).

Hagler, G. S. W., Yelverton, T. L. B., Vedantham, R., Hansen, A. D. A., & Turner, J. R. (2011). *Post-processing method to reduce noise while preserving high time resolution in aethalometer real-time black carbon data*. Aerosol and Air Quality Research, 11(5), 539–546. https://doi.org/10.4209/aaqr.2011.05.0055.

Hansen, A.D.A., Rosen, H., Novakov, T. (1984). *The aethalometer — An instrument for the real-time measurement of optical absorption by aerosol particles*. Science of the Total Environment (Vol. 36, pp. 191-196). https://doi.org/10.1016/0048-9697(84)90265-1.

Friedrich, A., Dahl, J., *bcMeter – low cost aethalometer – open source black carbon measurement*. Retrieved December 16, 2024, from https://bcmeter.org/.

Asbach, C., Kuhlbusch, T.A.J., Quass, U., Kaminski, H. (2020). *10 jahre Messungen der Anzahl und ungendeponierbaren Oberflächenkonzentration ultrafeiner Partikel im städtischen Hintergrund im Ruhrgebiet, Gefahrstoffe* - Reinhaltung der Luft 80: 25-35. https://doi.org/10.37544/0949-8036-2020-01-02-27.

Morabito, E., Zendri, E., Piazza, R., Ganzerla, R., Montalbani, S., Marcoleoni, E., Bonetto, F., Scandella, A., Barbante, C., & Gambaro, A. (2012). Deposition in St. Mark's Basilica of Venice. Environmental Science and Pollution Research 2012 20:4, 20(4), 2579–2592. https://doi.org/10.1007/S11356-012-1162-Z

Ente Italiano di Normazione. (2025). *Ergonomia dell'ambiente fisico – Strumenti per la valutazione della qualità dell'aria interna* [Ergonomics of the physical environment – Tools for the evaluation of indoor air quality] (Standard No. UNI 11976:2025)

He, C., Morawska, L., Hitchins, J., & Gilbert, D. (2004). Contribution from indoor sources to particle number and mass concentrations in residential houses. *Atmospheric Environment*, *38*(21), 3405–3415. https://doi.org/10.1016/J.ATMOSENV.2004.03.027

Caseiro, A., Schmitz, S., & von Schneidemesser, E. (2024). Particle number size distribution evaluation of Plantower PMS5003 low-cost PM sensors – a field experiment. Environmental Science: Atmospheres, 4(10), 1183–1194. https://doi.org/10.1039/D4EA00086B

Tesi di dottorato realizzata nell'ambito del progetto MUSA finanziato dal PNRR Missione 4 Componente 2 Investimento 1.5, finanziato dall'Unione Europea - NextGenerationEU - CUP H43C22000550001

Finanziato dall'Unione europea NextGenerationEU
Ministero dell'Università e della Ricerca
Italiadomani PIANO NAZIONALE DI RIPRESA E RESILIENZA